NASA
Technical
Paper
2393

May 1985

NASA-TP-2393 19850018394

Planning Fuel-Conservative Descents in an Airline Environment Using a Small Programmable Calculator

Algorithm Development and Flight Test Results

Charles E. Knox,
Dan D. Vicroy,
and David A. Simmon

NASA

NASA Technical Paper 2393

1985

Planning Fuel-Conservative Descents in an Airline Environment Using a Small Programmable Calculator

Algorithm Development and Flight Test Results

Charles E. Knox
and Dan D. Vicroy
Langley Research Center
Hampton, Virginia

David A. Simmon
United Airlines, Inc.
Chicago, Illinois

National Aeronautics
and Space Administration

Scientific and Technical Information Branch

Contents

Summary

The Federal Aviation Administration (FAA) is implementing an automated, time-based metering form of air traffic control with profile descent procedures for arrivals into the terminal area. These concepts provide fuel savings by matching the arrival flow of airplanes to the airport acceptance rate through time-control computations and by allowing the pilot to descend at his discretion from cruise altitude to a designated metering fix in an idle-thrust clean configuration (with landing gear up, flaps zero, and speed brakes retracted). Although substantial fuel savings have resulted from these procedures, a potential for further fuel savings exists. Currently, the radar controller maintains time management for each airplane through either speed control or path stretching with radar vectors. This often results in more fuel being consumed than would have been if the descent planned by the pilot had been flown. Work load for the pilot is also high since he must plan for an idle-thrust descent to the metering fix by using various rules of thumb.

The National Aeronautics and Space Administration (NASA) has developed an airborne descent algorithm compatible with time-based metering and profile descent procedures and designed to improve the accuracy of delivering an airplane during a fuel-efficient descent to a metering fix at a time designated by the air traffic control (ATC) system. This algorithm provides open-loop guidance for an airplane to make an idle-thrust, clean-configured descent to arrive at the metering fix at a predetermined time, altitude, and airspeed. The algorithm also provides open-loop guidance for fuel-conservative descents when time constraints are not a consideration.

An investigation into the feasibility of using the open-loop guidance in an airline operational environment was conducted. The algorithm was programmed on a small programmable calculator for use with a McDonnell Douglas DC-10-10 airplane. Flight tests were conducted on routine airline flights into various major airports. The resulting mean distance and time errors to actually achieve the predicted speed and altitude conditions at the end of the descent profile were 2.3 n.mi. long and 1.3 sec early, respectively, based on 19 test runs. The mean arrival time error at the metering fix was 8.4 sec early (compared with approximately 1 to 2 min when vectored by ATC). The subject pilots reported that the calculator was easy to use and did not interfere with normal flight duties. They felt that the open-loop guidance provided by the calculator would be of most value while flying descents at nonstandard speeds or during time-metered operations.

Introduction

In an effort to improve the efficiency of terminal area operations, the Federal Aviation Administration (FAA) is implementing an automated time-based metering form of air traffic control (ATC) with profile descent procedures. The time-based metering concept is based upon airplane arrivals crossing a metering fix (typically 30 to 40 n.mi. from the airport) at a specified altitude, airspeed, and time. The time metering derandomizes the arrivals to the airport prior to entering the terminal area and results in a reduction of the low-altitude, high-fuel-consumption flight normally used to sequence airplanes to a common final approach path. The proper sequencing and spacing of enroute traffic also allows for increased airport productivity (refs. 1 and 2). The profile descent procedure allows the pilot to plan and fly a descent that is fuel conservative for his particular airplane, thus resulting in additional fuel savings.

With the current time-based metering/profile descent procedures, the air traffic controller is responsible for the time management of each airplane. The controller can adjust the airplane time of arrival at the metering fix by increasing the flight path length through heading changes or by requesting the pilot to change speed. The pilot is responsible for crossing the metering fix at the proper airspeed and altitude and must plan the descent carefully if fuel is to be conserved. The time management and the descent planning are both work load intensive and interdependent. Since limited or no guidance is available to either the controller or the pilot, their tasks must be accomplished independently through various rules of thumb and past experience. With this present operational concept, airplanes typically cross the metering fix with a time accuracy between 1 and 2 min (ref. 3). When the controller must lengthen the path or change the speed of the airplane for time control (even though the time-based metering and profile descent procedures are saving fuel), additional fuel must be used.

During the summer of 1979, the National Aeronautics and Space Administration (NASA) developed and flight tested, in its Transport Systems Research Vehicle (TSRV, previously designated the Terminal Configured Vehicle) Boeing 737 research airplane, a flight-management descent algorithm designed to provide closed-loop guidance for a fuel-conservative descent and to reduce the metering-fix crossing-time dispersion. The flight-management algorithm, which was based on an idle-thrust, clean-configured descent (with landing gear up and flaps and spoilers retracted), was designed to place the airplane at the metering fix at the proper altitude,

airspeed, and ATC-designated time. The results of the flight tests showed that the closed-loop guidance provided by the guidance and display system could reduce the time error when the metering fix is crossed to approximately 12 sec, based on 19 test runs (ref. 4).

This research was continued in June of 1981 with a T-39A (Sabreliner) airplane to determine if similar results could be obtained with open-loop guidance and a conventional complement of cockpit instrumentation (ref. 5). A version of the flight-management descent algorithm was implemented on a Hewlett-Packard HP-41CV programmable calculator. Open-loop guidance was provided by the calculator in the form of the Mach number and airspeed at which the descent should be flown and the point at which the pilot was to reduce the thrust to flight idle and begin the descent. The descent was then flown with reference to the airplane Mach and airspeed indicators and by maintaining an altitude profile computed by the calculator as a function of distance to the metering fix. Flight tests using this open-loop guidance resulted in an average time error when crossing the metering fix of 20 sec, based on 12 runs. This version of the descent algorithm was designed to operate in both the time-based metered and the conventional air traffic control environment, in which metering-fix times are not assigned.

Having determined the viability of the open-loop descent guidance, additional research was conducted to evaluate the feasibility of using such a descent planning tool in an airline operational environment. The airplane used in this study was the McDonnell Douglas DC-10-10. This report contains a description of the programmable calculator software, the DC-10 descent performance model used in the algorithm computations, and the results of the model-validation and pilot-evaluation flight tests.

Symbols and Abbreviations

ATC	air traffic control
A_{gw}	coefficient for gross-weight multiplication factor, lb^{-1}
A_I	coefficient for constant IAS descent rate equation, ft/sec
A_M, B_M	coefficients for constant Mach descent rate equation, ft
a_0, a_1, a_2	coefficients for quadratic curve fits of altitude as a function of time
B_{gw}	coefficient for gross-weight multiplication factor
B_I	coefficient for constant IAS descent rate equation, $knots^{-1}$
b_0	modeled vertical speed at sea level, ft/sec
b_1	slope of linear model for $\dot{h}$ during constant IAS descent, (ft/sec)/ft
CRS	magnetic course from entry fix to metering fix, deg
C_I	coefficient for constant IAS descent rate equation, sec^{-1}
C_M	coefficient for constant Mach descent rate equation, sec^2/ft
c_0	constant in model for $\dot{h}_{M_d}$, sec^2/ft
c_1	constant in model for $\dot{h}_{M_d}$, ft
DME	distance measuring equipment
D_w	magnetic wind direction, deg
$D_{w,h}$	magnetic wind direction evaluated at altitude h, deg
$D_{w,s}$	magnetic wind direction computed for sea-level altitude, deg
dD_w/dH	wind direction gradient with respect to altitude H, deg/ft
EF	entry fix
EF_{DME}	DME reading at entry fix, n.mi.
GSc	ground speed at cruise altitude, knots
GS_5	average ground speed on segment 5, knots
GW	gross weight, lb
H	pressure altitude, ft
H_{av}	average pressure altitude, ft
H_{bod}	pressure altitude at bottom of descent, ft
H_c	pressure altitude at cruise, ft
H_{MF}	pressure altitude of metering fix, ft
H_{XO}	pressure altitude at transition from constant Mach descent to constant airspeed descent, ft
h	geopotential altitude, ft
h_c	cruise altitude, ft
h_{MF}	metering-fix altitude, ft

h_{XO}	altitude at transition from constant Mach descent to constant airspeed descent, ft
$\dot{h}$	rate of change of altitude (vertical speed), ft/sec
$\dot{h}_g$	rate of change of altitude due to wind gradient, ft/sec
$\dot{h}_{IAS_d}$	rate of change of altitude evaluated at indicated airspeed IAS_d, ft/sec
$\dot{h}_{M_d}$	rate of change of altitude evaluated at descent Mach number M_d, ft/sec
$\dot{h}'_{M_d}$	rate of change of altitude, normalized for gross weight, evaluated at descent Mach number M_d, ft/sec
IAS	indicated airspeed, knots
IAS_d	indicated airspeed used during descent, knots
$IAS_{d,initial}$	indicated airspeed of initial descent for speed-iteration computations, knots
$IAS_{d,i}$	indicated airspeed of descent computed on ith iteration, knots
$IAS_{d,max}$	maximum indicated airspeed limit during descent, knots
$IAS_{d,min}$	minimum indicated airspeed limit during descent, knots
IAS_{MF}	indicated airspeed to cross metering fix, knots
IDL_{DME}	DME indication of point at which thrust should be reduced to flight idle, n.mi.
ISA	ICAO Standard Atmosphere
K	interpolation factor computed for speed-iteration purposes
K_g	coefficient in rate of change of altitude due to wind gradient equation, (ft/sec)/knots/ft
K_{gw}	gross-weight multiplication factor for altitude rate
$K_{\dot{h},XO}$	substitution variable in DME→H routine
$K_{\dot{h},250}$	substitution variable in segment 2 computation
Δl_j	length of path segment j, n.mi.
l_t	distance between entry fix and metering fix, n.mi.
Δl	distance increment, n.mi.
M	Mach number
M/IAS	Mach number and indicated airspeed
$M/IAS_{d,initial}$	initial Mach number and indicated airspeed for speed-iteration computations, knots
MF	metering fix
MF_{DME}	DME indication of metering fix, n.mi.
MSL	mean sea level
M_c	cruise Mach number
M_d	descent Mach number
$M_{d,initial}$	initial descent Mach number for speed-iteration purposes
N	number of wind data points
N_{reg}	storage register number
N_{seg}	segment number
N_{sub}	subroutine number
OAT	outside air temperature, °C
S_w	wind speed, knots
$S_{w,h}$	wind speed evaluated at altitude h, knots
$S_{w,s}$	wind speed computed for sea-level altitude, knots
dS_w/dH	wind speed gradient with respect to altitude H, knots/ft
TAS	true airspeed, knots
TAS_{av}	average true airspeed, knots
TAS_f	final true airspeed of level flight segment, knots
TAS_i	initial true airspeed of level flight segment, knots
TRK	airplane magnetic track angle along ground, deg
TSRV	Transport Systems Research Vehicle
T_c	temperature measured at cruise altitude, K
$T_{ISA,c}$	International Standard Atmospheric temperature at cruise altitude c, K

$T_{ISA,H}$	International Standard Atmospheric temperature at altitude H, K
T_o	standard sea-level air temperature, K
T'_o	nonstandard sea-level air temperature, K
$T_{st,c}$	static air temperature measured at cruise altitude, K
$T_{st,H}$	static air temperature at altitude H, K
T_{trop}	static air temperature at tropopause, K
ΔT	difference between actual temperature and standard temperature, K
t	time, sec
t_E	time error for descent speed convergence criterion, sec
$t_{E,initial}$	initial time error, sec
t_{EF}	time that entry fix was crossed, hr:min:sec
t_{IDL}	crossing time of point at which throttles are reduced to flight idle, hr:min:sec
t_{MF}	metering-fix crossing time, hr:min:sec
Δt	time increment, sec
$\Delta t_{initial}$	time required to fly initial descent profile, sec
Δt_j	time required to fly on path segment j, sec
Δt_{req}	time required to fly between entry fix and metering fix, sec
VAR	magnetic variation in descent area, deg
V	indicated airspeed used in flow chart
V_f	final speed of level flight segment, knots
V_i	initial speed of level flight segment, knots
W_c	difference between actual and computed ground speeds at cruise altitude, knots
$W_{H,h}$	head-wind component along airplane ground track evaluated at altitude h, knots
W_{H,h_c}	head-wind component along airplane ground track in cruise, knots
$W_{H,h_{MF}}$	head-wind component along airplane ground track at metering fix, knots
X	distance variable in DME→H routine, n.mi.
X_{DME}	input DME reading used in DME→H routine, n.mi.
$\ddot{x}$	acceleration, knots/sec
Y_1, Y_2, Y_3	substitution variables used in DME→H routine

Airport abbreviations:

BDL	Bradley International, Windsor Locks, Connecticut
BOS	Logan International, Boston, Massachusetts
DEN	Stapleton International, Denver, Colorado
EWR	Newark International, Newark, New Jersey
HNL	Honolulu International, Honolulu, Hawaii
LAX	Los Angeles International, Los Angeles, California
ORD	O'Hare International, Chicago, Illinois
SFO	San Francisco International, San Francisco, California

Description of Flight-Management Descent Algorithm

Description of General Profile

The flight-management descent algorithm computes the parameters required to describe a seven-segment cruise and descent profile (fig. 1) between an arbitrarily located entry fix and an ATC-defined metering fix. The descent profile is computed based on empirical modeling of airplane performance for an idle-thrust, clean-configured descent. The descent Mach/airspeed schedule, airplane gross weight, wind, wind gradient, and nonstandard temperature effects are also considered in these calculations.

Figure 1 shows the vertical-plane geometry of the path between the entry fix and the metering fix. Each path segment, starting at the metering fix, is numbered according to the order in which it

is calculated by the algorithm. To be compatible with standard airline operating practices, the path is calculated based upon the descent being flown first at a constant Mach number with a subsequent transition to a constant indicated airspeed and with all speed reductions made in level flight.

The first segment traversed on the profile is segment 7, which begins at the entry fix and is flown at constant cruise altitude and Mach number. Segment 6 is a relatively short, level-flight path segment in which the pilot reduces thrust to flight idle so that the airplane will slow from the cruise Mach number to the descent Mach number. Segment 6 is eliminated if the descent and cruise Mach numbers are the same. Once the descent Mach number is attained, the constant Mach descent segment (segment 5) is started. As altitude is decreased along this path segment, the indicated airspeed will increase because of increasing air pressure. Segment 4 begins when the desired indicated airspeed is attained for descent. The descent is continued along this segment at the desired, constant indicated airspeed. When the metering-fix altitude has been reached, the airplane is flown at a constant altitude along segment 3 and is slowed from the descent airspeed to the designated airspeed over the metering fix. Segments 1 and 2 are not computed.

If the metering fix is below 10 000 ft MSL and the descent airspeed flown on segment 4 is greater than 250 knots, the airplane must be slowed to comply with an ATC-imposed speed limit of 250 knots below 10 000 ft MSL. In this case, segments 1 and 2 are computed as depicted in figure 1. Segment 3 then becomes a level-flight segment at 10 000 ft MSL in which the airspeed is reduced to 250 knots. The descent is then continued at 250 knots along segment 2. When the metering-fix altitude has been reached, the airplane is flown at a constant altitude along segment 1 and is slowed from 250 knots to the designated airspeed over the metering fix. Path segment 1 is not computed if the metering-fix crossing airspeed is also 250 knots.

The flight-management descent algorithm can be used in either of two modes. The first mode was designed for time-metered operations. In this mode, instead of specifying the M/IAS descent schedule, the pilot enters the time that the entry fix was crossed and the metering-fix arrival time that was assigned by ATC. The descent profile is then calculated based on an M/IAS descent schedule, which is computed through an iterative process, that will closely satisfy the crossing time specified for the metering fix. During this iterative process, the Mach number used for the descent is set equal to the cruise Mach number in an effort to reduce computational requirements and operational complexity. The airspeed is adjusted to satisfy the time constraints. A check is made within the profile computations to ensure that the descent airspeed IAS_d is within the minimum and maximum speed limits for the particular airplane modeled. For the DC-10 airplane, these limits were

$$220 \leq \mathrm{IAS}_d \leq 350 \quad \text{[knots]}$$

An additional constraint was that IAS_d would not be less than the airspeed at which the airplane was to cross the metering fix. This eliminated the need to accelerate the airplane to a higher airspeed, which results in greater fuel usage. If the ATC-assigned metering-fix crossing time requires a descent airspeed less than the airplane minimum descent airspeed limit, the profile is computed based on the minimum airspeed limit and a message is displayed to the pilot to "hold" (delay) for the required amount of time. A similar "late" message is displayed with the time error if a descent airspeed schedule greater than the maximum allowed is required.

The second mode is called the speed mode. In this mode the pilot must enter the desired M/IAS to be flown during descent. The descent profile is then computed, based on this descent speed schedule, without consideration of a constraint on metering-fix arrival time. This mode would be used when time-based metering is not being used.

Logic Flow of Profile Descent Algorithm

Figure 2 shows the general logic flow of the profile descent computations. Pilot inputs used to compute the profile may be entered prior to flight and modified, as required, prior to the descent. These parameters include cruise altitude and Mach number, airplane gross weight, outside air temperature, wind velocity at various altitudes selected by the pilot, entry-fix and metering-fix descriptions, and the course direction to the metering fix. In addition to these parameters, the pilot may enter either a particular Mach number and indicated airspeed to be used during the descent or the entry-fix crossing time and the ATC-assigned metering-fix crossing time.

If the M/IAS descent speed schedule has been entered in the calculator, the computations will be based on a nonmetered traffic environment. The pilot initiates the computations by pushing the "compute" key. The descent profile is then computed in a single iteration, and the point where thrust should be reduced to flight idle to start the descent is indicated as a DME distance on the calculator display.

If the entry-fix crossing time and the ATC-assigned metering-fix crossing time have been entered in the calculator, the time required to fly between the fixes Δt_{req} will be computed and subsequent calcu-

lations will be based on a time-metered traffic environment. Once the pilot has initiated the computations by pushing the "compute" key, an iterative process is started to determine an appropriate IAS descent speed that will satisfy the time constraints. The Mach number used for the descent is set equal to the cruise Mach number in an effort to reduce computational requirements and operational complexity.

The iterative process starts with the computation of the time to fly from the entry fix to the metering fix $\left(\sum_{j=1}^{7} \Delta t_j\right)_{\text{initial}}$ at the following descent speed schedule:

$$M_{d,\text{initial}} = M_c$$

$$\text{IAS}_{d,\text{initial}} = \begin{cases} 280 & \text{[knots]} \quad (\text{if } \text{IAS}_{\text{MF}} \leq 280) \\ \text{IAS}_{\text{MF}} & \text{[knots]} \quad (\text{if } \text{IAS}_{\text{MF}} > 280) \end{cases}$$

The $\text{IAS}_{d,\text{initial}}$ value of 280 knots is used because it is the approximate midpoint between the maximum and minimum allowable descent airspeeds and because it is a descent speed typically used by the airlines.

A check is made with the following transition-time inequality to determine if the time-convergence criterion t_E has been satisfied. (For the purposes of these tests, $t_E = 5$ sec.)

$$\left|\Delta t_{\text{req}} - \sum_{j=1}^{7} \Delta t_j\right| \leq t_E \qquad \text{[sec]}$$

where

$$\Delta t_{\text{req}} = t_{\text{MF}} - t_{\text{EF}} \qquad \text{[sec]}$$

If this inequality is satisfied, the computations are complete and the idle-thrust descent point is displayed to the pilot. If the inequality is not satisfied, the descent computations will be repeated by using the operational airspeed limits as follows:

$$M_d = M_c$$

$$\text{IAS}_d = \begin{cases} 350 & \text{[knots]} \quad \left(\text{if } \Delta t_{\text{req}} < \left(\sum_{j=1}^{7} \Delta t_j\right)_{\text{initial}}\right) \\ \text{IAS}_{\text{MF}} & \text{[knots]} \quad \text{otherwise} \end{cases}$$

A check is then made to determine if the time criterion has been satisfied or if a speed greater than 350 knots or less than IAS_{MF} would be required to satisfy the time constraints. If the time criterion is satisfied, the idle-thrust descent point is displayed to the pilot. If either the upper or lower airspeed limit must be violated to satisfy the time constraints, the appropriate speed limit will be used in the descent computations and the resulting time error for crossing the metering fix will be displayed to the pilot.

If the time criterion has not been satisfied and neither the upper nor lower airspeed limitation will be violated, a revised descent airspeed IAS_d and associated descent time will be computed and compared with Δt_{req}. This iterative process will continue until the time-convergence criterion has been satisfied.

The computation of the revised IAS_d is graphically depicted in figure 3, which shows a plot of the time required to fly between a specified entry fix and metering fix at a specified cruise Mach number over the complete IAS_d range of the airplane. The descent airspeed is revised through a modified linear interpolation of the desired Δt_{req} within a range of time bounded by an initial value and a computed variable value. The initial value $\left(\sum_{j=1}^{7} \Delta t_j\right)_{\text{initial}}$ was the resulting time computed with the $M/\text{IAS}_{d,\text{initial}}$ descent speed schedule on the first iteration. The variable time value $\left(\sum_{j=1}^{7} \Delta t_j\right)_{i-1}$ is the time computed for the $M/\text{IAS}_{d,i-1}$ descent speed schedule on the last $(i-1)$ iteration. The revised descent speed schedule $M/\text{IAS}_{d,i}$ is computed as follows:

$$M_d = M_c$$

$$\text{IAS}_{d,i} = \text{IAS}_{d,\text{initial}} + (\text{IAS}_{d,i-1} - \text{IAS}_{d,\text{initial}})K - \frac{\text{IAS}_{d,i-1} - \text{IAS}_{d,\text{initial}}}{\left(\sum_{j=1}^{7} \Delta t_j\right)_{\text{initial}} - \left(\sum_{j=1}^{7} \Delta t_j\right)_{i-1}} \times 5\sin(180K) \qquad \text{[knots]}$$

where

$$K = \frac{\left(\sum_{j=1}^{7} \Delta t_j\right)_{\text{initial}} - \Delta t_{\text{req}}}{\left(\sum_{j=1}^{7} \Delta t_j\right)_{\text{initial}} - \left(\sum_{j=1}^{7} \Delta t_j\right)_{i-1}}$$

and i is the ith iteration.

The last term of the computations for $\text{IAS}_{d,i}$ is a compensation factor for the difference in curvature between the plot of time required to fly between the entry fix and the metering fix as a function of descent airspeed and the straight line used in the linear interpolation.

The following numerical example will illustrate the interpolation process. The entry fix is crossed at an altitude of 37 000 ft and at a cruise Mach number of 0.81. ATC has assigned a metering-fix crossing time for 15 min (900 sec) later at an altitude of 8000 ft and at an airspeed of 280 knots.

An initial airspeed of 280 knots has been programmed into the interpolation routine. At this

speed, 934.8 sec are needed to fly this profile. Since the ATC time required to fly the profile is 900 sec, the maximum limit airspeed of 350 knots is chosen by the calculator for the second iteration. The time needed to fly the profile with a descent airspeed of 350 knots was computed to be 842.5 sec.

An interpolation for the next descent airspeed can now be made between the speed and time points of 280 knots and 934.8 sec and of 350 knots and 842.5 sec, respectively. A simple linear interpolation between these points for 900 sec results in a speed of 306.4 knots. However, when the compensation factor term is applied to correct for the straight-line interpolation effects, a slightly lower airspeed of 302.9 knots is obtained for further computations.

At a descent airspeed of 302.9 knots, 890.2 sec is needed to fly the profile. Since this exceeds the 5-sec time-convergence criterion (900 − 890.2 = 9.8 sec), another iteration is necessary to select a new descent airspeed. A linear interpolation between the speed and time points of 280 knots and 934.8 sec and of 302.9 knots and 890.2 sec, respectively, results in an airspeed of 297.9 knots for a time of 900 sec. A slightly lower airspeed of 296.2 knots is obtained after the compensation factor term is applied. The time needed to fly the profile with a descent airspeed of 296.2 knots is 901.4 sec. This satisfies the 5-sec time criterion (900 − 901.4 = −1.4 sec) and completes the iteration process. The descent airspeed displayed to the pilot is 296 knots.

Empirical Representation of Airplane Performance Characteristics

Computer memory limitations with the programmable calculator preclude the use of detailed aerodynamic and performance tables to represent the airplane for profile descent calculations. Instead, an empirical model of the performance of the DC-10 airplane was developed from flight data collected during idle-thrust, clean-configured descents and during level-flight speed reductions.

A portable voice recorder, a stop watch, and conventional flight instruments were used to collect data for descent performance modeling. Altitude, speed, temperature, and time were recorded at altitude increments of approximately 500 ft during the descents. Speed, temperature, and time were recorded at 10-sec intervals during constant-altitude speed changes. Gross weights were recorded at the beginning and end of each test run.

Constant IAS descent model. The performance model for the constant indicated airspeed descents consisted of linear approximations of vertical speed as a function of an approximated geopotential altitude for a range of airspeeds between 220 and 350 knots. The vertical speed was adjusted to compensate for variations in gross weight.

The first step in the development of the vertical performance model for constant IAS_d was to approximate, for each descent, geopotential altitude as a function of time as a quadratic equation through a least-squares curve-fit analysis. The general form assumed for this equation was

$$h = a_2 t^2 + a_1 t + a_0 \qquad \text{[ft]}$$

Figure 4 shows a typical plot of the data and resulting curve fit for a descent flown at a constant IAS_d of 280 knots.

Vertical speed was determined by differentiating this equation with respect to time. This resulted in an equation of the form

$$\dot{h} = 2a_2 t + a_1 \qquad \text{[ft/sec]}$$

A plot of $\dot{h}$ as a function of h was then developed for each descent. Figure 5 shows typical data for various descent speeds. These plots indicated that vertical speed was approximately linear as a function of geopotential altitude and were modeled with an equation of the form

$$\dot{h} = b_1 h + b_0 \qquad \text{[ft/sec]}$$

The slope b_1 was approximately the same for all descent speeds and was equal to -3.5×10^{-4} (ft/sec)/ft. The modeled vertical speed at sea level b_0 was corrected for gross-weight variations by dividing by the gross-weight multiplication factor K_{gw} (to be discussed subsequently). The b_0 data varied exponentially as a function of descent airspeed. A plot of these data with the exponential model of b_0 is shown in figure 6.

The vertical-speed model was also adjusted with a correction factor $\dot{h}_g$ due to head-wind gradient (to be discussed subsequently) to account for changes in the vertical speed due to head-wind component variations during the descent. The resulting model of vertical speed, for a DC-10 airplane, corrected for gross-weight variations and head-wind gradient effects, was

$$\dot{h}_{IAS_d} = (-3.5 \times 10^{-4})h + K_{gw}[\dot{h}_g - 3.07783 \exp(8.158681 \times 10^{-3} \times IAS_d)] \qquad \text{[ft/sec]}$$

Constant Mach number descent model. The performance model for constant Mach number descents consisted of parabolic approximations of vertical speed as a function of approximated geopotential altitude for a range of Mach numbers between 0.73 and 0.85. The vertical speed was adjusted to compensate for variations in gross weight.

The procedures used to develop the descent model for constant Mach number were similar to those used for development of the model for constant IAS descents. A quadratic equation for altitude as a function of time was derived for each descent through a least-squares curve-fit analysis. These equations were differentiated with respect to time to determine vertical speed as a function of time. The vertical speed was adjusted for gross-weight variations by dividing by the gross-weight correction factor K_{gw} (to be discussed subsequently).

The vertical speed $\dot{h}$, adjusted for gross-weight variation, was then plotted as a function of altitude. Typical plots of these data are shown in figure 7. The resulting curves were parabolic in nature and were modeled with an equation of the following form:

$$\dot{h}'_{M_d} = -[(h - c_1)/c_0]^{1/2} \qquad \text{[ft/sec]}$$

The magnitude of the coefficient c_0 was subjectively selected based on the shape of a generic parabola that would overlay the descent data. A value of $c_0 = -1.85$ sec^2/ft was selected and resulted in the parabola shown by the dashed line in figure 7.

The coefficient c_1 was calculated for each descent at an altitude approximately 2000 ft below cruise altitude for $c_0 = -1.85$ sec^2/ft. The resulting values for c_1 are plotted as a function of the descent Mach number in figure 8. A linear regression analysis resulted in an equation of c_1 as a function of the Mach number. However, the slope of this model was increased slightly to ensure that c_1 would be greater than the maximum cruise altitude of the airplane (defined by the altitude limits shown in fig. 8), thus ensuring that an imaginary root would not be obtained from the equation for $\dot{h}_{M_d}$. The maximum altitude limits are defined by the maximum operating altitude (42 000 ft) of the airplane and by the altitudes corresponding to a minimum airspeed of 220 knots for Mach numbers less than 0.79. The resulting model for c_1 is

$$c_1 = 25\,750M_d + 22\,167 \qquad \text{[ft]}$$

The correction factor $\dot{h}_g$ due to head-wind gradient was added to the descent-rate equation similarly as in the constant indicated airspeed case. The resulting equation for vertical speed for a constant Mach number descent was

$$\dot{h}_{M_d} = -K_{gw}\left[\frac{h - (25\,750M_d + 22\,167)}{-1.85}\right]^{1/2} - \dot{h}_g \qquad \text{[ft/sec]}$$

Acceleration performance model. Acceleration performance data were obtained for idle-thrust, clean-configured speed reductions on level flight paths for typical cruise and metering-fix altitudes. Indicated airspeed and time data were recorded during the speed reductions. The indicated airspeeds were converted to approximate true airspeeds to reduce computational requirements within the descent algorithm. Figure 9 shows a plot of approximate true airspeed, as a function of time, that resulted during speed reductions at various altitudes and gross weights. The average slope of each of these test runs was approximately the same. Hence, acceleration for the DC-10 airplane was modeled as constant and was approximated by

$$\ddot{x} = -1.3 \qquad \text{[knots/sec]}$$

Gross-weight variation. The effects of gross-weight variation on the descent performance of the airplane were accounted for with a single multiplication factor applied to the vertical performance models developed for both constant airspeed and constant Mach number descents. The multiplication factor K_{gw} is a linear, nondimensional expression.

The multiplication factor was derived for the DC-10 airplane by plotting the vertical speeds obtained during descents (conducted at the same indicated airspeed) against the gross weight of the airplane. Figure 10 shows the vertical speed at sea level as a function of gross weight for descents conducted at constant airspeeds of 250, 280, 300, and 340 knots. A linear curve fit was applied to the data points for the 280-knot descents since more descents were flown at this speed and since a wider range of gross weights existed in the data. This plot also shows that the model derived for the 280-knot descents may be shifted vertically (maintaining approximately the same slope) to overlay the descent data obtained at the other speeds. Since the same slope could be approximated for all airspeeds, changes to the vertical speed due to gross-weight variations were modeled independent of airspeed. The plot in figure 10 was then nondimensionalized by dividing the abscissa by 304 000 lb and the ordinate by -30.2 ft/sec (in which $b_0 = -30.2$ ft/sec at an airspeed of 280 knots and a gross weight of 304 000 lb). Nondimensionalization allowed the gross-weight variation model derived with the 280-knot descent data to be expressed in a

form useful for descents at any airspeed. The resulting multiplication factor K_{gw} for gross-weight variations was

$$K_{gw} = (-3.863133 \times 10^{-6})\text{GW} + 2.174392369$$

where

$$260\,000 \leq \text{GW} \leq 350\,000 \qquad \text{[lb]}$$

Head-wind gradient effect. The head-wind-gradient effect is an adjustment to the vertical-speed model required when the head-wind component of the airplane changes during an idle thrust, constant airspeed, or Mach number descent. If the head-wind component decreases during the descent, indicated airspeed will also decrease unless the pilot lowers the pitch angle of the airplane to maintain the airspeed. When the pitch angle is lowered, vertical speed will increase. Similarly, vertical speed must be decreased if the head-wind component increases during the descent.

The head-wind-gradient effect was quantified with an adjustment factor K_g computed from data obtained during a series of piloted descents with a DC-10 simulator. The idle-thrust descents were conducted at a constant indicated airspeed of 280 knots, at a gross weight of 300 000 lb, and in the presence of head-wind components that decreased 2, 3, and 10 knots per 1000 ft of descent. A quadratic regression analysis was applied to the data from each descent to obtain an equation for altitude as a function of time. The derivative of this equation resulted in a computed, smoothed vertical speed for each of the descents. The average vertical speed obtained for each of the descents with the wind gradients was then subtracted from the average vertical speed obtained during a descent with no wind gradient. The difference in vertical speed was divided by the magnitude of the wind gradient encountered during the descent. The results of these computations were then averaged to obtain a head-wind-gradient factor equal to a change in vertical speed of -1.28 ft/sec for a 1-knot decrease in head-wind component for each 1000 ft of change in altitude (i.e., $K_g = -1280$ (ft/sec)/knots/ft). The effect that the head-wind gradient had on vertical speed $\dot{h}_g$ could then be calculated based on the modeled wind and the cruise and metering-fix altitudes as shown in the following equation:

$$\dot{h}_g = K_g \frac{W_{H,h_c} - W_{H,h_{\text{MF}}}}{H_c - H_{\text{MF}}} \qquad \text{[ft/sec]}$$

Approximation of True Airspeed

It is necessary to determine true airspeed from both Mach number and calibrated airspeed, as required for each path segment, so that a head-wind component can be added to obtain ground speed for time calculations. True airspeed, as a function of Mach number and static air temperature $T_{\text{st},H}$, was defined by the following equation (ref. 4):

$$\text{TAS} = 38.96M(T_{\text{st},H})^{1/2} \qquad \text{[knots]}$$

True airspeed, as a function of calibrated airspeed and altitude h, was approximated with the following empirical equation:

$$\text{TAS} = \frac{\text{IAS}}{1 - (0.12 \times 10^{-4})h} \qquad \text{[knots]}$$

where

$$h \leq 42\,000 \qquad \text{[ft]}$$

$$220 \leq \text{IAS} \leq 360 \qquad \text{[knots]}$$

Wind Modeling Technique

A two-component linear wind model was used to represent the wind speed and the wind direction as functions of altitude. The coefficients of the wind model were computed via a linear regression analysis of data from winds-aloft reports and forecasts in the descent area. Winds-aloft data for the linear regression analysis were inserted through the calculator keyboard in a format similar to that used in standard aviation winds-aloft forecasts. Although wind speed and direction from only two altitudes were required to define a wind model, the pilot could choose to insert additional wind data based on both forecasts and pilot reports.

The magnitude of the wind speed and the direction of the wind defined by the linear wind model were computed for each segment of the profile based on the middle altitude of each segment. The following equations were used for these computations:

$$S_{w,h} = \frac{dS_w}{dH}\, h + S_{w,s} \qquad \text{[knots]}$$

$$D_{w,h} = \frac{dD_w}{dH}\, h + D_{w,s} \qquad \text{[deg]}$$

A head-wind component for each segment was computed automatically during the profile computations by multiplying the wind speed with the cosine of the angle between the airplane ground track and the wind direction. A head-wind-component correction factor, based on the actual winds encountered during cruise flight, could also be added to the wind model if the pilot determined it was necessary. The correction factor was obtained by first computing the term W_c, which was the difference between the actual

ground speed along the cruise segment (computed by the pilot) and the predicted ground speed based on the modeled winds and cruise Mach number. This term was assumed to be proportional to altitude and decreased linearly to 0 at sea level ($h = 0$). The corrected head-wind component $W_{H,h}$ used in the profile computations was defined by the following equation:

$$W_{H,h} = S_{w,h} \cos(D_{w,h} - \text{TRK}) + (h/h_c)W_c \qquad \text{[knots]}$$

where

$$\text{TRK} = \text{CRS} - \text{VAR}$$

Compensation for Effects of Nonstandard Atmospheric Temperature

Various flight instruments, including the Mach meter and the altimeter, are designed to display true indications in a standard atmosphere. However, standard atmospheric conditions are rarely encountered. This results in slight errors in speed and indicated altitude. The profile descent algorithm compensates for nonstandard temperatures as they affect the Mach number calculations and altimeter indications.

Nonstandard temperatures are computed by the algorithm based on a standard atmospheric temperature model with a bias correction based on the difference between the actual and the standard temperatures. The standard-temperature model is a two-segment linear profile defined as a function of altitude. This temperature model uses a slope equal to a temperature lapse rate of -1.978×10^{-3} °C/ft for altitudes below the tropopause ($H \leq 36\,152$ ft). At higher altitudes ($H > 36\,152$ ft), it was assumed that flight was being conducted within the tropopause where temperature remains constant with changes in altitude. The standard-temperature model is represented mathematically as

$$T_{\text{ISA},H} = 216.65 \qquad \text{[K]}$$

where $H > 36\,152$ ft and as

$$T_{\text{ISA},H} = 216.65 + (1.978 \times 10^{-3})(36\,152 - H) \qquad \text{[K]}$$

where $H \leq 36\,152$ ft.

The following bias correction ΔT, representing the difference between the actual temperature measured at cruise altitude T_c and the standard temperature for cruise altitude $T_{\text{ISA},c}$, is added to the standard atmospheric temperature profile to define static temperature $T_{\text{st},H}$ completely at any altitude H as follows:

$$\Delta T = T_c - T_{\text{ISA},c} \qquad \text{[K]}$$

$$T_{\text{st},H} = T_{\text{ISA},H} + \Delta T \qquad \text{[K]}$$

The static temperature is then used for conversion of Mach number to true airspeed.

Pressure altitudes H used to define the end points of each segment are corrected to approximate geopotential altitudes by multiplying the pressure altitude by a temperature ratio of nonstandard and standard sea-level temperatures (ref. 6) as follows:

$$h = H(T'_o/T_o) \qquad \text{[ft]}$$

The standard sea-level air temperature T_o is 288.15 K; the nonstandard sea-level air temperature T'_o is computed from the static temperature model for $H = 0$.

Computations of Descent Path

The point where the pilot is to reduce power to idle thrust to start the descent was defined by summing the distances required to fly segments 1 through 6. Each segment length was determined by first computing the required time to traverse the segment and then multiplying by the average ground speed computed for the segment. Times for the level-flight segments requiring airspeed or Mach reductions were determined by dividing the required speed change by the deceleration capability of the airplane. Times for the path segments requiring descents were determined from equations derived by integrating the equation of the vertical-speed model over the altitude change required. The average ground speed at which the airplane was to fly each segment was determined by summing the computed true airspeed and the head-wind component evaluated for each segment.

The cruise segment (segment 7) at level flight and constant Mach number had no influence on the location of the point where idle thrust was to begin. This segment was significant only during the time-metered mode and was used for the calculations to satisfy the time constraints. Segments 1 and 2 were computed only if the ATC-imposed limit of 250 knots indicated airspeed for flight below 10 000 ft MSL was applicable. The details of these calculations are presented in the following paragraphs.

M/IAS transition altitude. As the airplane descends at a constant Mach number, the indicated airspeed increases because of an increase in the air pressure. The altitude at which the desired descent airspeed is obtained is called the M/IAS transition altitude and defines the point at which the constant Mach segment ends and the constant IAS segment begins. The general equation for this transition altitude was determined by equating true airspeed

as a function of indicated airspeed and altitude, with true airspeed as a function of Mach number and altitude. Solving for altitude results in the following equation to define the altitude for transition of Mach number to indicated airspeed:

$$h_{XO} = 1.77675 \times 10^5 - \left[8.90046 \times 10^9 + (3.42936 \times 10^7)\frac{IAS_d}{M_d}\right]^{1/2} \quad [ft]$$

Segment 1. Path segment 1 is a level-flight segment on which the airplane is slowed from an indicated airspeed of 250 knots to the metering-fix crossing speed. If the metering-fix crossing speed is less than or equal to 250 knots, or if the metering-fix altitude is equal to or greater than 10 000 ft MSL, this segment is not computed. The equations for time and length in segment 1 are, respectively,

$$\Delta t_1 = \frac{IAS_{MF} - 250}{\ddot{x}[1 - (0.12 \times 10^{-4})h_{MF}]} \quad [sec]$$

where $\ddot{x} = -1.3$ knots/sec, and

$$\Delta l_1 = \left[\frac{(IAS_{MF} + 250)/2}{1 - (0.12 \times 10^{-4})h_{MF}} - W_{H,h_{MF}}\right]\frac{\Delta t_1}{3600} \quad [n.mi.]$$

Segment 2. Segment 2 is an idle-thrust descent flown at a constant 250 knots from 10 000 ft MSL to the metering-fix altitude. Segment 2 is not computed if the metering-fix altitude is equal to or greater than 10 000 ft MSL or if the descent speed IAS_d flown on segment 4 is 250 knots or less. The equations for time and length in segment 2 are, respectively,

$$\Delta t_2 = \frac{1}{C_I}\ln\left[\frac{h_{MF}C_I + K_{gw}(K_{\dot{h},250} + \dot{h}_g)}{10\,000 C_I \frac{T'_o}{T_o} + K_{gw}(K_{\dot{h},250} + \dot{h}_g)}\right] \quad [sec]$$

where

$$K_{\dot{h},250} = A_I e^{250 B_I} \quad [ft/sec]$$
$$A_I = -3.07783 \quad [ft/sec]$$
$$B_I = 8.158681 \times 10^{-3} \quad [knots^{-1}]$$
$$C_I = -3.5 \times 10^{-4} \quad [sec^{-1}]$$

and

$$\Delta l_2 = \left[\frac{250}{1 - (0.12 \times 10^{-4})h} - W_{H,h}\right]\frac{\Delta t_2}{3600} \quad [n.mi.]$$

where

$$h = [(10\,000 + H_{MF})T'_o/T_o]/2 \quad [ft]$$

Segment 3. Segment 3 is a level-flight segment on which the airplane is slowed from the descent speed IAS_d to the metering-fix crossing speed (or 250 knots if segments 1 and 2 are computed). The equations for time and length in segment 3 are, respectively,

$$\Delta t_3 = \frac{IAS_{MF} - IAS_d}{\ddot{x}[1 - [0.12 \times 10^{-4})h]} \quad [sec]$$

where $\ddot{x} = -1.3$ knots/sec, and

$$\Delta l_3 = \left[\frac{(IAS_d + IAS_{MF})/2}{1 - (0.12 \times 10^{-4})h} - W_{H,h}\right]\frac{\Delta t_3}{3600} \quad [n.mi.]$$

where

$$h = \begin{cases} h_{MF} & [ft] \quad \text{(if segments 1 and 2 are not computed)} \\ 10\,000\frac{T'_o}{T_o} & [ft] \quad \text{(otherwise)} \end{cases}$$

Segment 4. Segment 4 is an idle-thrust descent flown at a constant indicated airspeed IAS_d. The descent begins at the transition altitude h_{XO} and ends at the metering-fix altitude (or at 10 000 ft MSL, if segments 1 and 2 are computed). The equations for time and length of segment 4 are, respectively,

$$\Delta t_4 = \frac{1}{C_I}\ln\left[\frac{C_I H_{bod}\frac{T'_o}{T_o} + K_{gw}\left(A_I e^{B_I\,IAS_d} + \dot{h}_g\right)}{C_I H_{XO}\frac{T'_o}{T_o} + K_{gw}\left(A_I e^{B_I\,IAS_d} + \dot{h}_g\right)}\right] \quad [sec]$$

where

$$H_{bod} = \begin{cases} 10\,000 \quad [ft] & \text{(if segments 1 and 2 are computed)} \\ H_{MF} \quad [ft] & \text{(otherwise)} \end{cases}$$

and

$$\Delta l_4 = \left[\frac{IAS_d}{1 - (0.12 \times 10^{-4})h} - W_{H,h}\right]\frac{\Delta t_4}{3600} \quad [n.mi.]$$

where

$$h = [(H_{XO} + H_{bod})T'_o/T_o]/2 \quad [ft]$$

Segment 5. Segment 5 is a constant Mach descent flown at idle-thrust power settings. This segment begins at cruise altitude h_c and ends when IAS_d is attained at the transition altitude h_{XO}. The

equations for time and length of segment 5 are, respectively,

$$\Delta t_5 = \frac{2C_M}{K_{gw}} \left\{ \left(\frac{H_c \frac{T'_o}{T_o} - c_1}{C_M} \right)^{1/2} - \dot{h}_g - K_{\dot{h},XO} - \dot{h}_g \ln \left[\frac{K_{\dot{h},XO}}{\left(\frac{H_c \frac{T'_o}{T_o} - c_1}{C_M} \right)^{1/2} - \dot{h}_g} \right] \right\} \quad [\text{sec}]$$

where

$$K_{\dot{h},XO} = \left(\frac{H_{XO} \frac{T'_o}{T_o} - c_1}{C_M} \right)^{1/2} - \dot{h}_g$$

$$c_1 = M_d A_M + B_M \quad [\text{ft}]$$
$$A_M = 25\,750 \quad [\text{ft}]$$
$$B_M = 22\,167 \quad [\text{ft}]$$
$$C_M = -1.85 \quad [\text{sec}^2/\text{ft}]$$

and

$$\Delta l_5 = [38.96(T_{st,5})^{1/2} M_d - W_{H,h}] \frac{\Delta t_5}{3600} \quad [\text{n.mi.}]$$

where

$$h = [(H_c + H_{XO}) T'_o / T_o]/2 \quad [\text{ft}]$$

The static temperature $T_{st,5}$ and the head-wind component are evaluated at the average altitude between the cruise and transition altitudes.

Segment 6. Segment 6 is a level-flight speed change from the cruise Mach number to the descent Mach number. If the cruise and descent Mach numbers are the same, this segment is not computed. The equations for time and length of segment 6 are, respectively,

$$\Delta t_6 = 38.96(T_{st,c})^{1/2} \frac{M_d - M_c}{\ddot{x}} \quad [\text{sec}]$$

where $\ddot{x} = -1.3$ knots/sec, and

$$\Delta l_6 = \left[38.96(T_{st,c})^{1/2} \frac{M_c + M_d}{2} - W_{H,h_c} \right] \frac{\Delta t_6}{3600} \quad [\text{n.mi.}]$$

Segment 7. Segment 7 is the remaining path between the entry fix and the beginning of segment 6. The length of segment 7 is the difference between the total distance between the entry fix and metering fix l_t and the sum of the distances of the remaining six segments. The length is given as follows:

$$\Delta l_7 = l_t - \sum_{j=1}^{6} \Delta l_j \quad [\text{n.mi.}]$$

Segment 7 time Δt_7 is found by dividing the distance to be flown by the ground speed as follows:

$$\Delta t_7 = \frac{3600\ \Delta l_7}{38.96(T_{st,c})^{1/2} M_c - W_{H,h_c}} \quad [\text{sec}]$$

Input/Output Requirements

The data required for the profile descent equations are obtained from the preprogrammed calculator memory and from pilot entries through the keyboard shown in figure 11. Even though all the data necessary to compute the descent are entered prior to takeoff, these parameters may be updated during cruise to obtain more accurate results.

The wind data are entered through the keyboard and the wind model coefficients are automatically computed and stored in the proper memory locations. The wind data, correlated to altitude, are inserted in a data format similar to that found on an aviation weather forecast. To insert the wind data, the pilot must first push the key labeled "*", followed by the key labeled "*Wind". The display will request the altitude for the wind speed and direction data with the message "H=?FT". The altitude is keyed into the display and entered into memory by pushing the "New Entry" key. The calculator will then request the wind direction and speed with the message "DIR.SPD?". Wind direction and speed are keyed into the display and entered into memory by pushing the "New Entry" key. This process will be repeated until all wind data have been inserted in the calculator. The linear regression analysis will be completed after the pilot inserts a negative altitude to indicate that no more wind data will be inserted. The calculator will then display a "WIND IN" message.

The wind data used by the pilot to compute the wind model could contain some errors since that information is usually based on aviation forecasts that may not be current. A procedure was developed that allows the pilot to modify the wind model with a correction factor based on the difference between the computed and actual ground speeds along the cruise segment (segment 7). The computed ground speed used in the profile descent computations may be displayed by pushing the "*" key followed by the "*GSc" key. The difference between the displayed ground speed and the actual ground speed represents the wind modeling error along the magnetic course

of the airplane to the metering fix. If the ground speeds are different, the actual ground speed may be keyed into the display. Then, by pushing the "New Entry" key, the difference between the ground speeds is computed and stored in memory for use in subsequent descent and ground-speed computations.

The operational parameters affected by ATC constraints or pilot desires, and not accurately known until just prior to the start of descent, were designed to be single key inputs. To enter these data, the pilot presses the particular key dedicated to the parameter to be changed. After the key has been pressed, the display will show the name of the parameter and its current value that is stored in the calculator. Another numerical value may be keyed on the display and then stored in the proper memory location by simply pressing the "New Entry" key. If the current value shown is satisfactory, no more keyboard actions will be required for that parameter.

The operational parameters may be inserted in any order, or they may be changed at any time prior to initiating the descent calculations. When the magnitudes of the parameters are satisfactory to the pilot, the profile descent computations are initiated by pressing the "Profile" key. Computations typically require less than 2 min for completion in the time-metered mode of operation and approximately 25 sec in the nonmetered mode.

The operational parameters to be entered by the flight crew through the keyboard, as well as their symbology as presented on the keyboard and the display, are shown in table I.

If the descent speed schedule has been specified, a zero flag, indicating that the algorithm is in a speed mode, will be shown in the middle of the calculator display. While in the speed mode the entry-fix and metering-fix crossing times must remain unassigned. If these times are specified through the keyboard, the zero flag will not be shown and the algorithm will be in the time mode. While in the time mode the proper descent speed schedule will be computed and stored in the correct memory location for recall by the pilot.

When the computations are completed, the display will normally show the DME indication where thrust should be reduced to flight idle for the descent to the metering fix. It should be noted that the distance displayed is the point where an instantaneous thrust reduction and descent should be started. The pilot should start the descent 1 to 2 miles prior to the computed descent point to ensure that good passenger ride qualities are maintained during the transition to descent. If the assigned metering-fix crossing time cannot be attained in the time-metered mode because of airplane operational speed limitations, a message will be displayed indicating the amount of time required to delay (hold) before starting the descent or the amount of time that the airplane will arrive late at the metering fix.

After the profile descent computations have been completed, the value of any operational parameters, including those required for input, may be displayed by pressing the particular designated key on the keyboard. Parameters that may be displayed after the descent computations, and their designated names, are shown in table II.

Open-loop guidance in the form of desired altitude as a function of distance along the profile may also be computed by the pilot. This is accomplished by keying a DME mileage indication into the display and pushing the "DME→H" key. The desired altitude corresponding to that distance will then be computed and displayed to the pilot. The "DME→H" feature may be used as guidance throughout the descent.

A program flow chart showing the steps used in the algorithm computations is included in appendix A. It is in a generalized format and may be used to aid in programming the algorithm on any computer. The actual program listing used with the HP-41CV calculator is included in appendix B.

Flight Test Objectives

The flight tests consisted of two phases: (1) the performance-model validation phase, and (2) the operational evaluation phase. The objectives of the performance-model validation phase were to document the accuracy of the vertical performance model programmed into the calculator and to investigate the effect of variations in pilot technique on the arrival accuracy at the metering fix. These objectives were achieved by evaluating flight data in the form of time, speed, altitude, and DME indications. These data were recorded with a portable voice recorder on the flight segment between the entry fix and the metering fix.

The objectives of the operational evaluation phase were to determine if the concept of providing open-loop descent guidance with a small, hand-held electronic computing device was acceptable to the pilot and if the concept was operationally feasible in an airline cockpit environment. These objectives were achieved by using quantitative data as recorded in the performance-model validation phase and subjective data in the form of pilot comments and test observer notes.

Description of Airplane and Cockpit Instrumentation

The airplane type used during the flight tests

was a McDonnell Douglas DC-10-10 wide-body trijet commercial transport configured to carry 254 passengers. Flight tests were conducted on various DC-10-10 airplanes within the United Airlines fleet. The actual airplanes used in the tests were arbitrarily chosen. Even though all the DC-10 airplanes in the United Airlines fleet are powered by the same engines, rated at 39 300 lb takeoff thrust, certified maximum takeoff weight varied between 410 000 and 430 000 lb. In addition, some of the test airplanes had been aerodynamically modified to reduce drag.

Specific flight instruments used by the pilot to fly the descent included an airspeed indicator and Mach number meter combined in one instrument, an altimeter, and a digital DME indicator. The airspeed indicator, Mach meter, and altimeter were driven by an air data computer that corrected pitot-static system inputs for sensor-position error and angle-of-attack effects. Static air temperature was also computed by the air data computer and displayed digitally on the instrument panel. DME indications were displayed digitally to tenths of a nautical mile in both upper left- and right-hand corners of the horizontal situation indicator. If the inertial navigation system were used, distance to, or from, the next way point would be displayed in place of the DME indications.

Data Recording

A portable voice recorder and conventional flight instruments were used to collect data for descent performance and acceleration modeling. Altitude, Mach number, static air temperature, and DME readings were recorded at altitude increments of approximately 500 ft during the descents and at airspeed increments of approximately 10 knots during the idle-thrust, level-flight speed reductions. A stop watch was used to correlate the data with time during postflight analysis.

When the calculator was used to provide descent guidance, the contents of the calculator memory were printed with a portable printer after completing each descent. These data included all parameters inserted by the pilots and the results of intermediate computations that allowed reconstruction of the guidance computations for postflight analysis.

Flight notes were also recorded by the test conductor during the descents. These notes contained the resulting time and DME indication at which the metering-fix crossing altitude and airspeed were actually obtained, ATC instructions related to the descent, pilot comments, and other observations pertinent to the tests (i.e., turbulence, wind shear, and variations in pilot technique).

Test Procedure

Performance-model validation tests. During the model validation flight tests, the calculator inputs were made by either the flight crew or the NASA test engineers. The tests were conducted on selected line flights and coordinated with ATC in an effort to yield, to the extent possible, uninterrupted descents. The pilot was asked to fly a specified M/IAS speed schedule as accurately as possible, beginning the descent at the DME indication computed by the calculator.

Pilot-evaluation tests. During the pilot-evaluation tests, the subject pilots were given a briefing on the use of the descent calculator prior to the flight tests. During the tests, the subject pilots were asked to use the calculator in whatever manner they felt most useful. The NASA test engineers observed how the calculator was used and answered any questions about its use. The same subject pilots were used on 2 to 3 consecutive days on regular line flights to various large cities (Chicago, Denver, Boston, Newark, and Windsor Locks). Four to six descents were flown per subject pilot during both peak and off-peak traffic periods. There was no special ATC coordination during these tests. However, on some flights into Denver, a metering-fix crossing time (computed by the Denver Air Route Traffic Control Center enroute metering program) was given to the pilot by ATC. The metering-fix crossing time is normally retained for use by the ATC controller. When each subject pilot completed his series of descents, he was interviewed to obtain a subjective evaluation of the descent calculator.

Results and Discussion

Validation and Evaluation Criteria

The results of the performance-model validation and pilot-evaluation tests, as well as the results of a parametric sensitivity analysis conducted on the algorithm, were quantified in terms of the errors in time, altitude, and airspeed when the airplane crossed the metering fix and in terms of the time and distance required to achieve the desired metering-fix crossing altitude and airspeed. The results of the subjective evaluations by the subject pilots were summarized and are presented in a later section.

Parametric Sensitivity Analysis

A parametric sensitivity analysis was conducted to determine the effects that uncertainties in the magnitudes of the operational parameters input for the descent computations would have upon the time

and distance predictions for crossing the metering fix. This analysis was conducted by comparing the output (i.e., time and distance predictions) of the descent computations for a nominal case with the output of a descent profile constructed to reflect the flight path resulting from an off-nominal flight condition. Each off-nominal descent was constructed by using the predicted time and distance computed with the same inputs used for the nominal case, except for the specific input parameter to be examined. The descent profile computed for the off-nominal case was shifted so that the idle-thrust descent point computed for the off-nominal case corresponded to the DME indication computed for the nominal case. Then, the resulting time and airspeed errors for crossing the metering fix were calculated. The magnitude of each parameter examined in the sensitivity analysis was varied throughout a range of values that could typically be encountered.

Nominal case. The magnitudes of the parameters used to compute the nominal case were as follows:

Cruise altitude = 37 000 ft
Cruise Mach number = 0.830
Airplane gross weight = 304 000 lb
Outside static air temperature = −56.5°C (ISA at 37 000 ft)
Descent Mach number = 0.830
Descent airspeed = 280 knots
Metering-fix crossing altitude = 8000 ft
Metering-fix crossing speed = 230 knots
No wind
Entry-fix location = 100 n.mi. from metering fix

The following results were obtained from the profile descent computations by using the nominal inputs. Thrust was to be reduced to flight idle to start the descent 83.0 n.mi. from the metering fix. A constant Mach number of 0.830 was to be maintained during the descent until an airspeed of 280 knots was obtained. The 280-knot airspeed was to be maintained until reaching an altitude of 10 000 ft MSL. At 10 000 ft MSL, the airplane was to be slowed to 250 knots in level flight. After obtaining 250 knots, the descent was to be continued to 8000 ft MSL at which point the airplane would be flown at a constant altitude and slowed to 230 knots airspeed. The metering fix would be crossed as 230 knots was obtained. The time to fly from the idle-thrust point to the metering fix would be 802 sec.

The following parameters were varied in the sensitivity analysis: static air temperature, gross weight, Mach number, descent airspeed, wind magnitude, and wind gradient. The results of the sensitivity analysis, shown in figure 12 as plots of altitude error, airspeed error, and time error that would result when the airplane crossed the metering fix, are shown for the range of values computed for each parameter. The distance prior to or past the metering fix where the desired metering-fix altitude and airspeed were attained is also plotted.

Static-air-temperature sensitivity. Static air temperature is used in the descent computations to convert pressure altitude to an approximate geopotential altitude and to compute true airspeed (in knots) from Mach number. The effects of static-air-temperature error on the descent profile were calculated by biasing the nominal temperature profile through a range from 10°C warmer to 10°C colder than standard. Temperatures warmer than standard resulted in an increase in both geopotential altitudes and true airspeed; temperatures colder than standard resulted in decreases. The metering-fix crossing errors resulting from temperature errors are plotted in figure 12(a).

With a temperature profile 5°C warmer than standard, the increased altitudes and airspeeds would cause the metering fix to be crossed 9.8 sec early, at an airspeed 20 knots faster than desired. The desired crossing airspeed and altitude would be attained 1.2 n.mi. past the metering fix. For a temperature profile 5°C colder than standard, the desired crossing speed would be attained 1.1 n.mi. prior to the metering fix. The fix would be crossed 9.0 sec later than predicted. Although no altitude and airspeed error would occur with the colder temperature, extra fuel would be used to maintain altitude and airspeed.

Gross-weight sensitivity. The effects of gross-weight variations on the descent profile were calculated for a weight range from 270 000 to 350 000 lb. These weights represented the minimum and maximum landing gross weights, respectively, that would likely be encountered in routine operations. The metering-fix crossing errors resulting from variations in gross-weight errors are plotted in figure 12(b).

The descent parameter most significantly affected by gross-weight variations was the point at which thrust should be retarded to flight idle for beginning the descent. An airplane that was 3.3 percent (10 000 lb) heavier than that for the nominal case (304 000 lb) would require a path 2.6 n.mi. longer than that predicted for the descent, since it must be flown at a slightly higher lift/drag ratio (same indicated airspeeds) that would result in a shallower descent angle. The metering fix would be crossed 14.4 sec earlier and 20 knots faster than desired. The desired airspeed would be achieved 2.6 n.mi. past the fix. For the 10 000-lb lighter-than-nominal case, the

desired crossing speed and altitude would be achieved 2.5 n.mi. prior to crossing the metering fix. This would result in an arrival-time error of 12.1 sec late. Extra fuel would be used to maintain altitude and airspeed.

Mach number sensitivity. The effects of Mach number variations on the descent profile were calculated for two separate scenarios. In the first scenario, the cruise Mach number was constant and equal to 0.83 and the descent Mach number was varied for a range between 0.74 and 0.86. The metering-fix crossing errors resulting from these variations are plotted in figure 12(c). The variation in the descent Mach number yielded the least relative variation in the metering-fix crossing errors. This was due primarily to the relatively short duration of the Mach descent segment.

In the second scenario, both the cruise and the descent Mach number were biased by a 0.02 Mach increment faster and slower to represent an error in the Mach indicator on board the airplane. At the higher Mach number (0.85), the metering fix was crossed 8.9 sec early with an airspeed 15 knots higher than desired. The desired 230-knot airspeed was attained 1.0 n.mi. past the metering fix. At the lower Mach number (0.81), the metering fix was crossed 12.3 sec late. The desired airspeed and altitude were attained 1.2 n.mi. prior to the metering fix and were maintained at a cost of increased fuel.

Descent airspeed sensitivity. The effects of descent airspeed variations on the descent profile were calculated for an airspeed range between 230 and 350 knots. Metering-fix crossing errors were plotted in figure 12(d) for variations of airspeed at altitudes above 10 000 ft MSL. The distance error plot shows that variations in the descent airspeed resulted in corresponding changes in the distance required to attain the metering-fix crossing conditions. A 10-knot speed increase (290-knot descent airspeed) resulted in attaining the metering-fix conditions 3.0 n.mi. prior to crossing the metering fix; a 10-knot airspeed decrease, 2.9 n.mi. past the fix. The time error to cross the metering fix, when flown at the slower airspeeds, also resulted in a corresponding increase. (A 270-knot airspeed resulted in a 11.1-sec late time error.) However, when airspeeds higher than the nominal speed were used, time error was not significantly changed. (A 290-knot airspeed resulted in a 2.5-sec early time error.) This was caused by the fact that the metering-fix altitude and airspeed conditions were attained prior to crossing the metering fix. The additional time required to fly to the metering fix would then offset the time saved with the higher descent speed and would eventually result in crossing the metering fix later than desired, as shown in figure 12(d).

Wind modeling sensitivity. The effects of wind modeling errors were calculated first, by assuming a constant 20-knot error in the head-wind component for the entire flight path between the entry fix and the metering fix. These calculations were then repeated by assuming a 20-knot tail-wind error.

With an unknown 20-knot head wind, the resulting ground speed would be decreased proportionately and would result in a crossing-time error of 76.8 sec later than predicted. The desired airspeed and altitude for crossing the metering fix would be attained 4.5 n.mi. prior to the metering fix. Thrust would be required to maintain airspeed and altitude to the metering fix. With the 20-knot tail wind, the metering fix would be crossed 58.9 sec earlier than predicted, but with an airspeed 20 knots faster than desired. The desired final airspeed and altitude would be achieved 4.4 n.mi. past the metering fix.

It should be noted that the time error is accumulated both in the descent and cruise portions of flight between the entry and metering fixes. Hence, this time error will also be a function of distance between the fixes. If the time error incurred during the cruise portion is not considered, the time error for the head-wind case would be 71.1 sec late; and for the tail-wind case, 53.7 sec early.

The potential for significant errors occurring in wind modeling is high because of a constantly changing atmosphere and the vagaries of forecasting winds aloft. However, the wind modeling accuracy problem may be reduced if the pilot modifies the wind model based upon the winds actually encountered during the cruise portion of his flight through the cruise ground-speed function (*GSc key). By pushing the "*" and the "*GSc" keys, the ground speed will be computed for the cruise segment of flight based on the wind model in the calculator. If the computed and actual ground speeds are different, the actual ground speed can be entered into the calculator so that the wind model will be modified for subsequent computations. The wind model will be changed by summing an error component to the original wind model. The error component is equal to the difference in the computed and actual ground speeds, linearly decreased to 0 from cruise altitude to sea level.

Wind-gradient sensitivity. The effects of wind gradient (change in head-wind component due to a change in altitude) were calculated for a range of magnitudes between −4 knots/1000 ft (increasing head wind from cruise to the metering fix) and

4 knots/1000 ft (decreasing head wind from cruise to the metering fix). The wind gradients were input such that the average head wind from cruise to the metering fix was 0. The results of these changes are shown in figure 12(e).

The effect of an increasing head wind on the airplane as it descends is to lengthen the distance required to attain the metering-fix crossing conditions. This results in an early arrival at the metering fix at a higher airspeed than desired. The increased distance to descend is due to the shallowing of the flight path angle that is required to maintain the desired descent airspeed.

Performance-Model Validation Tests

The purpose of the initial flight testing and data analysis was to validate and refine the descent performance model used in the profile descent algorithm. Altitude, DME, airspeed, and temperature data were recorded continuously during the descent so that the flight profile could be reconstructed for postflight analysis. The same subject pilot flew each of the descents during this phase of the evaluation. The subject pilot also advised ATC that NASA fuel conservation tests were in progress and requested an unrestricted descent.

The criterion used to evaluate the performance that resulted with the open-loop guidance was the accuracy in terms of the descent time and the descent distance required to achieve the desired metering-fix altitude h_{MF} and airspeed IAS_{MF} and the accuracy in terms of the resulting time error when the metering fix was crossed. These errors are presented in table III. The mean and standard deviation for these errors are presented at the bottom of the table. The origin and destination airports and the M/IAS descent speed schedule for each test run are also shown in the table.

The time error associated with attaining the desired metering-fix airspeed and altitude was an indication of the accuracies with which the airplane descent performance data had been modeled and how closely the airplane had been flown on the predicted profile with the open-loop guidance. This particular form of time error was not affected by horizontal winds since it was a time associated with attaining airspeeds and altitudes that are air-mass referenced. However, wind-speed-gradient effects (the change in head-wind component due to a change in altitude) can have an effect upon this form of time error. Runs 10 and 16 are examples in which large time errors resulted in the presence of a known wind-speed gradient recorded from airborne, inertial navigation system data. The mean and standard deviation of the time error to attain the desired airspeed and altitude for the 19 test runs were 1.3 sec early and 22.4 sec, respectively, for descents lasting between 5 and 14.3 min. Based on these time errors, it was concluded that the airplane descent performance data were adequately modeled and that the time required to attain the desired airspeed and altitude could be adequately predicted with the open-loop guidance provided by the Mach and airspeed indicators.

The distance error that resulted while attaining the desired metering-fix speed and altitude and the time error associated with crossing the metering fix were indicators of the same error components associated with the descent time error discussed previously and, in addition, indicators of the accuracy of wind modeling. The resulting mean and standard deviation for the distance error for these test runs were 2.3 n.mi. past the metering fix and 2.3 n.mi., respectively. The mean and standard deviation for the crossing-time error at the metering fix were 24.4 sec early and 28.3 sec, respectively. These errors are consistent (i.e., approximately 1/2 min is required to fly 2.3 n.mi. past the metering fix) and are referenced to Earth-fixed axes (i.e., the metering fix) and, as such, are affected by the wind. Since a much smaller time error to attain the desired altitude and airspeed (air-mass referenced) was achieved, it was concluded that the data inserted into the wind model may have been in error.

Experience obtained during the profile descent tests with the Advanced Transport Operating Systems TSRV Boeing 737 airplane (ref. 4) and with the NASA T-39A airplane (ref. 5) indicates that the linear wind model is sufficient to model the wind during the descent, provided that the model is based on reasonably accurate wind data. However, the winds-aloft weather forecast may be based on observations more than 12 hr old and, as such, may be subject to some error.

Variation in Pilot Technique

Variation in pilot technique in flying the descent can have an effect upon the crossing errors at the metering fix. Three phases of the descent were noted during these tests as having a significant impact on the crossing accuracy. They were the thrust reduction and the pitch rate used at the start of the descent, the pilot technique used to control the pitch attitude of the airplane during the constant Mach number descent segment, and the technique used to make the transition to the level flight on the speed-reduction segments.

It was initially assumed that the pilot would reduce the thrust to flight idle with a rather short deliberate action. However, in the interest of passenger

comfort, the pilot would gradually reduce the throttles over a 10- to 20-sec interval and would slowly decrease the pitch attitude of the airplane to begin the descent. In addition, all three throttles were seldom reduced in unison to avoid the simultaneous shifting of engine bleed air valves which causes loud noises in the pressurization system. Because of the gradual thrust reduction, it was found that some anticipation of the idle-thrust point was required for the throttles to be at idle at that point. The amount of lead distance required varied with the speed with which the pilot reduced the throttle. The method utilized by most pilots was to gradually reduce power to idle thrust on the left and right engines about 2 n.mi. prior to the computed idle-thrust descent point. After the left and right engines were reduced to flight idle, the center engine would be similarly reduced.

The second phase of the descent in which the metering-fix crossing accuracy could be affected was in the constant Mach number descent segment. To maintain a constant Mach number during an idle-thrust descent, the pitch attitude of the airplane must be continuously decreased as altitude is lost. As a result, cabin deck angles may become excessive for passenger comfort during high-speed descents. Some pilots approximated the constant Mach descent segment by flying a constant vertical-speed descent instead. If the airspeed that will be used in the constant airspeed descent segment is low, then the Mach segment will be short and the resulting errors small. If the constant airspeed segment is to be flown at higher airspeeds, the Mach segment will be longer and greater errors will accrue. As an example, from a cruise altitude of 37 000 ft, with a descent speed schedule of 0.830/280 knots, only 2600 ft must be lost during the constant Mach segment; with a descent speed schedule of 0.830/340 knots, 10 800 ft must be lost.

The last phases of the descent, in which piloting technique affected the vertical performance, were the level-flight deceleration segments at 10 000 ft and at the bottom of the descent. If the pilot gradually decreased the descent rate, by beginning 1000 to 2000 ft above the level-flight altitude to achieve a gradual transition to level flight, the distance required to decelerate from the descent speed to the metering-fix crossing speed was longer than if the pilot chose to descend slightly below the level-flight altitude and gradually climb back up to it. The pilot could use either of these techniques to null distance or time error.

Pilot-Evaluation Test Phase

Five subject pilots were briefed on the use of the calculator during the pilot-evaluation phase of the tests. Each pilot participated in four, or more, descents while using the calculator. Twenty-two descents were completed during the pilot-evaluation phase of the tests.

The flight test results achieved during this phase are presented in table IV. These results include the metering-fix crossing errors that were defined as the difference between the actual and the computed crossing time, altitude, and indicated airspeed. Also tabulated were the origin and destination airports, the airport arrival time, if ATC altered or constrained the descent clearance, if the calculator was unusable, if the pilot used an M/IAS speed schedule or the DME$\rightarrow H$ feature for descent guidance, and remarks about any anomalies incurred during the descent.

Each subject pilot followed the same general procedures when using the calculator. Preliminary inputs to the calculator were made prior to takeoff from a computerized flight plan normally provided by the company flight dispatcher. Data from the computerized flight plan input to the calculator included an estimated gross weight, cruise altitude, cruise Mach number, winds-aloft forecast, and outside air temperature. The pilot would estimate altitude and airspeeds to cross the metering fix based on previous flight experience at the destination airport. The pilot would then compute a preliminary descent profile. He would update the input parameters later in the flight and recompute the descent profile as required. The final descent profile would typically be computed 150 to 200 n.mi. from the metering fix. However, on several occasions during this phase of the test, to satisfy ATC constraints, the pilot was required to reprogram the calculator just prior to the top-of-descent point and during the descent.

The mean and standard deviation of the crossing errors at the metering fix are shown at the bottom of table IV. Except for the mean time error at the metering fix, the crossing errors were larger than those obtained during the performance-model validation tests because of ATC clearance changes. Only 6 of the 22 runs were completed without receiving an amended ATC clearance. Amended clearances received during the descent were more difficult to modify on the calculator than those received prior to the descent. On four of the descents, the calculator was not used at all because of numerous ATC clearance changes received throughout the descent. On five of the descents, the guidance provided by the calculator was used for only a portion of the descent because of ATC requests for spacing and sequencing.

Data in the calculator were modified by the pilot just prior to the descent to accommodate amended ATC clearances on six of the descents. However,

some of the amended clearances did not require data modification. As an example, if the pilot was told to descend early to an intermediate altitude, the pilot would descend to, and remain at, the intermediate altitude until he had reacquired the original profile as determined from the DME→H feature. The idle-thrust descent would then be continued by using the guidance provided by the calculator.

If an amended ATC clearance were received in enough time prior to the top-of-descent point, the flight crew could modify the data in the calculator and then the full benefits of fuel conservation from use of the guidance could be obtained. Amended clearances received after the descent has begun may, or may not, preclude the use of the guidance provided by the calculator. However, amended clearances received after the descent has begun will almost always result in more fuel being used. Amended ATC clearances may be necessary for safe and expeditious movement of airplanes in a very dynamic environment. It was noted, however, that an amended clearance was received on only one of the descents during the performance-model validation tests during which the pilot told ATC that fuel-conservation tests were in progress.

The time mode of the calculator was used on only three of the descents during the pilot-evaluation test phase. All these descents were into Denver since this was the only destination terminal of the various flights actively using time-based metering. On these flights the pilot input the actual time that the airplane crossed an arbitrary entry fix (typically about 130 n.mi. from the metering fix) and the metering-fix crossing time assigned by ATC. The pilot would then start the computation of the descent profile. The computations typically required about 2 min to complete.

On two of the three time-metered flights, the crossing-time accuracy was within ±6 sec. On flight 20, however, the pilot started the descent late and used a higher descent speed in an attempt to reacquire the computed descent profile. Even though the altitude error was nulled, the metering fix was crossed 50 sec earlier than desired and 35 knots faster than planned.

On seven descents, the pilot used the M/IAS speed schedule provided by the calculator as the primary descent guidance. On 11 of the descents, the altitude profile generated by the calculator through the DME→H function was used as the primary descent guidance. When the DME→H function was used, one of the nonflying crew would operate the calculator and call out the altitudes corresponding to upcoming DME indications. When this form of guidance was used instead of maintaining an M/IAS descent speed schedule, slightly earlier arrival times at the metering fix resulted. These results occurred because the airplane was typically initially high on the computed vertical profile since the pilots would make the transition from cruise flight into the descent slowly because of passenger ride-comfort considerations. As the pilot increased the vertical speed of the airplane to correct back to the vertical profile, a higher airspeed would result. If the airplane were below the computed profile, it would be expected that the metering fix would be crossed at a later time.

Pilot Comments

Each pilot was interviewed at the conclusion of the series of descents to obtain a subjective evaluation of the descent calculator concept. All subject pilots in general derived the same consensus. A compendium of the pilot comments is as follows:

1. The work load required to operate the calculator was acceptable provided that major modifications to the data were not required during the descent. The pilots felt that the use of the calculator did not interfere with their normal flight duties or ever compromise safety.

2. All the pilots felt that some training period would be required to use the calculator operationally. All but one of the pilots felt that the calculator was much easier to learn to operate than an inertial navigation system.

3. Most of the pilots felt that they could plan the descent as well by using various rules of thumb for their standard airline-policy M/IAS descent. However, for descents at other than standard M/IAS speed schedules or for time-metered descents, the calculator was very useful.

4. All the pilots felt that the guidance provided by the DME→H function was very useful.

5. Even though no operational problems due to the computation speed were encountered during these tests, it was felt that the computation time should be reduced, especially for the time-metered computations.

6. Some of the pilots wanted to be able to recall the wind data that was input so that key-punching errors could be rechecked and corrected. With the present software configuration, wind inputs can be checked only prior to pushing the "New Entry" key.

7. All the pilots felt that the display was difficult to read at night in reduced lighting. This is typical of all liquid-crystal displays that are not backlighted.

Suggested Modifications

During the flight tests, situations arose which highlighted areas in which design improvements to

the descent calculator could enhance its use. The following is a list of features which should be considered in any future design of a descent planning calculator:

1. The DME distance term presently used in the DME→H function represents the distance between the airplane and the DME ground station parallel to the Earth's surface. The DME indication in the airplane represents the distance directly between the airplane and the DME ground station (called slant range). The difference between the horizontal distance and the slant range distance should be included in the algorithm so as to yield a more accurate altitude computation.

2. The altimeter setting of the destination airport should be included in the calculator inputs so that a correction for the change in the indicated altitude can be accounted for when changing from a pressure altitude setting to a corrected altimeter setting.

3. The wind data used in generating the wind model should be stored so that they can be reviewed and modified.

4. The display should be lit so that it is readable in a reduced-lighting environment.

5. The computation time should be reduced. This could be accomplished by using a small portable computer rather than a programmable calculator to exercise the algorithm.

6. A function to compute the DME reading(s) corresponding to a given altitude should be included as an alternate form of guidance to the DME→H function (which provides the altitude corresponding to a given DME reading).

7. A function to compute the desired time corresponding to a DME distance input (similar to the DME→H function) should be included.

8. A revised temperature model that can account for nonstandard lapse rates and nonstandard troposphere altitudes may result in higher accuracy.

Concluding Remarks

A simple, airborne, flight-management descent algorithm, designed to aid the pilot in planning a fuel-efficient time-constrained descent, was programmed into a small programmable calculator. In a time-metered mode, the airborne algorithm computes the specific Mach number, airspeed, and point for the pilot to begin the descent to arrive at a metering fix at a predetermined airspeed, altitude, and time assigned by air traffic control (ATC). In the non-metered mode, the algorithm computes the point to begin the descent based on the Mach and airspeed descent schedule input by the pilot.

Flight test data obtained in an airline operational environment during normally scheduled flights indicated that the time and distance to descend could be satisfactorily predicted with the use of relatively simple equations and airplane-performance-characteristics modeling. The flight data also have shown that the descent profile could be satisfactorily flown with open-loop guidance provided by conventional cockpit Mach and airspeed indicators. However, pilot technique used to fly the descent can affect the accuracy of crossing the metering fix at the desired time.

The subject pilots commented that the use of the calculator to plan descents was particularly useful when nonstandard descent speeds were used or when the time to cross the metering fix had been assigned by ATC. They also found that the calculator did not interfere with their normal flight duties. Amended clearances received from ATC, after the descent had begun, precluded the use of the calculator for descent guidance when extensive modifications to the input data were required.

NASA Langley Research Center
Hampton, VA 23665
December 6, 1984

TABLE I. OPERATIONAL PARAMETERS REQUIRED FOR DESCENT COMPUTATIONS

Keyboard symbology	Display symbology	Operational parameter (symbol used in equations)
Mc	Mc	Cruise Mach number (M_c)
Hc	Hc	Cruise altitude (H_c), ft
*GSc	GSc	Ground speed at cruise altitude (GSc), knots
Md	Md	Descent Mach number (M_d)
IASd	IASd	Descent indicated airspeed (IAS_d), knots
Time MF	MF TM	Time assigned by ATC to cross metering fix (t_{MF}), hr:min:sec
Time EF	EF TM	Time to cross entry fix (t_{EF}), hr:min:sec
GW	GW	Airplane gross weight at top of descent (GW), lb
OAT	OAT	Static outside air temperature (OAT), °C
Metering Fix	H MF	Pressure altitude of metering fix (H_{MF}), ft
Metering Fix	IAS MF	Indicated airspeed to cross metering fix, (IAS_{MF}), knots
Metering Fix	MF DME	DME indication defining metering-fix location (MF_{DME}), n.mi.
Entry Fix	EF DME	DME indication defining entry-fix location; this mileage must be relative to same DME station used to define metering fix (EF_{DME}), n.mi.
Entry Fix	MAGCRS	Magnetic course from entry fix to metering fix (CRS), deg
Entry Fix	MAGVAR	Magnetic variation in descent area (VAR), deg

TABLE II. PARAMETERS COMPUTED BY DESCENT COMPUTATIONS

Keyboard symbology	Display symbology	Operational parameter (symbol used in equations)
Md	Md	Descent Mach number required to satisfy entry-fix and metering-fix time constraints (M_d)
IASd	IASd	Descent indicated airspeed required to satisfy entry-fix and metering-fix time constraints (IAS_d), knots
Idle DME	IDL DME	DME indication showing point where thrust should be reduced to flight idle (IDL_{DME}), n.mi.
2nd push of Idle DME	IDL TM	Incremental time to fly between entry fix and metering fix (Δt_{req}), sec
Late	LATE	Amount of time that airplane will be late in crossing metering fix, min:sec
Early	HOLD	Amount of time that airplane must delay before starting descent if crossing-time constraint at metering fix is to be satisfied, min:sec

TABLE III. TIME AND DISTANCE ERRORS TO ATTAIN METERING-FIX CONDITIONS DURING PERFORMANCE-MODEL VALIDATION TESTS

Run	Airport, origin—destination	M_d/IAS_d, knots	Descent distance to attain IAS_{MF} and h_{MF}, n.mi.			Descent time to attain IAS_{MF} and h_{MF}, sec			Time to cross metering fix, sec		
			Calculated	Actual	Error	Calculated	Actual	Error	Calculated	Actual	Error
1	ORD—DEN	0.730/250	68.3	70.1	−1.8	681	671	10	681	653	28
2	DEN—ORD	.710/250	81.4	84.7	−3.3	828	841	−13	828	799	29
3	ORD—DEN	.814/289	60.1	61.7	−1.6	538	540	−2	538	525	13
4	ORD—DEN	.830/296	60.0	60.0	0	540	535	5	540	535	5
5	DEN—ORD	.830/280	95.7	95.2	.5	867	836	31	867	844	23
6	ORD—DEN	.834/350	34.5	37.4	−2.9	300	298	2	300	273	27
7	DEN—LAX	.830/280	83.0	83.8	−.8	779	758	21	779	796	−17
8	LAX—DEN	.830/280	62.2	64.6	−2.4	526	540	−14	526	517	9
9	DEN—SFO	.820/280	70.8	76.0	−5.2	698	725	−27	698	660	38
10	SFO—HNL	.820/280	73.0	80.8	−7.8	716	752	−36	716	671	45
11	HNL—SFO	.820/280	97.2	97.8	−.6	898	860	38	898	852	46
12	SFO—DEN	.830/280	69.6	72.4	−2.8	567	605	−38	567	567	0
13	DEN—ORD	.820/280	73.9	78.4	−4.5	608	606	2	608	561	47
14	ORD—DEN	.820/280	61.1	59.0	2.1	555	565	−10	555	591	−36
15	DEN—SFO	.830/280	76.2	78.4	−2.2	692	700	−8	692	674	18
16	SFO—HNL	.800/280	55.3	59.9	−4.6	645	601	44	645	545	100
17	HNL—SFO	.830/320	70.2	71.9	−1.7	708	706	2	708	683	25
18	SFO—DEN	.830/280	65.4	69.0	−3.6	569	560	9	569	526	43
19	ORD—DEN	.830/280	64.9	65.9	−1.0	599	590	9	599	579	20
Mean					−2.3			1.3			24.4
Standard deviation					2.3			22.4			28.3

TABLE IV. PHASE II FLIGHT TEST RESULTS

Run	Airport origin—destination	Local airport arrival time, hr:min	Metering-fix crossing errors			ATC altered descent	Calculator was reprogrammed	Calculator was unusable	Descent was time metered	Primary guidance		Remarks
			Time (Early = +; Late = −), sec	Indicated airspeed (Fast = +; Slow = −), knots	Altitude (High = +; Low = −), ft					M/IAS	DME→H	
1	DEN—ORD	4:04 p.m.	85	40	0						X	Started descent late (1.0 n.mi.); flew higher airspeed to reacquire vertical profile.
2	ORD—BOS	8:17 p.m.	−6	15	0						X	
3	BOS—ORD	9:10 a.m.	18	40	600	X	X				X	ATC requested increase in airspeed; pilot maintained profile and added thrust; ATC later changed metering-fix altitude and location; calculator was reprogrammed accordingly.
4	ORD—DEN	11:43 a.m.	27	0	1400	X					X	ATC clearance to descend was 3.4 n.mi. past computed idle DME point; airplane was also held at intermediate altitude for traffic before being cleared for profile descent; pilot flew at faster airspeed to reacquire vertical profile.
5	DEN—ORD	4:04 p.m.				X		X				ATC changed clearance during descent too frequently to reprogram calculator.
6	ORD—BOS	8:17 p.m.	56	30	1200	X	X				X	ATC requested early descent to intermediate altitude; calculator was reprogrammed to reflect change; new descent started 5.9 n.mi. late; pilot flew at faster airspeed to reacquire vertical profile.
7	BOS—ORD	9:10 a.m.				X		X				ATC changed clearance during descent too frequently to reprogram calculator.

TABLE IV. Continued

Run	Airport origin—destination	Local airport arrival time, hr:min	Metering-fix crossing errors			ATC altered descent	Calculator was reprogrammed	Calculator was unusable	Descent was time metered	Primary guidance		Remarks
			Time (Early = +; Late = −), sec	Indicated airspeed (Fast = +; Slow = −), knots	Altitude (High = +; Low = −), ft					*M*/IAS	DME→*H*	
8	ORD—DEN	11:43 a.m.	6	5	1000	X			X	X		ATC requested decrease in airspeed midway through descent; calculator was not used after speed reduction.
9	ORD—BOS	2:44 p.m.	33	30	1000					X		
10	BOS—ORD	5:45 p.m.	−13	0	0	X	X			X		ATC requested early descent to intermediate altitude; calculator was reprogrammed accordingly.
11	ORD—EWR	2:40 p.m.	−52	0	0					X		Experienced large change in head wind during last third of descent.
12	EWR—ORD	5:40 p.m.	−21	0	−1000	X				X		ATC requested speed reduction and changed crossing restriction; pilot used speed brakes to increase descent rate.
13	ORD—DEN	8:10 p.m.	−47	0	0					X		Began descent off track because of ATC vectoring for spacing.
14	DEN—ORD	6:54 p.m.	13	5	−1000	X	X				X	ATC changed crossing restriction; calculator was reprogrammed; ATC requested speed increase.
15	BDL—ORD	12:18 p.m.	20	10	300	X	X				X	ATC changed metering fix midway through descent; calculator was reprogrammed; new vertical profile was acquired.
16	ORD—DEN	2:39 p.m.	21	−5	0	X	X				X	ATC requested speed reduction; calculator was reprogrammed; pilot held at intermediate altitude and idle thrust to slow and acquire new vertical profile.
17	DEN—ORD	10:50 p.m.				X		X				ATC changed clearance during descent too frequently to reprogram calculator.

TABLE IV. Concluded

Run	Airport origin—destination	Local airport arrival time, hr:min	Metering-fix crossing errors			ATC altered descent	Calculator was reprogrammed	Calculator was unusable	Descent was time metered	Primary guidance		Remarks
			Time (Early = +; Late = −), sec	Indicated airspeed (Fast = +; Slow = −), knots	Altitude (High = +; Low = −), ft					M/IAS	DME→H	
18	ORD—DEN	2:30 p.m.	−27	0	1100	X					X	Descent was interrupted because of intermediate altitude restriction; thrust was added at intermediate altitude to maintain airspeed until cleared to continue descent.
19	DEN—ORD	7:05 p.m.				X		X				ATC changed clearance during descent too frequently to reprogram calculator.
20	ORD—DEN	11:42 a.m.	50	35	0				X		X	Started descent about 1.0 n.mi. late; used higher airspeed to reacquire vertical profile.
21	DEN—ORD	3:57 p.m.	−6	0	÷500	X					X	ATC requested speed reduction near end of descent.
22	ORD—DEN	8:17 p.m.	−6	0	0				X	X		
Mean			8.39	11.39	228	Total						
Standard deviation			35.27	15.89	702	15	6	4	3	7	11	

Appendix A—Program Flow Chart

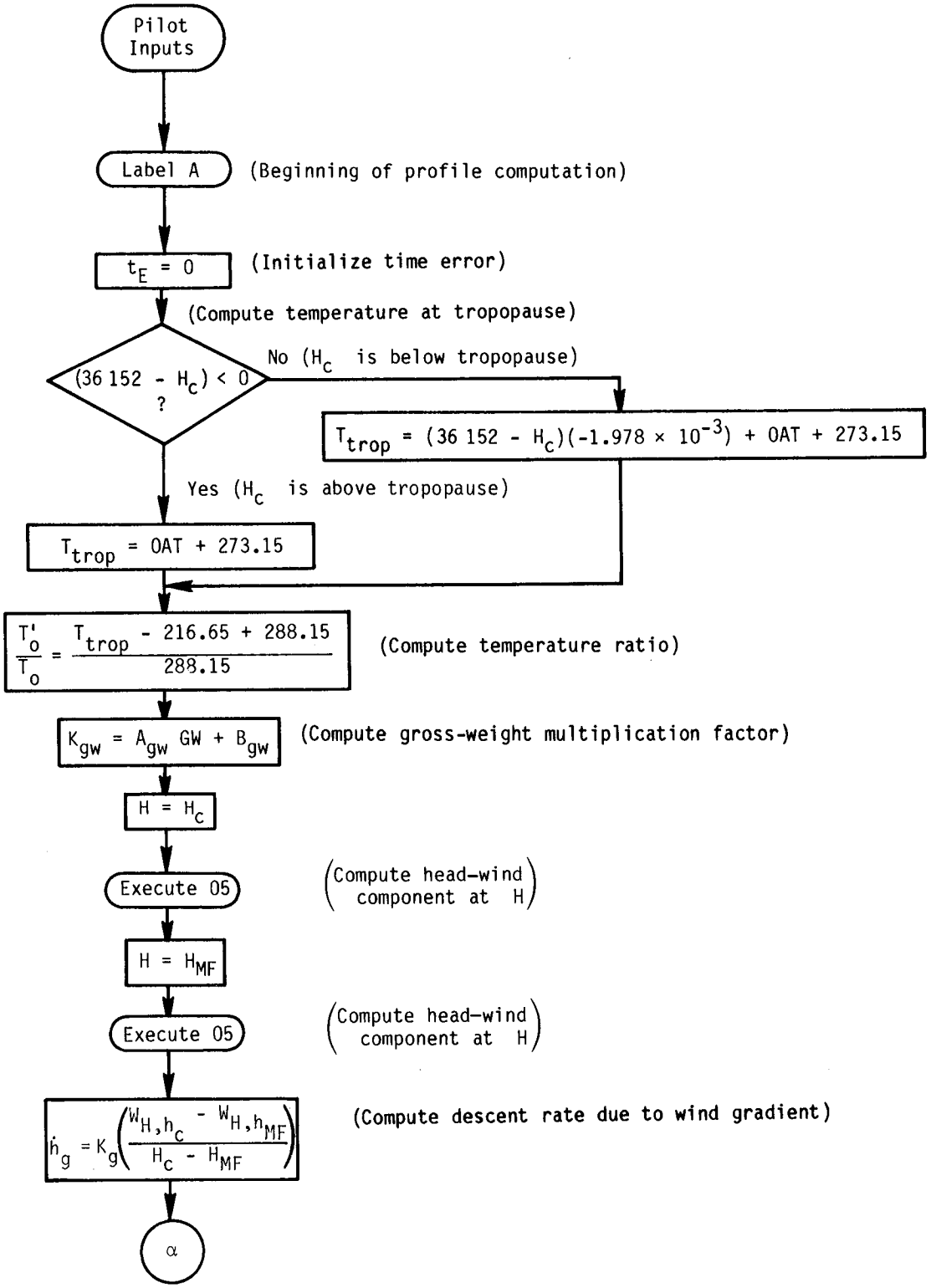

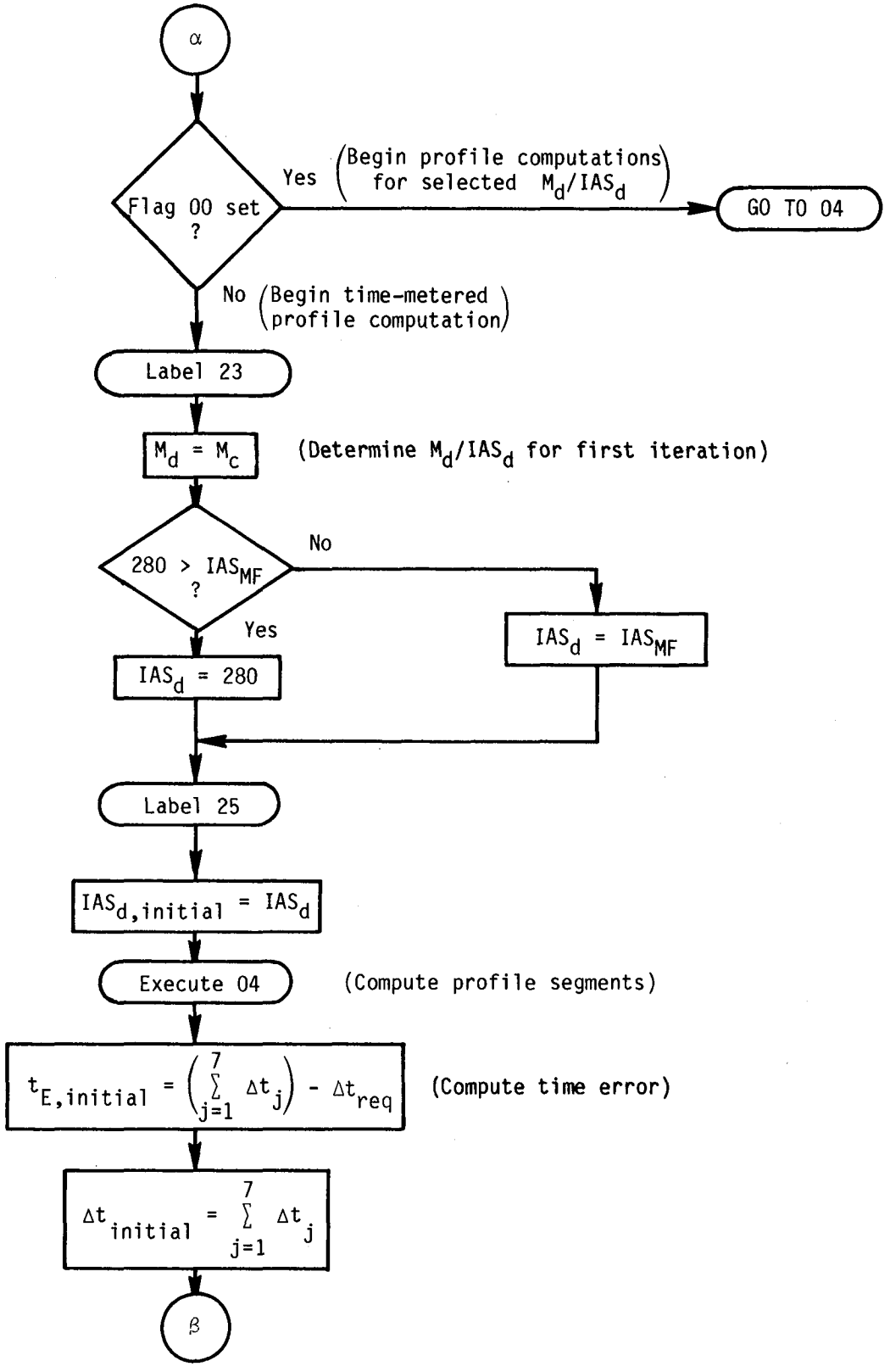
α
Flag 00 set ?
Yes
(Begin profile computations for selected M_d/IAS_d)
GO TO 04
No
(Begin time-metered profile computation)
Label 23
$M_d = M_c$
(Determine M_d/IAS_d for first iteration)
280 > IAS_{MF} ?
No
Yes
$IAS_d = IAS_{MF}$
$IAS_d = 280$
Label 25
$IAS_{d,initial} = IAS_d$
Execute 04
(Compute profile segments)
$t_{E,initial} = \left(\sum_{j=1}^{7} \Delta t_j\right) - \Delta t_{req}$
(Compute time error)
$\Delta t_{initial} = \sum_{j=1}^{7} \Delta t_j$
β

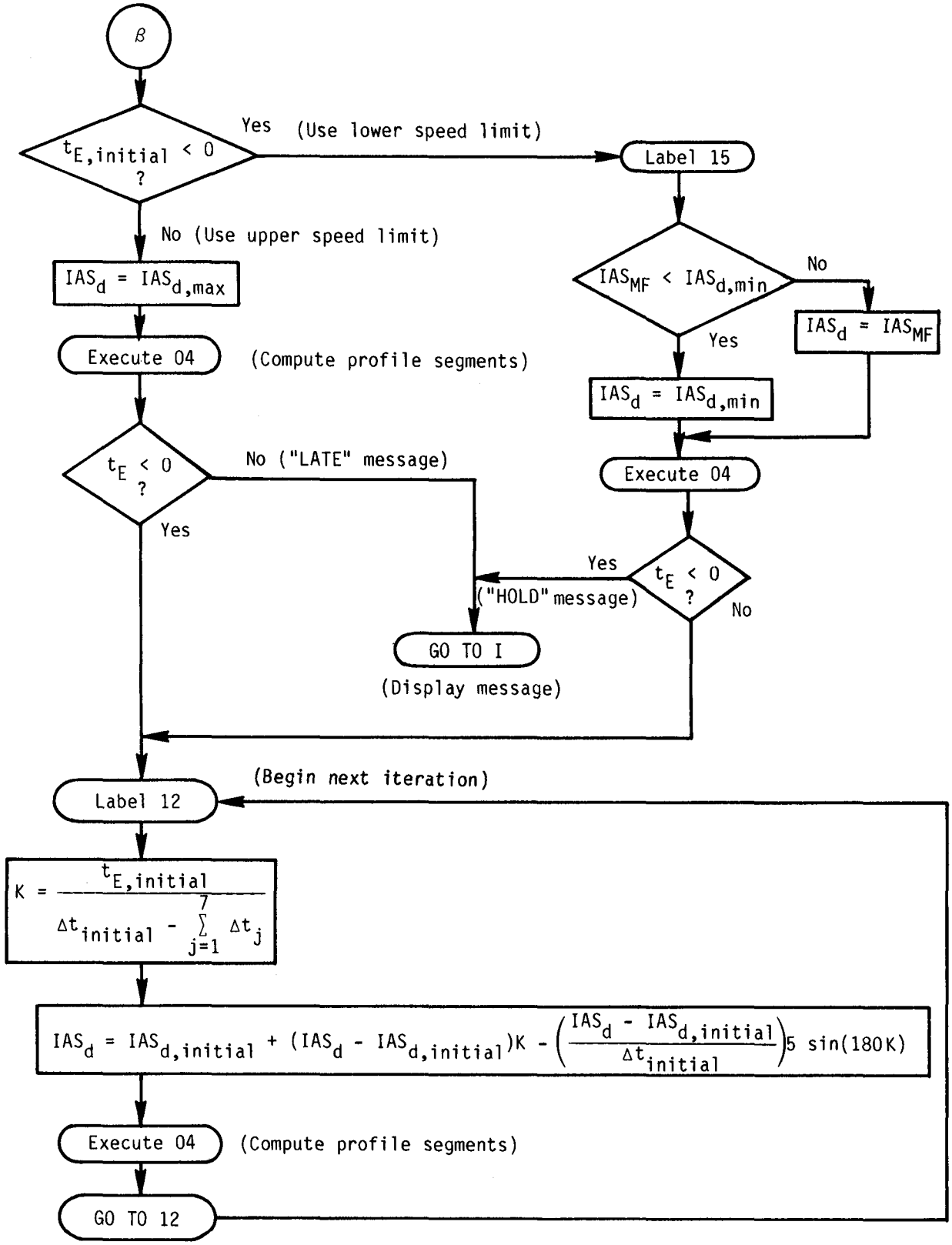
B
$t_{E,initial} < 0$?
Yes
(Use lower speed limit)
Label 15
No
(Use upper speed limit)
$IAS_d = IAS_{d,max}$
$IAS_{MF} < IAS_{d,min}$
No
$IAS_d = IAS_{MF}$
Yes
$IAS_d = IAS_{d,min}$
Execute 04
(Compute profile segments)
$t_E < 0$?
No ("LATE" message)
Yes
Execute 04
Yes
("HOLD" message)
$t_E < 0$?
No
GO TO I
(Display message)
(Begin next iteration)
Label 12
$K = \frac{t_{E,initial}}{\Delta t_{initial} - \sum_{j=1}^{7} \Delta t_j}$
$IAS_d = IAS_{d,initial} + (IAS_d - IAS_{d,initial})K - \left(\frac{IAS_d - IAS_{d,initial}}{\Delta t_{initial}}\right) 5 \sin(180K)$
Execute 04
(Compute profile segments)
GO TO 12

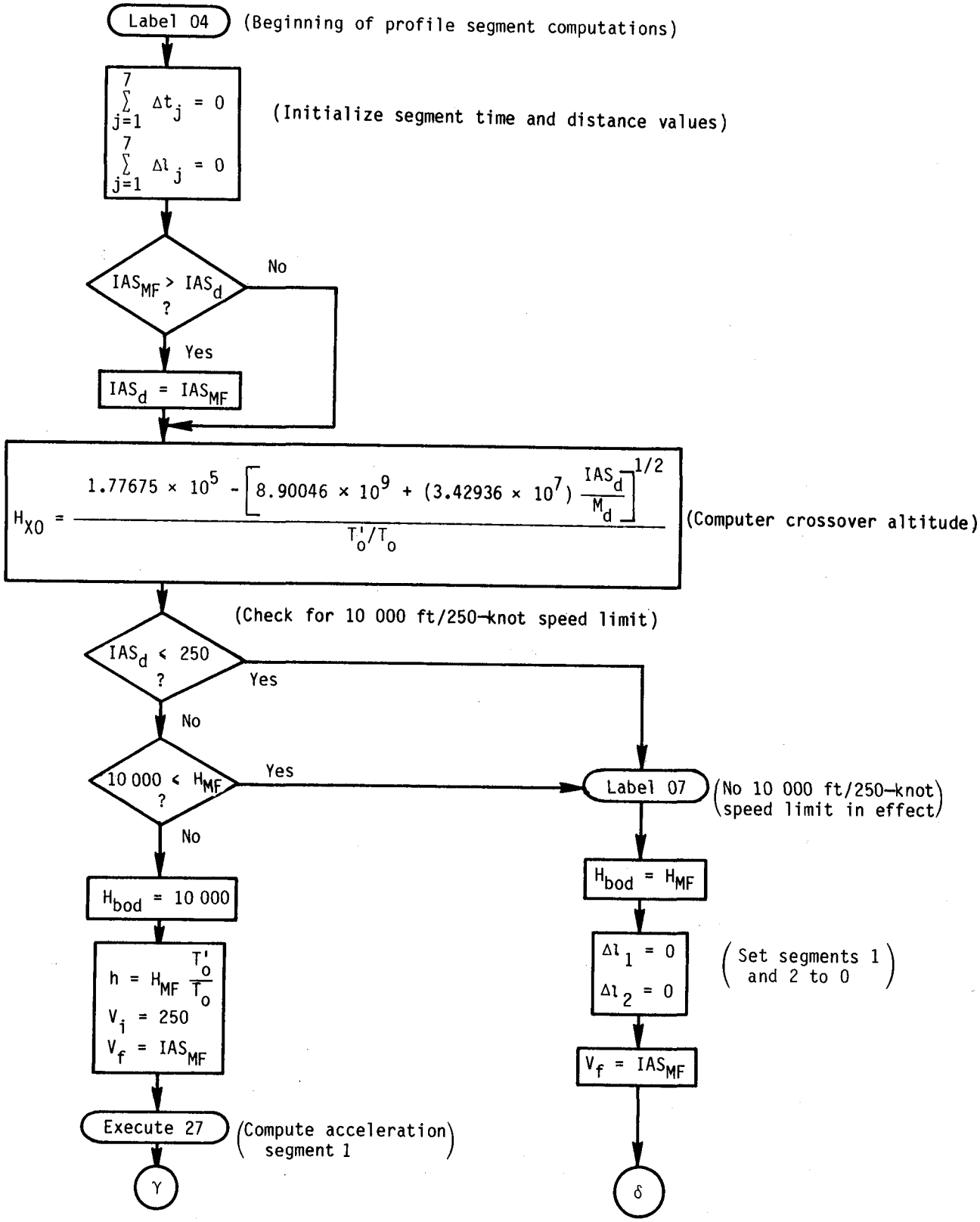
Label 04
(Beginning of profile segment computations)
$\sum_{j=1}^{7} \Delta t_j = 0$
$\sum_{j=1}^{7} \Delta l_j = 0$
(Initialize segment time and distance values)
$IAS_{MF} > IAS_d$?
No
Yes
$IAS_d = IAS_{MF}$
$H_{XO} = \frac{1.77675 \times 10^5 - \left[8.90046 \times 10^9 + (3.42936 \times 10^7) \frac{IAS_d}{M_d}\right]^{1/2}}{T'_o/T_o}$
(Computer crossover altitude)
(Check for 10 000 ft/250-knot speed limit)
$IAS_d < 250$?
Yes
No
$10\,000 < H_{MF}$?
Yes
No
Label 07
(No 10 000 ft/250-knot speed limit in effect)
$H_{bod} = H_{MF}$
$H_{bod} = 10\,000$
$h = H_{MF} \frac{T'_o}{T_o}$
$V_i = 250$
$V_f = IAS_{MF}$
$\Delta l_1 = 0$
$\Delta l_2 = 0$
(Set segments 1 and 2 to 0)
$V_f = IAS_{MF}$
Execute 27
(Compute acceleration segment 1)
γ
δ

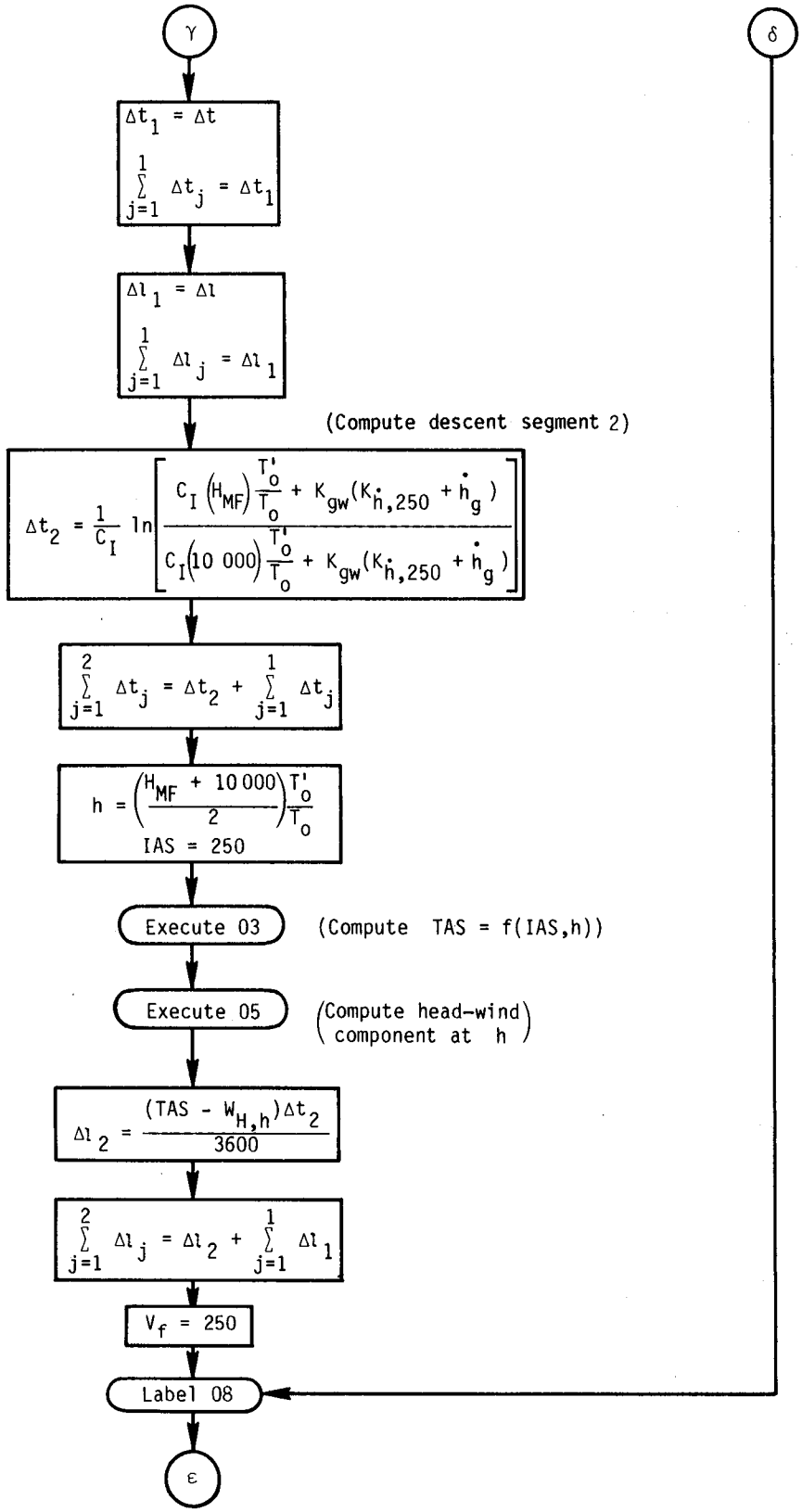
γ
δ
$\Delta t_1 = \Delta t$
$\sum_{j=1}^{1} \Delta t_j = \Delta t_1$
$\Delta l_1 = \Delta l$
$\sum_{j=1}^{1} \Delta l_j = \Delta l_1$
(Compute descent segment 2)
$\Delta t_2 = \frac{1}{C_I} \ln \left[\frac{C_I (H_{MF}) \frac{T'_o}{T_o} + K_{gw}(K_{\dot{h},250} + \dot{h}_g)}{C_I (10\,000) \frac{T'_o}{T_o} + K_{gw}(K_{\dot{h},250} + \dot{h}_g)} \right]$
$\sum_{j=1}^{2} \Delta t_j = \Delta t_2 + \sum_{j=1}^{1} \Delta t_j$
$h = \left(\frac{H_{MF} + 10\,000}{2} \right) \frac{T'_o}{T_o}$
IAS = 250
Execute 03
(Compute TAS = f(IAS,h))
Execute 05
(Compute head-wind component at h)
$\Delta l_2 = \frac{(TAS - W_{H,h}) \Delta t_2}{3600}$
$\sum_{j=1}^{2} \Delta l_j = \Delta l_2 + \sum_{j=1}^{1} \Delta l_1$
$V_f = 250$
Label 08
ε

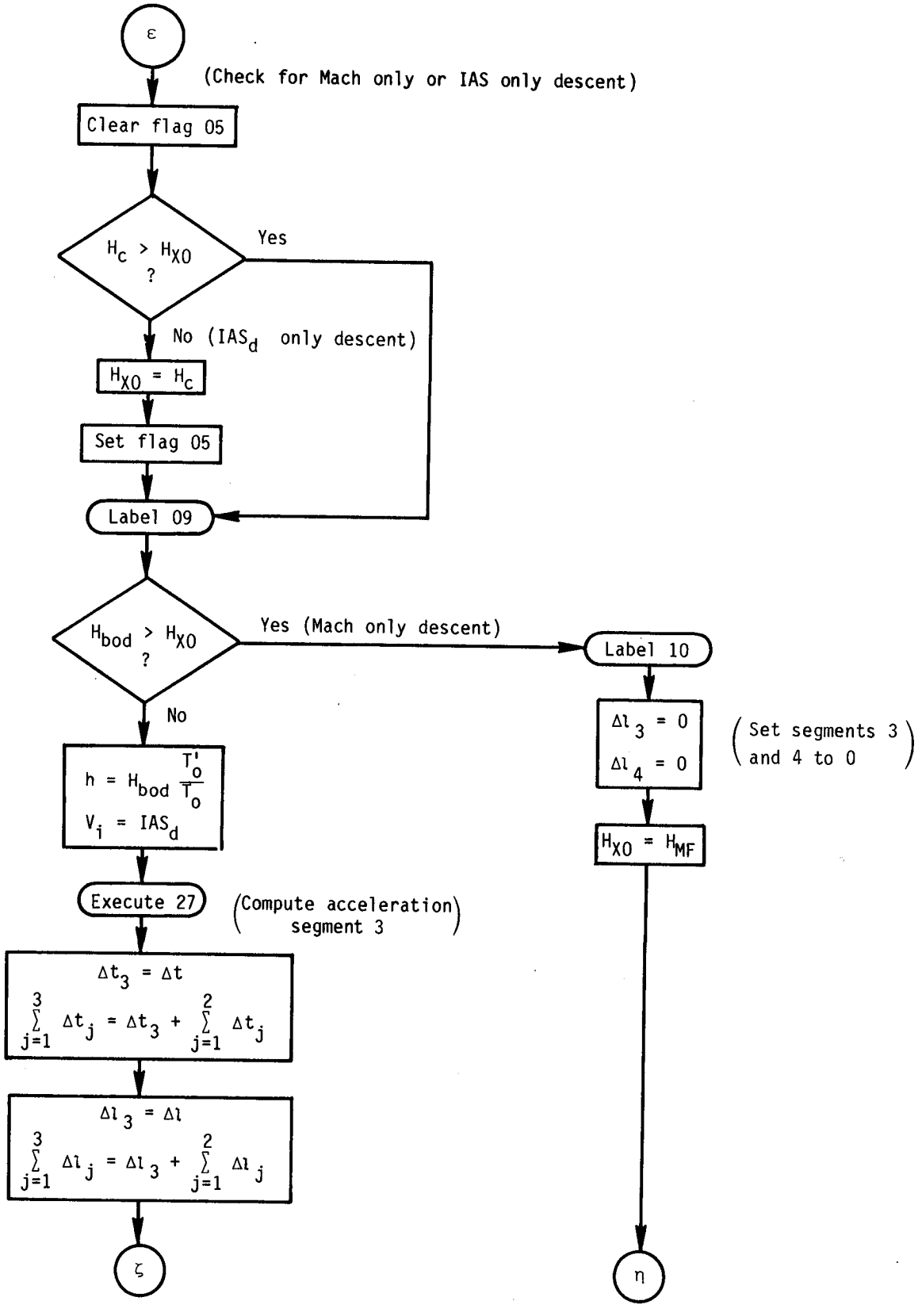
ε
(Check for Mach only or IAS only descent)
Clear flag 05
$H_c > H_{XO}$?
Yes
No (IAS_d only descent)
$H_{XO} = H_c$
Set flag 05
Label 09
$H_{bod} > H_{XO}$?
Yes (Mach only descent)
Label 10
$\Delta l_3 = 0$
$\Delta l_4 = 0$
(Set segments 3 and 4 to 0)
$H_{XO} = H_{MF}$
No
$h = H_{bod} \frac{T'_o}{T_o}$
$V_i = IAS_d$
Execute 27
(Compute acceleration segment 3)
$\Delta t_3 = \Delta t$
$\sum_{j=1}^{3} \Delta t_j = \Delta t_3 + \sum_{j=1}^{2} \Delta t_j$
$\Delta l_3 = \Delta l$
$\sum_{j=1}^{3} \Delta l_j = \Delta l_3 + \sum_{j=1}^{2} \Delta l_j$
ζ
η

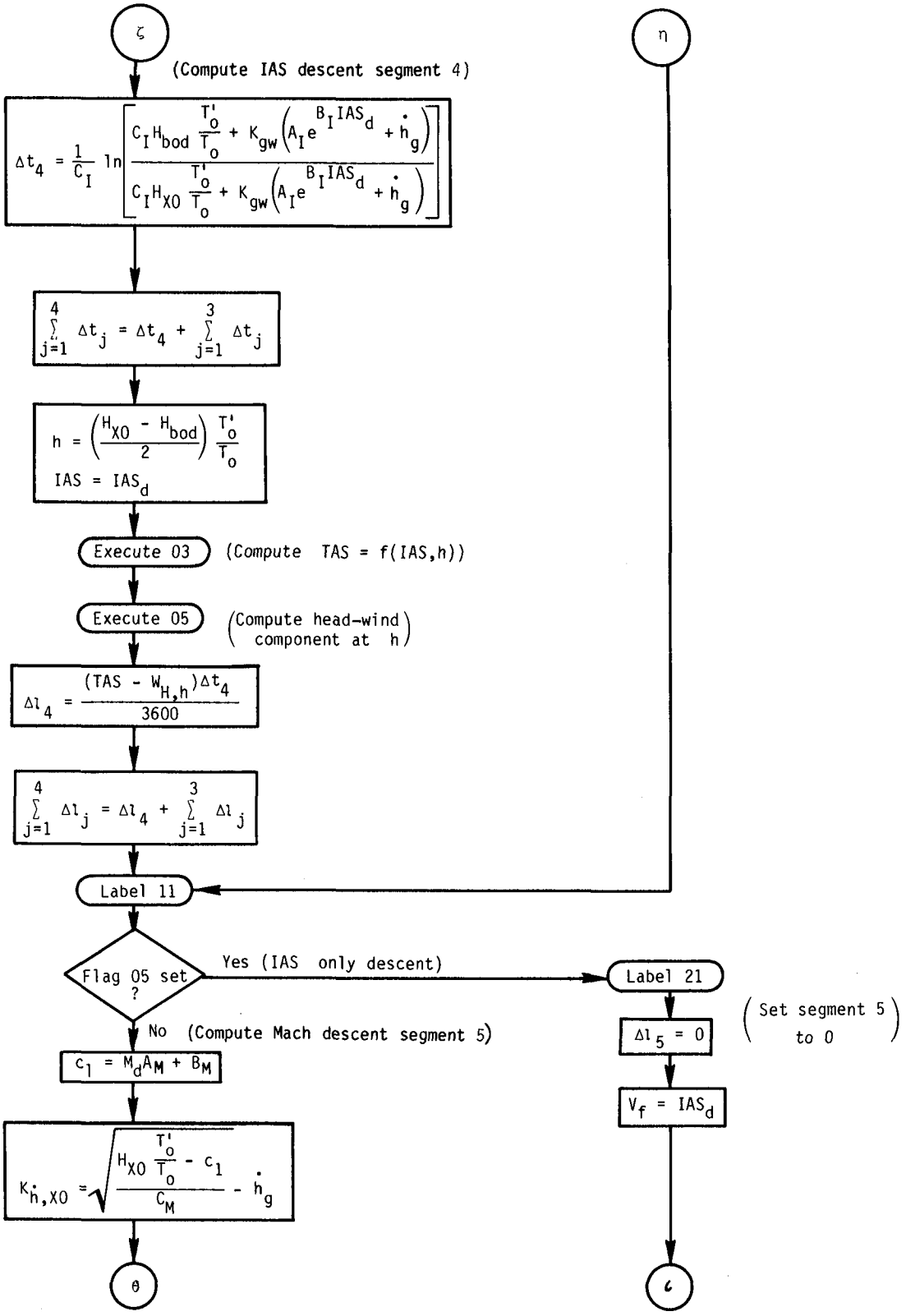
ζ
(Compute IAS descent segment 4)
$\Delta t_4 = \frac{1}{C_I} \ln \left[\frac{C_I H_{bod} \frac{T'_o}{T_o} + K_{gw}\left(A_I e^{B_I IAS_d} + \dot{h}_g\right)}{C_I H_{XO} \frac{T'_o}{T_o} + K_{gw}\left(A_I e^{B_I IAS_d} + \dot{h}_g\right)} \right]$
$\sum_{j=1}^{4} \Delta t_j = \Delta t_4 + \sum_{j=1}^{3} \Delta t_j$
$h = \left(\frac{H_{XO} - H_{bod}}{2}\right) \frac{T'_o}{T_o}$
$IAS = IAS_d$
Execute 03
(Compute TAS = f(IAS,h))
Execute 05
(Compute head-wind component at h)
$\Delta l_4 = \frac{(TAS - W_{H,h})\Delta t_4}{3600}$
$\sum_{j=1}^{4} \Delta l_j = \Delta l_4 + \sum_{j=1}^{3} \Delta l_j$
Label 11
Flag 05 set ?
Yes (IAS only descent)
Label 21
$\Delta l_5 = 0$
(Set segment 5 to 0)
$V_f = IAS_d$
No (Compute Mach descent segment 5)
$c_1 = M_d A_M + B_M$
$K_{\dot{h},XO} = \sqrt{\frac{H_{XO} \frac{T'_o}{T_o} - c_1}{C_M}} - \dot{h}_g$
θ
η
ι

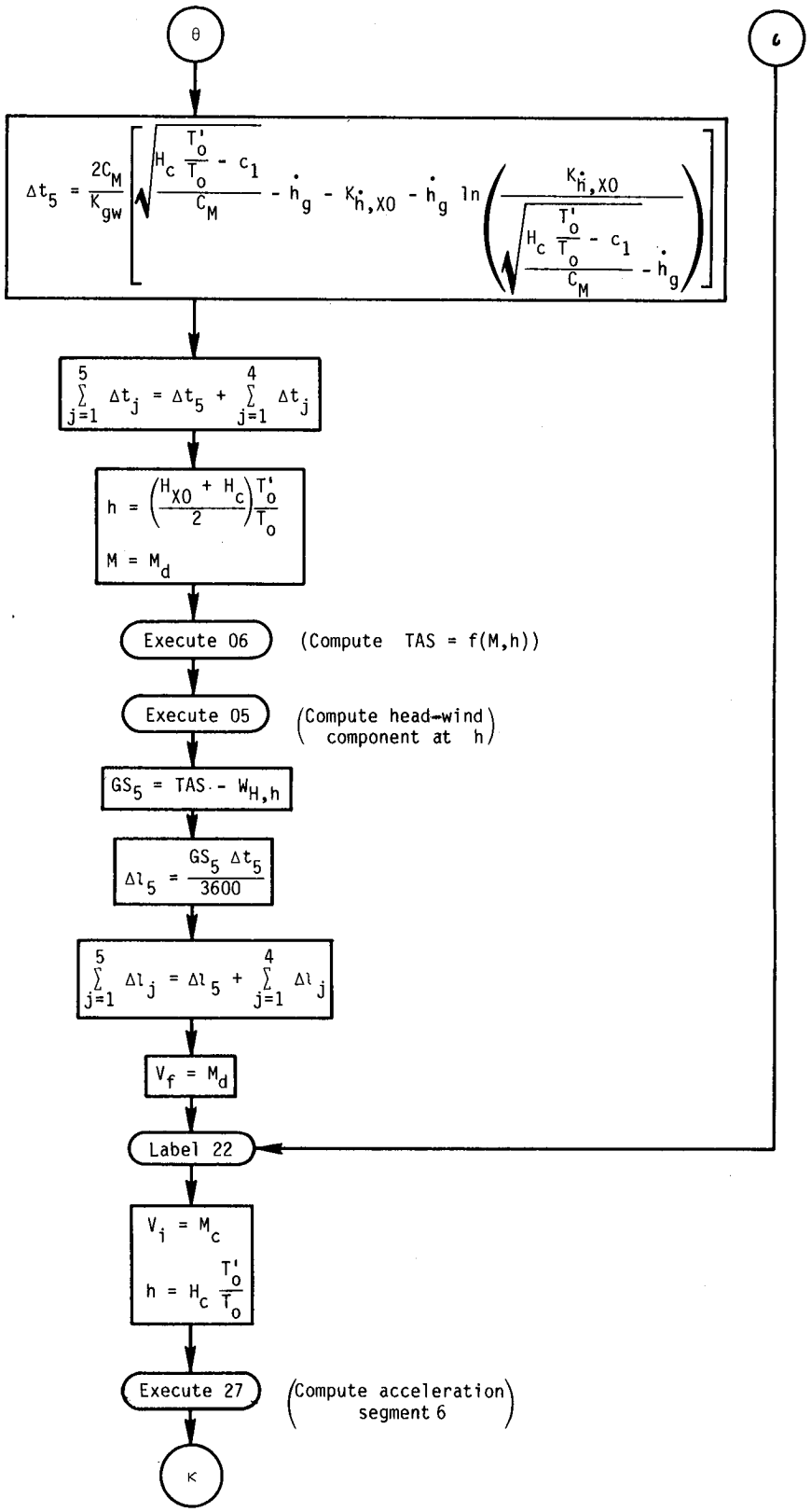
θ
6
$\Delta t_5 = \frac{2C_M}{K_{gw}}\left[\sqrt{\frac{H_c\frac{T'_o}{T_o} - c_1}{C_M}} - \dot{h}_g - K_{\dot{h},XO} - \dot{h}_g \ln\left(\frac{K_{\dot{h},XO}}{\sqrt{\frac{H_c\frac{T'_o}{T_o} - c_1}{C_M}} - \dot{h}_g}\right)\right]$
$\sum_{j=1}^{5} \Delta t_j = \Delta t_5 + \sum_{j=1}^{4} \Delta t_j$
$h = \left(\frac{H_{XO} + H_c}{2}\right)\frac{T'_o}{T_o}$
$M = M_d$
Execute 06
(Compute TAS = f(M,h))
Execute 05
(Compute head-wind component at h)
$GS_5 = TAS - W_{H,h}$
$\Delta l_5 = \frac{GS_5\ \Delta t_5}{3600}$
$\sum_{j=1}^{5} \Delta l_j = \Delta l_5 + \sum_{j=1}^{4} \Delta l_j$
$V_f = M_d$
Label 22
$V_i = M_c$
$h = H_c\frac{T'_o}{T_o}$
Execute 27
(Compute acceleration segment 6
K

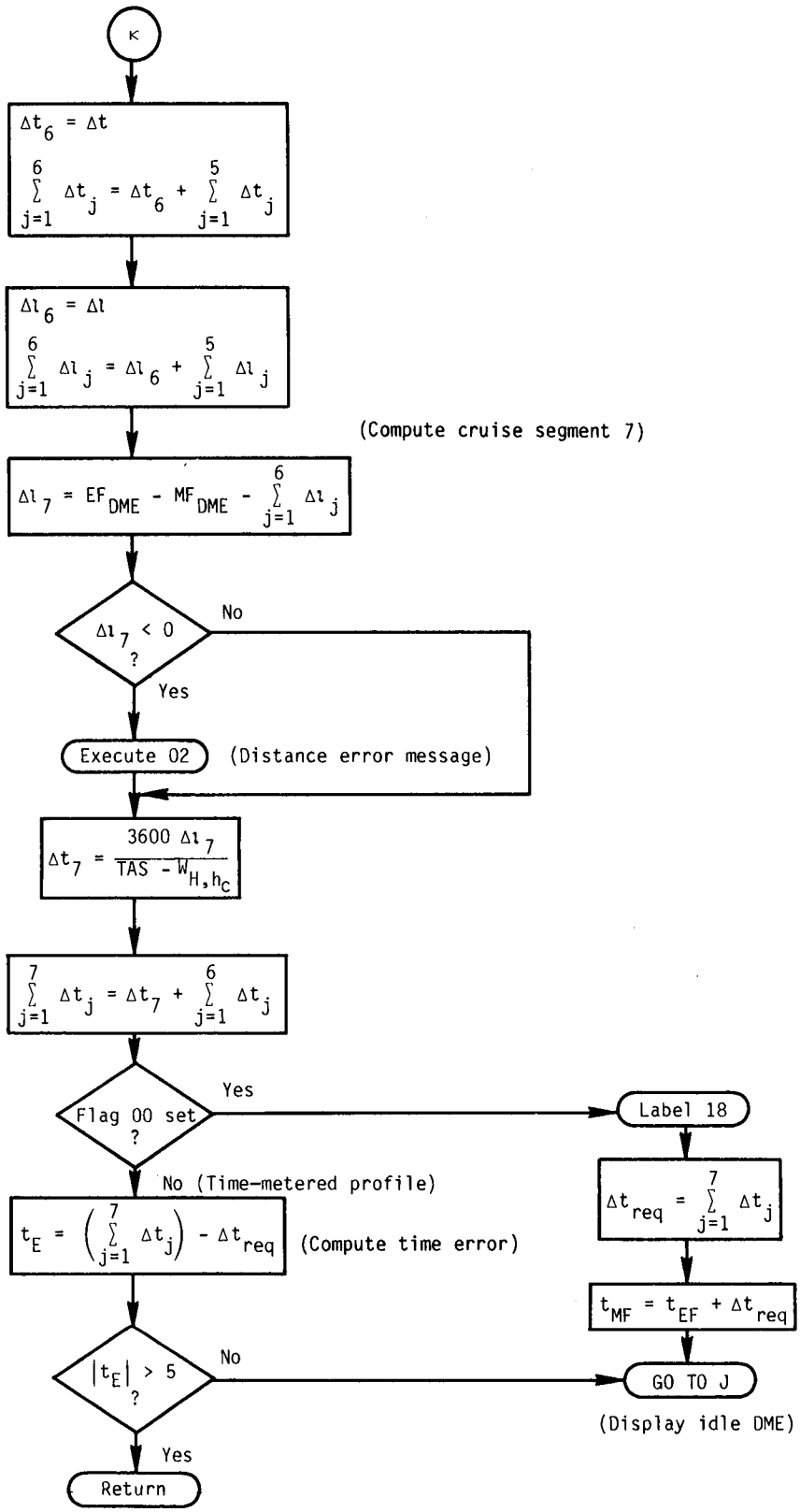
K
$\Delta t_6 = \Delta t$
$\sum_{j=1}^{6} \Delta t_j = \Delta t_6 + \sum_{j=1}^{5} \Delta t_j$
$\Delta l_6 = \Delta l$
$\sum_{j=1}^{6} \Delta l_j = \Delta l_6 + \sum_{j=1}^{5} \Delta l_j$
(Compute cruise segment 7)
$\Delta l_7 = EF_{DME} - MF_{DME} - \sum_{j=1}^{6} \Delta l_j$
$\Delta l_7 < 0$?
No
Yes
Execute 02
(Distance error message)
$\Delta t_7 = \frac{3600\ \Delta l_7}{TAS - W_{H,h_c}}$
$\sum_{j=1}^{7} \Delta t_j = \Delta t_7 + \sum_{j=1}^{6} \Delta t_j$
Flag 00 set ?
Yes
Label 18
No (Time-metered profile)
$\Delta t_{req} = \sum_{j=1}^{7} \Delta t_j$
$t_E = \left(\sum_{j=1}^{7} \Delta t_j\right) - \Delta t_{req}$
(Compute time error)
$t_{MF} = t_{EF} + \Delta t_{req}$
$|t_E| > 5$?
No
GO TO J
(Display idle DME)
Yes
Return

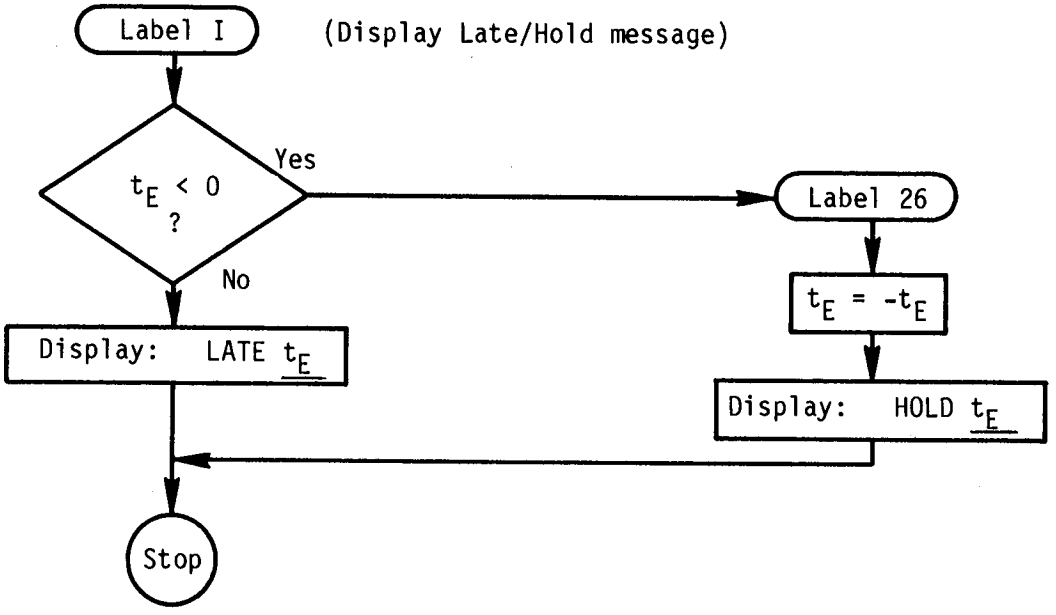
Label I
(Display Late/Hold message)
$t_E < 0$?
Yes
No
Label 26
$t_E = -t_E$
Display: LATE t_E
Display: HOLD t_E
Stop

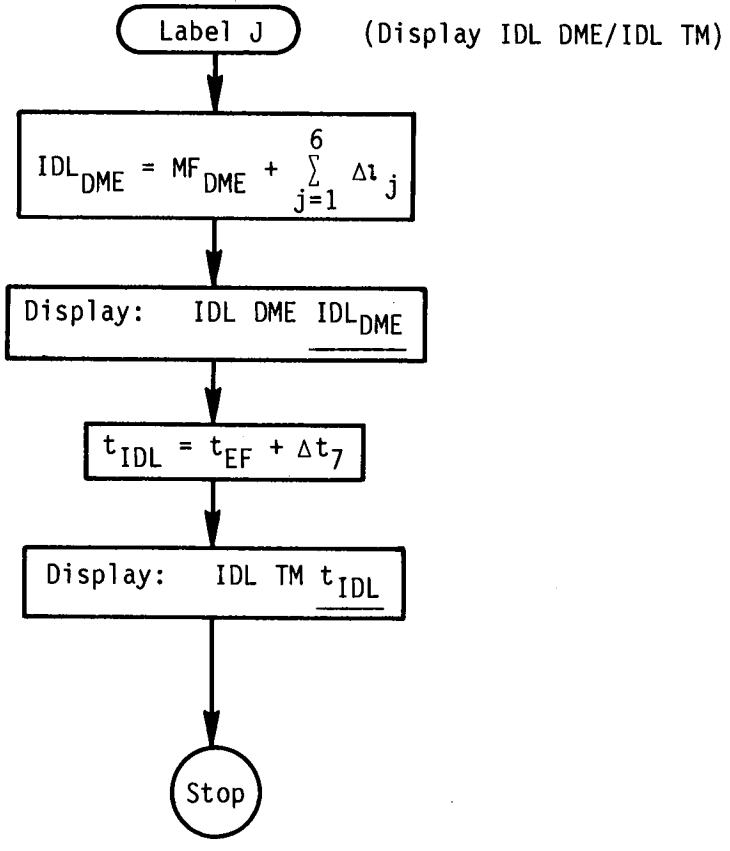
Label J
(Display IDL DME/IDL TM)
$IDL_{DME} = MF_{DME} + \sum_{j=1}^{6} \Delta i_j$
Display: IDL DME IDL_{DME}
$t_{IDL} = t_{EF} + \Delta t_7$
Display: IDL TM t_{IDL}
Stop

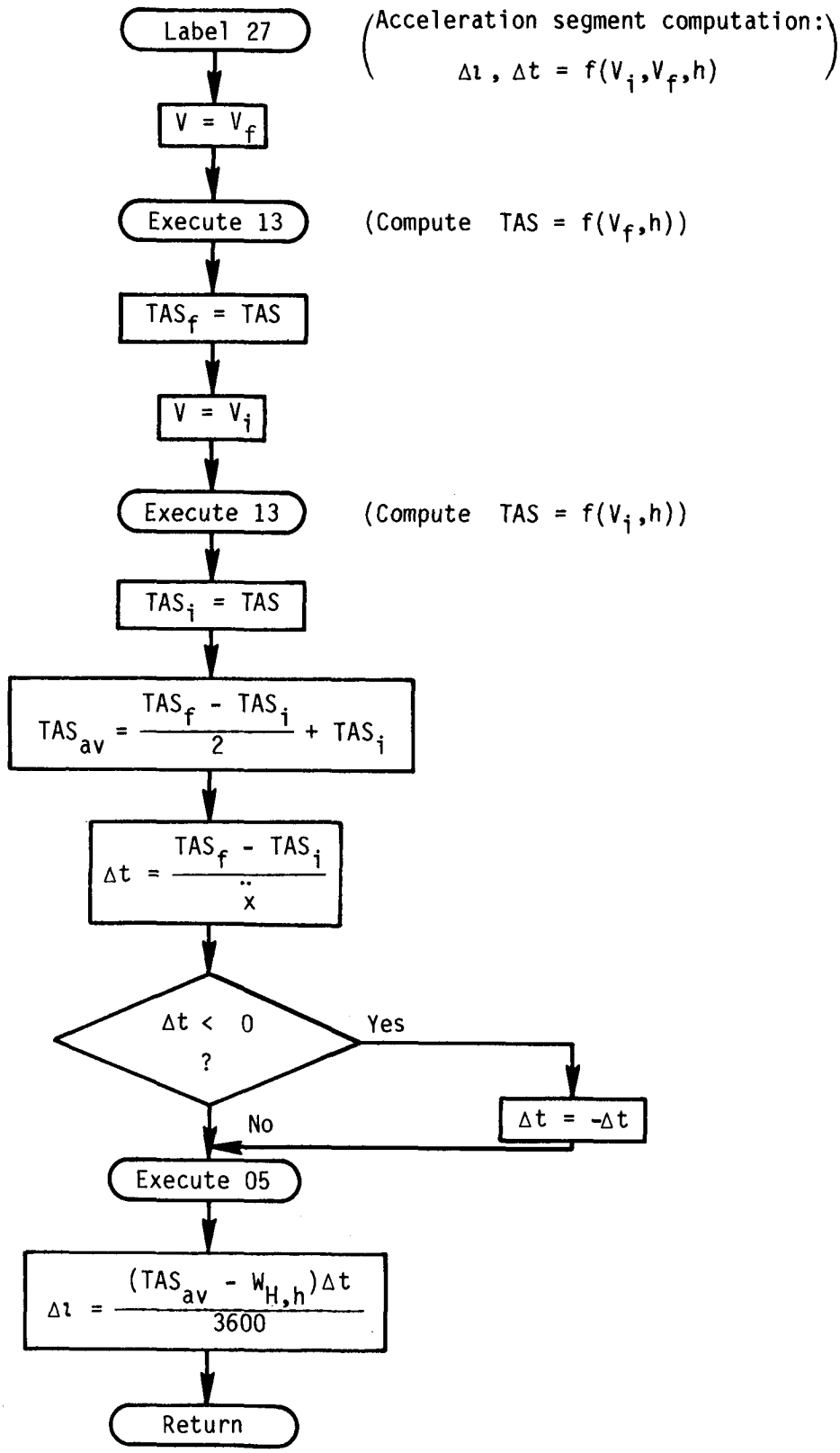
Label 27
(Acceleration segment computation:
Δl , Δt = f(V_i,V_f,h))
V = V_f
Execute 13
(Compute TAS = f(V_f,h))
TAS_f = TAS
V = V_i
Execute 13
(Compute TAS = f(V_i,h))
TAS_i = TAS
TAS_av = (TAS_f - TAS_i)/2 + TAS_i
Δt = (TAS_f - TAS_i)/ẍ
Δt < 0 ?
Yes
No
Δt = -Δt
Execute 05
Δl = (TAS_av - W_H,h)Δt/3600
Return

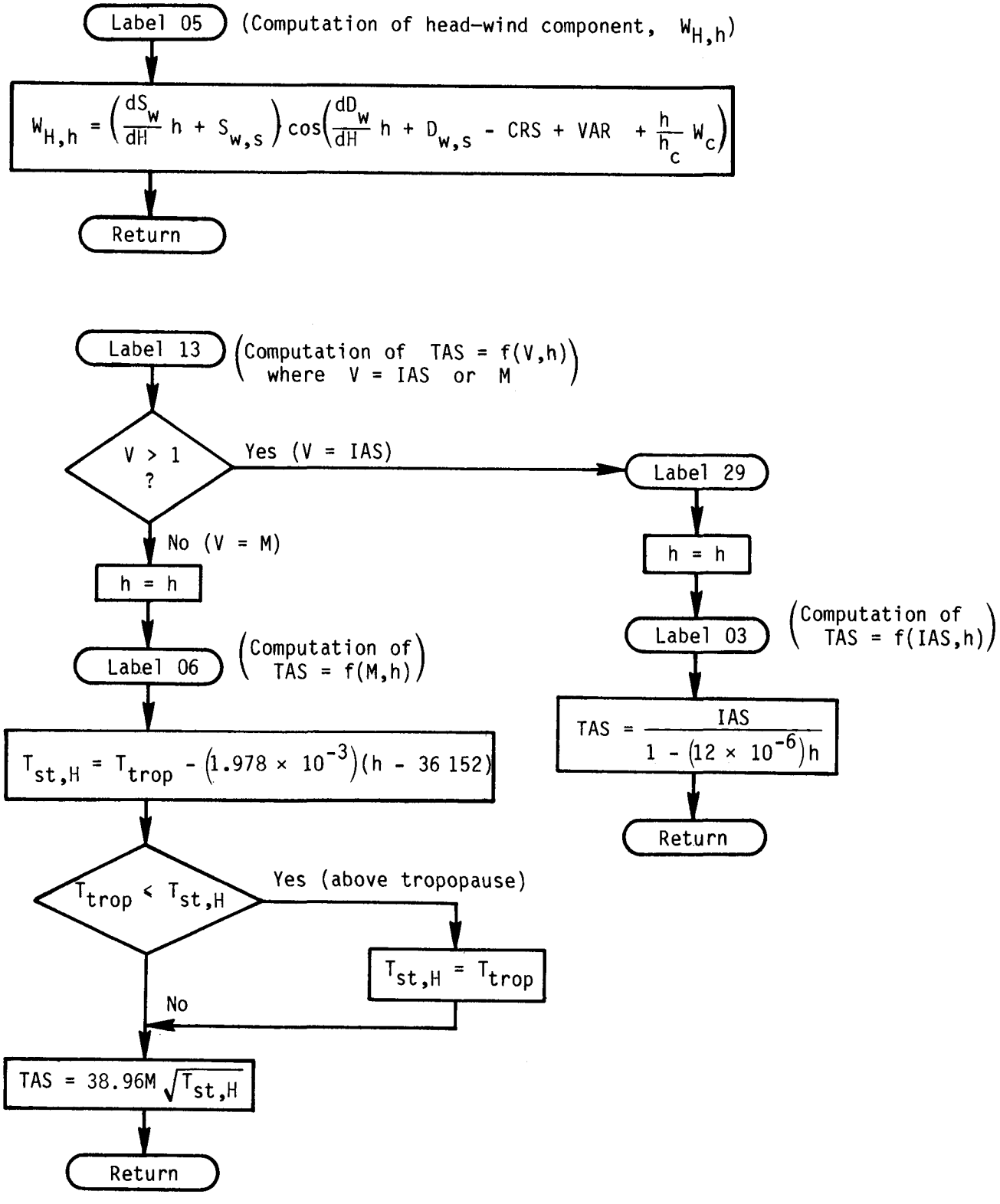
Label 05
(Computation of head-wind component, $W_{H,h}$)
$W_{H,h} = \left(\frac{dS_w}{dH} h + S_{w,s}\right) \cos\left(\frac{dD_w}{dH} h + D_{w,s} - CRS + VAR + \frac{h}{h_c} W_c\right)$
Return
Label 13
(Computation of TAS = f(V,h) where V = IAS or M)
V > 1 ?
Yes (V = IAS)
Label 29
h = h
Label 03
(Computation of TAS = f(IAS,h))
$TAS = \frac{IAS}{1 - (12 \times 10^{-6})h}$
Return
No (V = M)
h = h
Label 06
(Computation of TAS = f(M,h))
$T_{st,H} = T_{trop} - (1.978 \times 10^{-3})(h - 36\,152)$
$T_{trop} < T_{st,H}$
Yes (above tropopause)
$T_{st,H} = T_{trop}$
No
$TAS = 38.96M \sqrt{T_{st,H}}$
Return

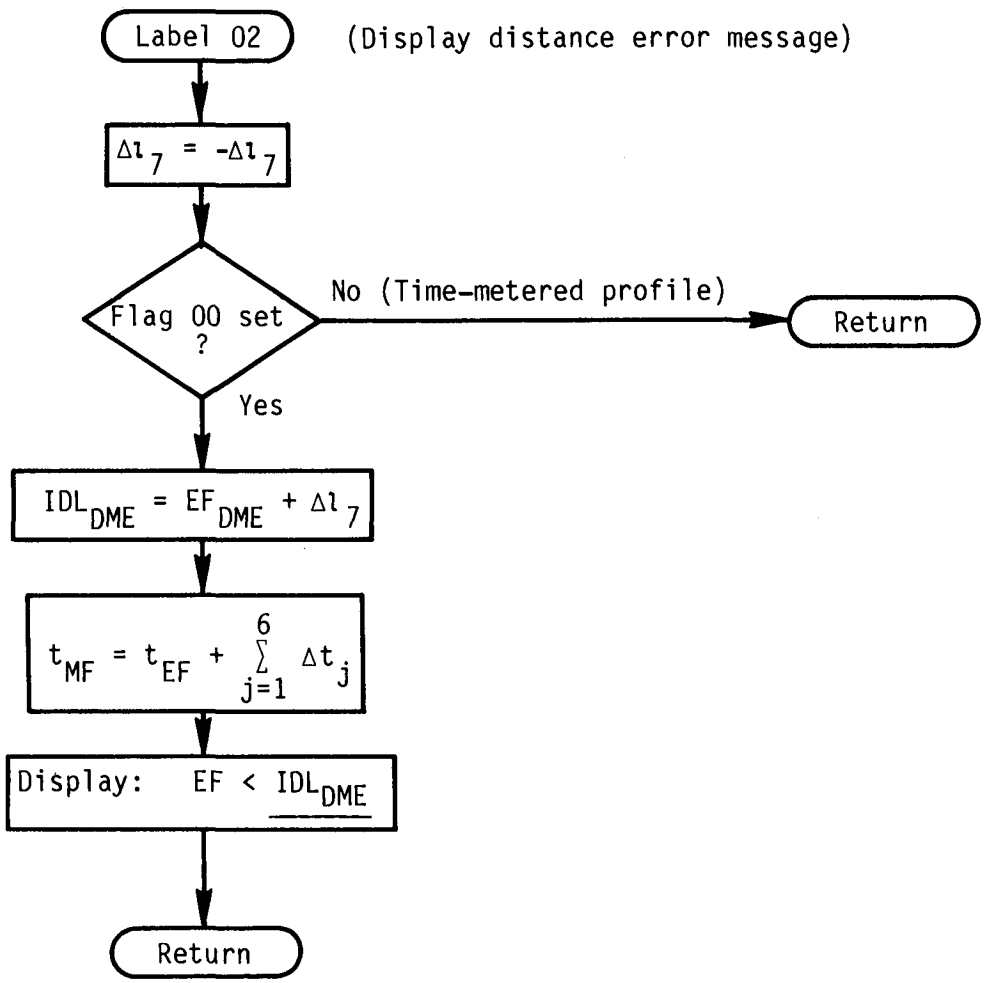
Label 02
(Display distance error message)
$\Delta l_7 = -\Delta l_7$
Flag 00 set ?
No (Time-metered profile)
Return
Yes
$IDL_{DME} = EF_{DME} + \Delta l_7$
$t_{MF} = t_{EF} + \sum_{j=1}^{6} \Delta t_j$
Display: EF < IDL_{DME}
Return

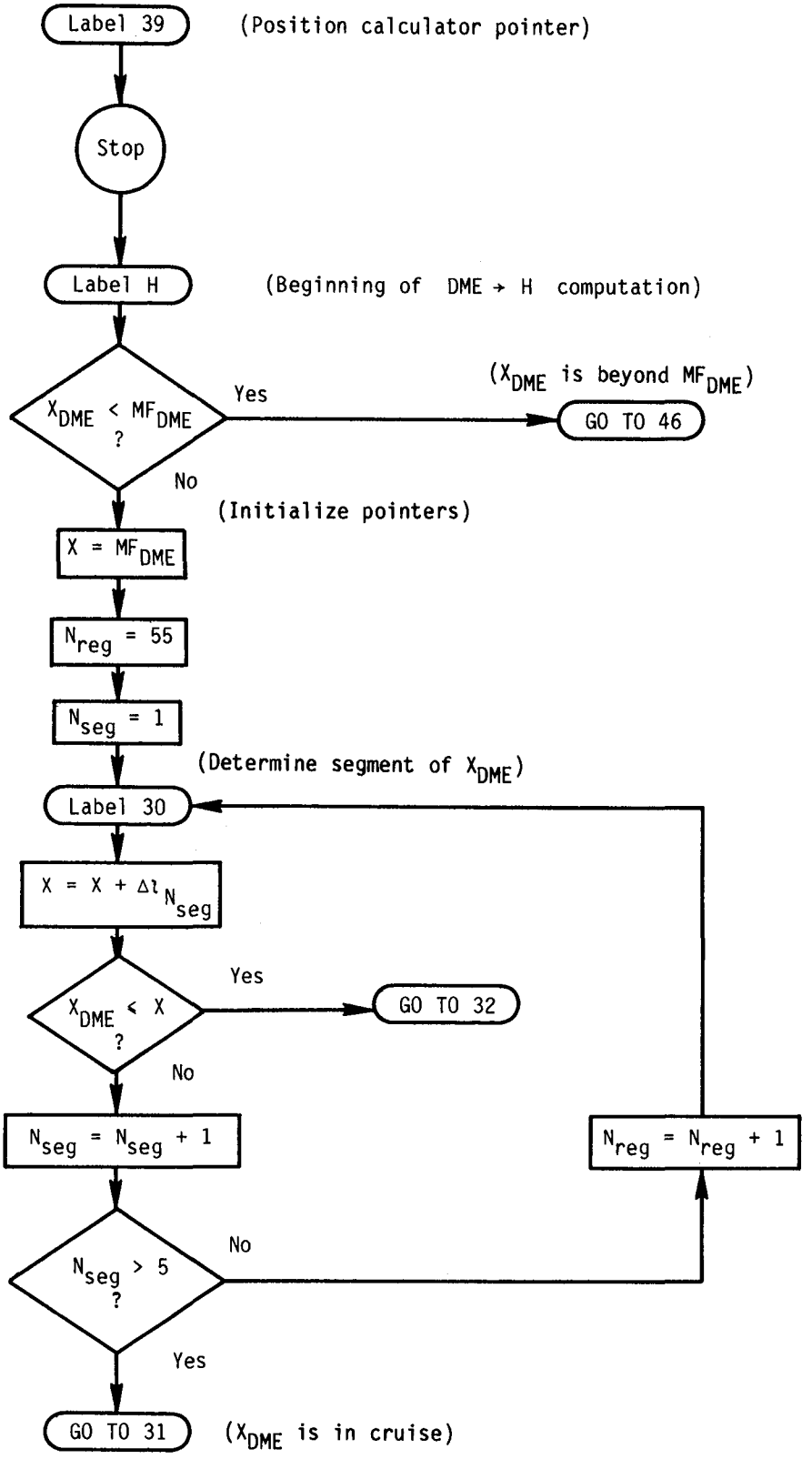
Label 39
(Position calculator pointer)
Stop
Label H
(Beginning of DME → H computation)
$X_{DME} < MF_{DME}$?
Yes
(X_{DME} is beyond MF_{DME})
GO TO 46
No
(Initialize pointers)
$X = MF_{DME}$
$N_{reg} = 55$
$N_{seg} = 1$
(Determine segment of X_{DME})
Label 30
$X = X + \Delta l_{N_{seg}}$
$X_{DME} < X$?
Yes
GO TO 32
No
$N_{seg} = N_{seg} + 1$
$N_{seg} > 5$?
No
Yes
$N_{reg} = N_{reg} + 1$
GO TO 31
(X_{DME} is in cruise)

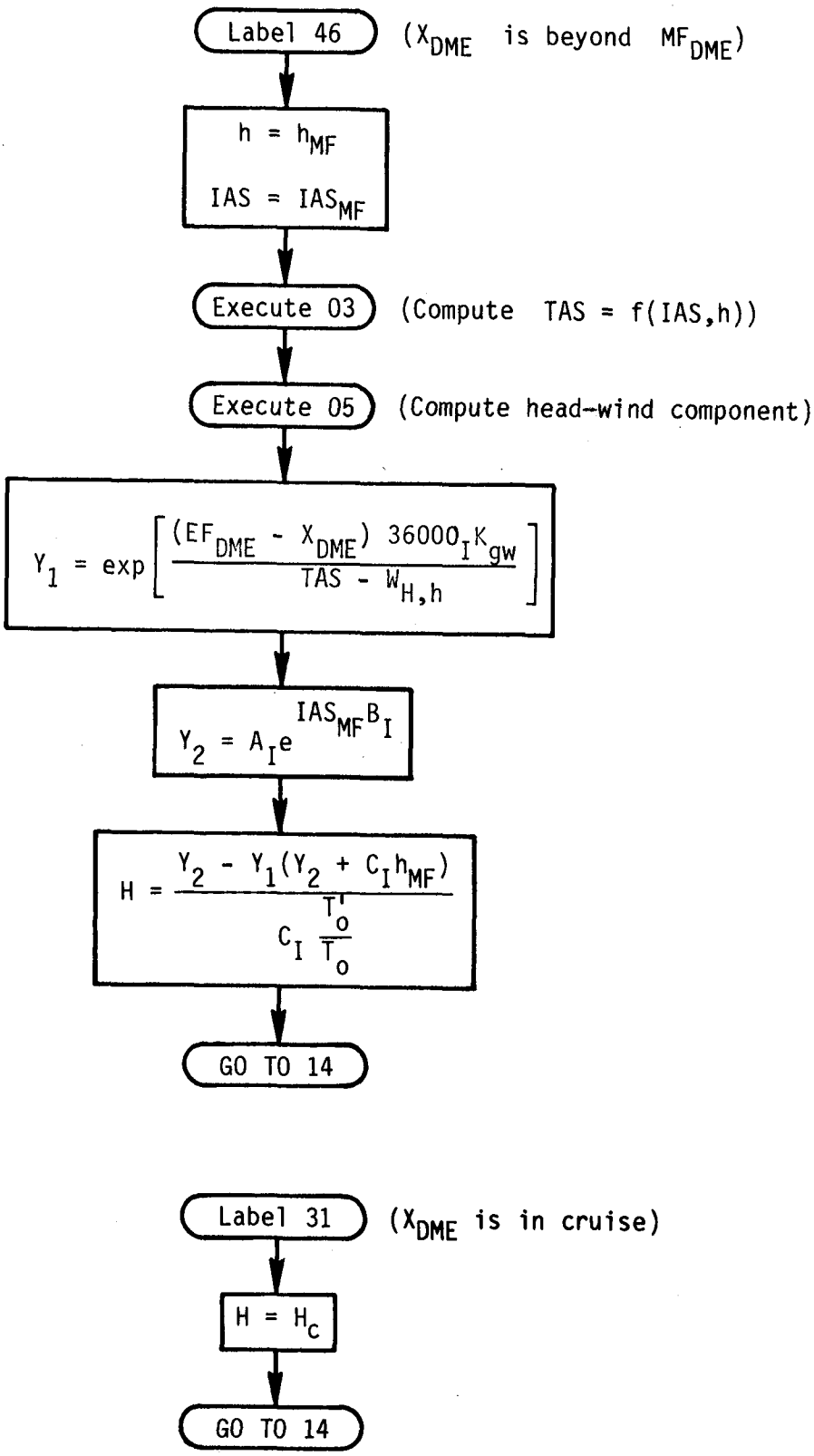
Label 46
(X_{DME} is beyond MF_{DME})
$h = h_{MF}$
$IAS = IAS_{MF}$
Execute 03
(Compute TAS = f(IAS,h))
Execute 05
(Compute head-wind component)
$Y_1 = \exp\left[\frac{(EF_{DME} - X_{DME})\ 36000_I K_{gw}}{TAS - W_{H,h}}\right]$
$Y_2 = A_I e^{IAS_{MF} B_I}$
$H = \frac{Y_2 - Y_1(Y_2 + C_I h_{MF})}{C_I \frac{T'_o}{T_o}}$
GO TO 14
Label 31
(X_{DME} is in cruise)
$H = H_c$
GO TO 14

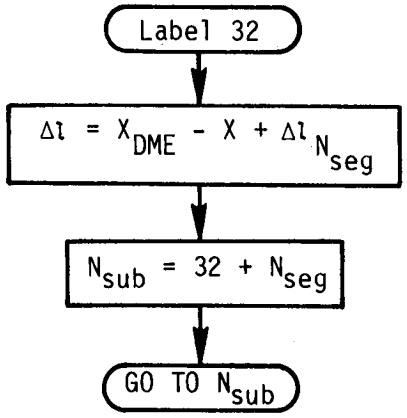

(Determine distance within segment)

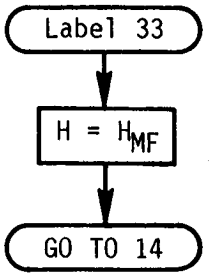

(X_{DME} is in segment 1)

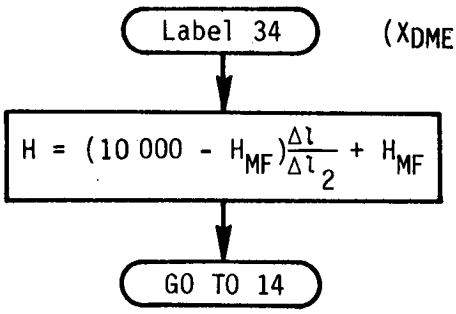

(X_{DME} is in segment 2)

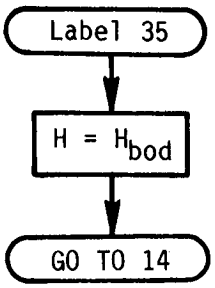

(X_{DME} is in segment 3)

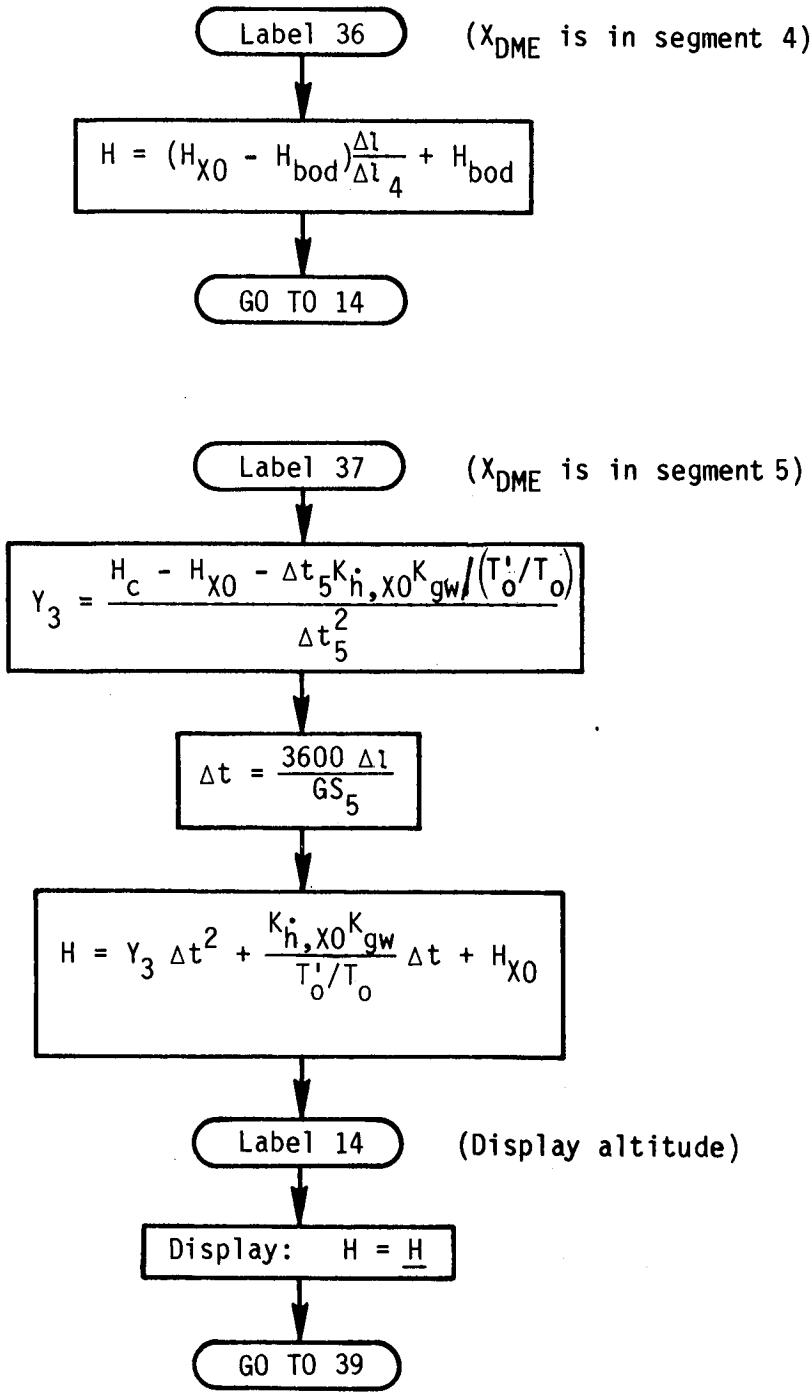
Label 36
(X_{DME} is in segment 4)
$H = (H_{XO} - H_{bod})\frac{\Delta l}{\Delta l_4} + H_{bod}$
GO TO 14
Label 37
(X_{DME} is in segment 5)
$Y_3 = \frac{H_c - H_{XO} - \Delta t_5 \dot{K}_{h,XO} K_{gw} / (T'_o/T_o)}{\Delta t_5^2}$
$\Delta t = \frac{3600\ \Delta l}{GS_5}$
$H = Y_3\ \Delta t^2 + \frac{\dot{K}_{h,XO} K_{gw}}{T'_o/T_o}\ \Delta t + H_{XO}$
Label 14
(Display altitude)
Display: H = H
GO TO 39

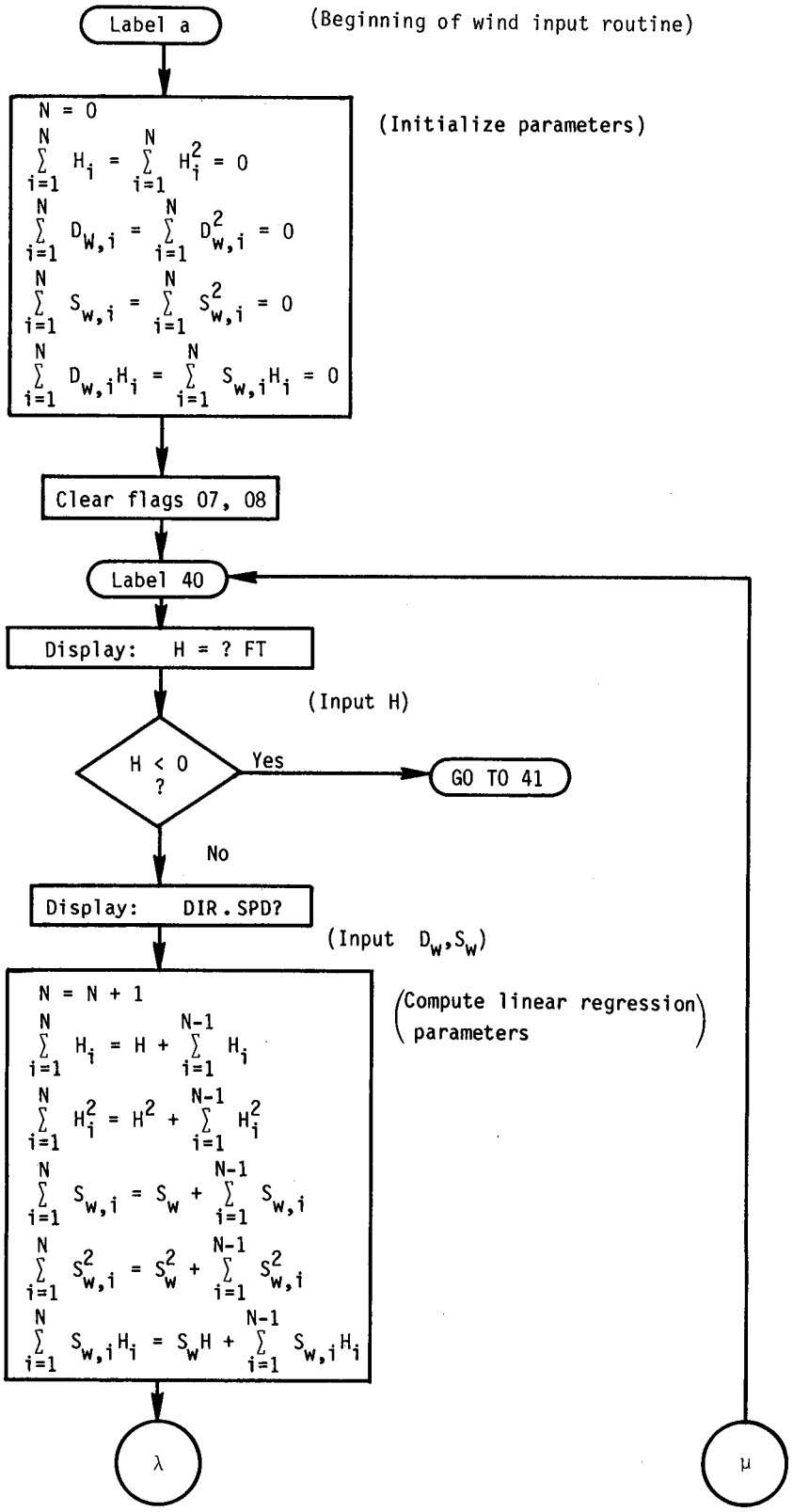
Label a
(Beginning of wind input routine)
N = 0
$\sum_{i=1}^{N} H_i = \sum_{i=1}^{N} H_i^2 = 0$
$\sum_{i=1}^{N} D_{W,i} = \sum_{i=1}^{N} D_{w,i}^2 = 0$
$\sum_{i=1}^{N} S_{w,i} = \sum_{i=1}^{N} S_{w,i}^2 = 0$
$\sum_{i=1}^{N} D_{w,i}H_i = \sum_{i=1}^{N} S_{w,i}H_i = 0$
(Initialize parameters)
Clear flags 07, 08
Label 40
Display: H = ? FT
(Input H)
H < 0 ?
Yes
GO TO 41
No
Display: DIR.SPD?
(Input D_W,S_W)
N = N + 1
$\sum_{i=1}^{N} H_i = H + \sum_{i=1}^{N-1} H_i$
$\sum_{i=1}^{N} H_i^2 = H^2 + \sum_{i=1}^{N-1} H_i^2$
$\sum_{i=1}^{N} S_{w,i} = S_w + \sum_{i=1}^{N-1} S_{w,i}$
$\sum_{i=1}^{N} S_{w,i}^2 = S_w^2 + \sum_{i=1}^{N-1} S_{w,i}^2$
$\sum_{i=1}^{N} S_{w,i}H_i = S_wH + \sum_{i=1}^{N-1} S_{w,i}H_i$
(Compute linear regression parameters)
λ
μ

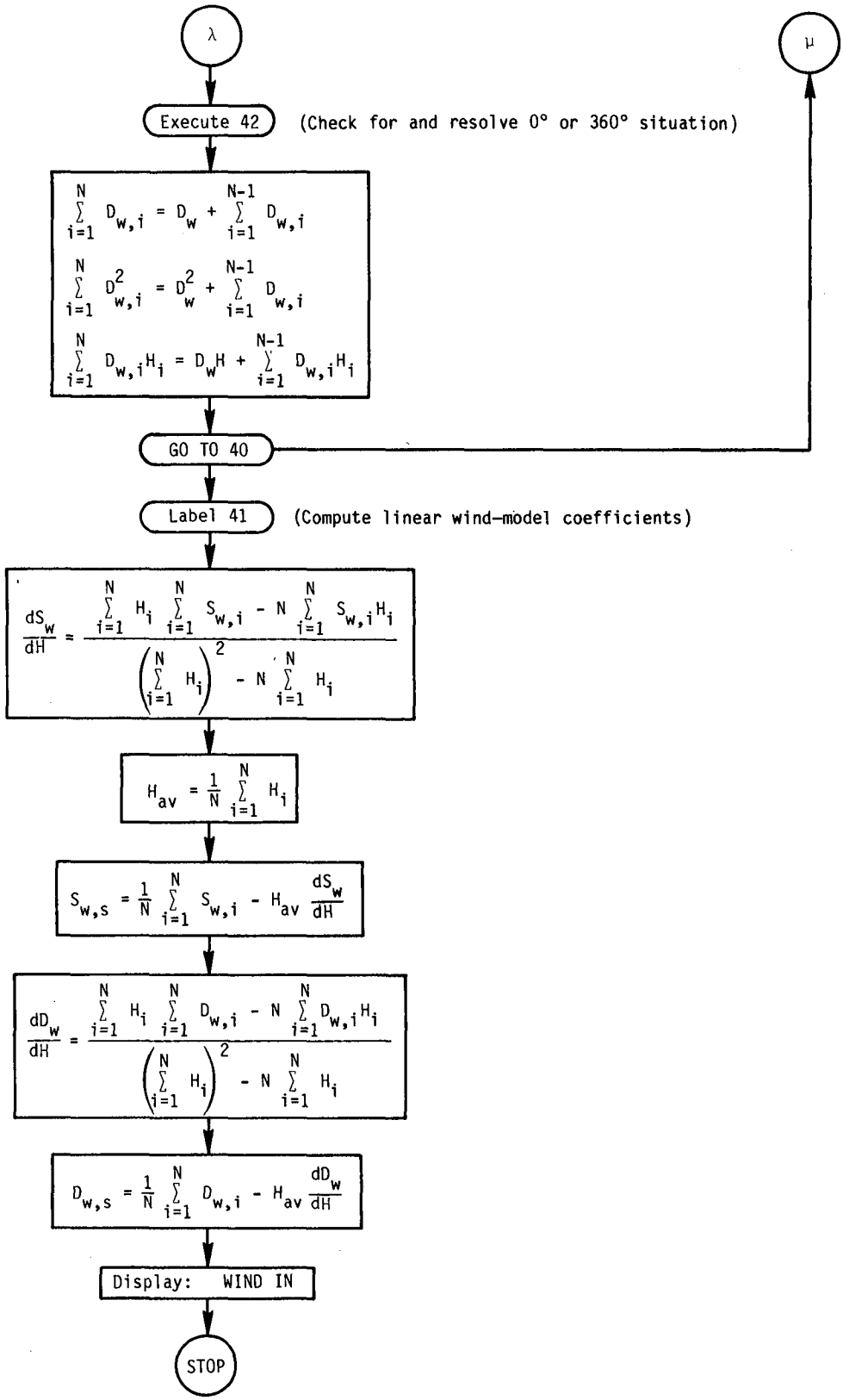
λ
μ
Execute 42
(Check for and resolve 0° or 360° situation)
$\sum_{i=1}^{N} D_{w,i} = D_w + \sum_{i=1}^{N-1} D_{w,i}$
$\sum_{i=1}^{N} D_{w,i}^2 = D_w^2 + \sum_{i=1}^{N-1} D_{w,i}$
$\sum_{i=1}^{N} D_{w,i}H_i = D_wH + \sum_{i=1}^{N-1} D_{w,i}H_i$
GO TO 40
Label 41
(Compute linear wind-model coefficients)
$\frac{dS_w}{dH} = \frac{\sum_{i=1}^{N} H_i \sum_{i=1}^{N} S_{w,i} - N \sum_{i=1}^{N} S_{w,i}H_i}{\left(\sum_{i=1}^{N} H_i\right)^2 - N \sum_{i=1}^{N} H_i}$
$H_{av} = \frac{1}{N} \sum_{i=1}^{N} H_i$
$S_{w,s} = \frac{1}{N} \sum_{i=1}^{N} S_{w,i} - H_{av} \frac{dS_w}{dH}$
$\frac{dD_w}{dH} = \frac{\sum_{i=1}^{N} H_i \sum_{i=1}^{N} D_{w,i} - N \sum_{i=1}^{N} D_{w,i}H_i}{\left(\sum_{i=1}^{N} H_i\right)^2 - N \sum_{i=1}^{N} H_i}$
$D_{w,s} = \frac{1}{N} \sum_{i=1}^{N} D_{w,i} - H_{av} \frac{dD_w}{dH}$
Display: WIND IN
STOP

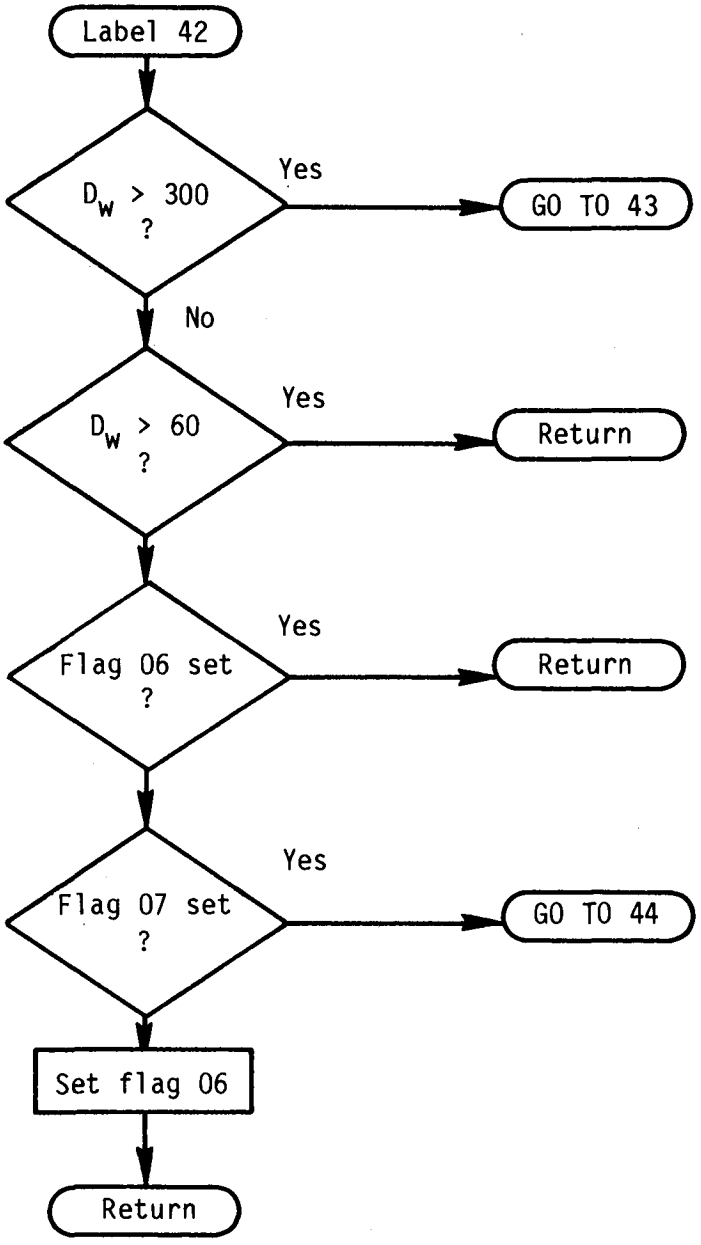
Label 42
D_W > 300 ?
Yes
GO TO 43
No
D_W > 60 ?
Yes
Return
Flag 06 set ?
Yes
Return
Flag 07 set ?
Yes
GO TO 44
Set flag 06
Return

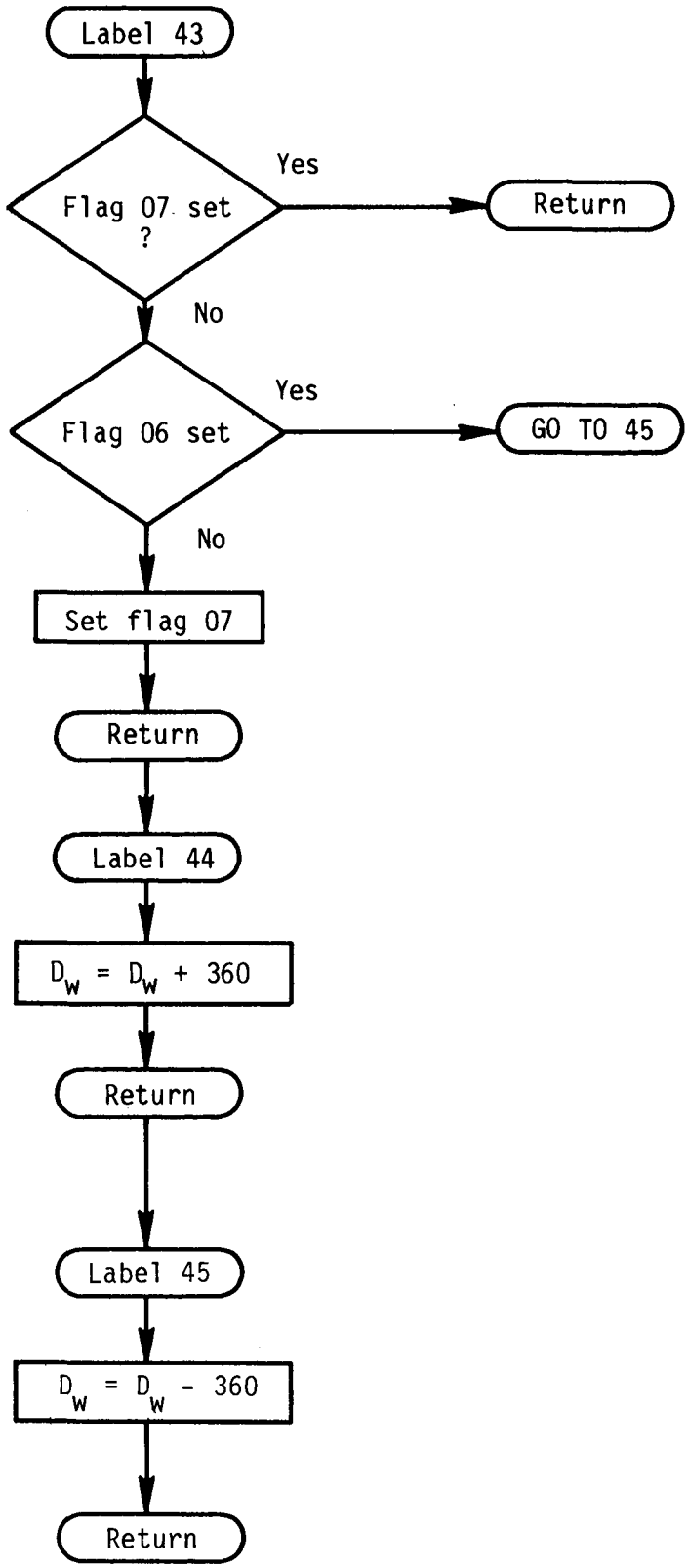
Label 43
Flag 07 set ?
Yes
Return
No
Flag 06 set
Yes
GO TO 45
No
Set flag 07
Return
Label 44
$D_W = D_W + 360$
Return
Label 45
$D_W = D_W - 360$
Return

Appendix B—Calculator Program

Storage Register Location of Descent Algorithm Variables (Numerical Values for the DC-10-10 Model)

Input Variables

17	M_c
18	H_c
08	M_d
10	IAS_d
21	t_{MF}
22	t_{EF}
23	GW
19	OAT
07	H_{MF}
26	$\mathrm{IAS}_{\mathrm{MF}}$
27	$\mathrm{MF}_{\mathrm{DME}}$
28	$\mathrm{EF}_{\mathrm{DME}}$
29	CRS
24	VAR

Computed Variables

00	Temporary
01	
02	
03	
04	
05	$\sum_{j=1}^{i} \Delta t_j \quad (i = 1, 7)$
06	$\sum_{j=1}^{i} \Delta l_j \quad (i = 1, 7)$
09	T_o'/T_o
11	H_{XO}
12	H_{bod}
13	K_{gw}
14	$t_{E,\mathrm{initial}}$
15	t_E
16	$\Delta t_{\mathrm{initial}}$
20	T_{trop}
25	Δt_{req}
55	Δl_1
56	Δl_2
57	Δl_3
58	Δl_4
59	Δl_5
60	Δt_5
61	GS_5
62	$K_{\dot{h},\mathrm{XO}}$
63	$\mathrm{IAS}_{d,i}$
64	GSc
65	$\dot{h}_g$
66	Δt_7

Wind Model Coefficients

50	dD_w/dH
51	$D_{w,s}$
52	dS_w/dH
53	$S_{w,s}$
54	W_{H,h_c}

Airplane Model Coefficients

30	$\mathrm{IAS}_{d,\mathrm{min}}$ (220 knots)
31	$\mathrm{IAS}_{d,\mathrm{max}}$ (350 knots)
32	A_M (25 750 ft)
33	B_M (22 167 ft)
34	C_M (-1.85 sec^2/ft)
35	A_I (-3.07783 ft/sec)
36	B_I (8.158681×10^{-3} knots^{-1})
37	C_I (-3.5×10^{-4} sec^{-1})
38	$\ddot{x}$ (-1.3 knots/sec)
39	A_{gw} (-3.863133×10^{-6} lb^{-1})
40	B_{gw} (2.174392369)
41	K_g (-1280 (ft/sec)/knots/ft)
42	$K_{h,250}$ (-24.70908254)

Computational Constants

43	10 000
44	250
45	3600
46	-1.978×10^{-3}
47	34 293 550
48	8 900 460 000
49	177 675

```
01♦LBL "PD DC10"
02♦LBL B
03 RCL 17
04 FIX 3
05 "Mc "
06 ARCL X
07 PROMPT
08 STO 17
09♦LBL B
10 RCL 18
11 FIX 0
12 "Hc "
13 ARCL X
14 PROMPT
15 STO 18
16 "OK"
17 PROMPT
18♦LBL b
19 FIX 0
20 RCL 19
21 273.15
22 +
23 SQRT
24 RCL 17
25 *
26 38.96
27 *
28 RCL 18
29 XEQ 05
30 +
31 STO 64
32 "GSc "
33 ARCL X
34 PROMPT
35 RCL 64
36 -
37 CHS
38 ST+ 54
39 "OK"
40 PROMPT
41♦LBL C
42 RCL 08
43 FIX 3
44 "Md "
45 ARCL X
46 PROMPT
47 STO 08
48 SF 00
49♦LBL C
50 RCL 10
51 FIX 0
52 "IASd "
53 ARCL X
54 PROMPT
55 STO 10
56 SF 00
57 "OK"
58 PROMPT
59♦LBL D
60 FIX 4
61 RCL 21
62 "MF TM "
63 ARCL X
64 PROMPT
65 STO 21
66 CF 00
67 XEQ 00
68♦LBL D
69 RCL 22
70 "EF TM "
71 ARCL X
72 PROMPT
73 STO 22
74 XEQ 00
75♦LBL D
76 FIX 1
77 RCL 25
78 "DEL TM "
79 ARCL X
80 PROMPT
81♦LBL 00
82 RCL 21
83 RCL 22
84 HMS-
85 HR
86 RCL 45
87 *
88 STO 25
89 RTN
90♦LBL E
91 FIX 0
92 RCL 23
93 "GW "
94 ARCL X
95 PROMPT
96 STO 23
97♦LBL E
98 FIX 1
99 RCL 19
100 "OAT C "
101 ARCL X
102 PROMPT
103 STO 19
104 "OK"
105 PROMPT
106♦LBL F
107 FIX 0
108 RCL 07
109 "H MF "
110 ARCL X
111 PROMPT
112 STO 07
113♦LBL F
114 RCL 26
115 "IAS MF "
116 ARCL X
117 PROMPT
118 STO 26
119♦LBL F
120 FIX 1
121 RCL 27
122 "MF DME "
123 ARCL X
124 PROMPT
125 STO 27
126 "OK"
127 PROMPT
128♦LBL G
129 FIX 1
130 RCL 28
131 "EF DME "
132 ARCL X
133 PROMPT
134 STO 28
135♦LBL G
136 FIX 0
137 RCL 29
138 "MAGCRS "
139 ARCL X
140 PROMPT
141 STO 29
142♦LBL G
143 RCL 24
144 "MAGVAR "
145 ARCL X
146 PROMPT
147 STO 24
148 "OK"
149 PROMPT
150♦LBL A
151 FIX 2
152 0
153 STO 15
154 36152
155 RCL 18
156 -
157 X<0?
158 0
159 RCL 46
```

```
160 *
161 RCL 19
162 273.15
163 +
164 +
165 STO 20
166 216.65
167 -
168 288.15
169 +
170 LASTX
171 /
172 STO 09
173 RCL 23
174 RCL 39
175 *
176 RCL 40
177 +
178 STO 13
179 RCL 18
180 XEQ 05
181 STO 01
182 RCL 07
183 XEQ 05
184 RCL 01
185 -
186 RCL 18
187 RCL 07
188 -
189 /
190 RCL 41
191 *
192 STO 65
193 FS? 00
194 GTO 04
195*LBL 23
196 RCL 17
197 STO 08
198 RCL 26
199 280
200 X>Y?
201 GTO 25
202 X<>Y
203*LBL 25
204 STO 63
205 STO 10
206 XEQ 04
207 LASTX
208 STO 14
209 RCL 05
210 STO 16
211 X<>Y
212 X<0?
213 GTO 15
214 RCL 31
215 STO 10
216 XEQ 04
217 LASTX
218 X<0?
219 GTO 12
220 GTO I
221*LBL 15
222 RCL 30
223 RCL 26
224 X<Y?
225 X<>Y
226 STO 10
227 XEQ 04
228 LASTX
229 X<0?
230 GTO I
231*LBL 12
232 RCL 14
233 RCL 16
234 RCL 05
235 -
236 /
237 STO 00
238 RCL 10
239 RCL 63
240 -
241 *
242 ENTER↑
243 ENTER↑
244 RCL 14
245 /
246 5
247 *
248 RCL 00
249 180
250 *
251 SIN
252 *
253 -
254 RCL 63
255 +
256 STO 10
257 XEQ 04
258 GTO 12
259*LBL 04
260 0
261 STO 05
262 STO 06
263 RCL 10
264 RCL 26
265 X>Y?
266 STO 10
267 RCL 10
268 RCL 08
269 /
270 RCL 47
271 *
272 RCL 48
273 +
274 SQRT
275 CHS
276 RCL 49
277 +
278 RCL 09
279 /
280 STO 11
281 RCL 44
282 RCL 10
283 X<=Y?
284 GTO 07
285 RCL 07
286 RCL 43
287 X<=Y?
288 GTO 07
289 STO 12
290 RCL 07
291 RCL 09
292 *
293 STO 00
294 RCL 26
295 STO 01
296 RCL 44
297 STO 02
298 XEQ 27
299 RCL 01
300 STO 05
301 RCL 02
302 STO 06
303 STO 55
304 RCL 07
305 RCL 09
306 *
307 RCL 37
308 *
309 RCL 42
310 RCL 65
311 +
312 RCL 13
313 *
314 +
315 RCL 43
316 RCL 09
317 *
318 RCL 37
```

```
319 *
320 RCL 42
321 RCL 65
322 +
323 RCL 13
324 *
325 +
326 /
327 LN
328 RCL 37
329 /
330 STO 01
331 ST+ 05
332 RCL 07
333 RCL 43
334 +
335 2
336 /
337 RCL 09
338 *
339 STO 02
340 RCL 44
341 X<>Y
342 XEQ 03
343 RCL 02
344 XEQ 05
345 +
346 RCL 01
347 *
348 RCL 45
349 /
350 ST+ 06
351 STO 56
352 RCL 44
353 STO 01
354 GTO 08
355♦LBL 07
356 RCL 07
357 STO 12
358 0
359 STO 55
360 STO 56
361 RCL 26
362 STO 01
363♦LBL 08
364 CF 05
365 RCL 11
366 RCL 18
367 X>Y?
368 GTO 09
369 STO 11
370 SF 05
371♦LBL 09
372 RCL 11
373 RCL 12
374 X>Y?
375 GTO 10
376 RCL 09
377 *
378 STO 00
379 RCL 10
380 STO 02
381 XEQ 27
382 RCL 01
383 ST+ 05
384 RCL 02
385 STO 57
386 ST+ 06
387 RCL 10
388 RCL 36
389 *
390 E↑X
391 RCL 35
392 *
393 RCL 65
394 +
395 RCL 13
396 *
397 STO 01
398 RCL 12
399 RCL 09
400 *
401 RCL 37
402 *
403 +
404 RCL 11
405 RCL 09
406 *
407 RCL 37
408 *
409 RCL 01
410 +
411 /
412 LN
413 RCL 37
414 /
415 ST+ 05
416 STO 01
417 RCL 11
418 RCL 12
419 +
420 2
421 /
422 RCL 09
423 *
424 STO 02
425 RCL 10
426 X<>Y
427 XEQ 03
428 RCL 02
429 XEQ 05
430 +
431 RCL 01
432 *
433 RCL 45
434 /
435 ST+ 06
436 STO 58
437 GTO 11
438♦LBL 10
439 0
440 STO 57
441 STO 58
442 RCL 07
443 STO 11
444♦LBL 11
445 FS? 05
446 GTO 21
447 RCL 08
448 RCL 32
449 *
450 RCL 33
451 +
452 STO 01
453 RCL 18
454 RCL 09
455 *
456 -
457 CHS
458 RCL 34
459 /
460 SQRT
461 STO 02
462 RCL 11
463 RCL 09
464 *
465 RCL 01
466 -
467 RCL 34
468 /
469 SQRT
470 RCL 65
471 -
472 STO 62
473 RCL 02
474 RCL 65
475 -
476 /
477 LN
```

```
478 RCL 65
479 *
480 CHS
481 RCL 62
482 -
483 RCL 65
484 -
485 RCL 02
486 +
487 2
488 *
489 RCL 34
490 *
491 RCL 13
492 /
493 ST+ 05
494 STO 60
495 STO 01
496 RCL 11
497 RCL 18
498 +
499 2
500 /
501 RCL 09
502 *
503 STO 04
504 RCL 08
505 X<>Y
506 XEQ 06
507 RCL 04
508 XEQ 05
509 +
510 STO 61
511 RCL 01
512 *
513 RCL 45
514 /
515 ST+ 06
516 STO 59
517 RCL 08
518 STO 01
519 GTO 22
520♦LBL 21
521 0
522 STO 59
523 RCL 10
524 STO 01
525♦LBL 22
526 RCL 17
527 STO 02
528 RCL 18
529 RCL 09
530 *
531 STO 00
532 XEQ 27
533 RCL 01
534 ST+ 05
535 RCL 02
536 ST+ 06
537 RCL 28
538 RCL 27
539 -
540 RCL 06
541 -
542 X<0?
543 XEQ 02
544 RCL 45
545 *
546 RCL 03
547 RCL 04
548 +
549 /
550 STO 66
551 ST+ 05
552 FS? 00
553 GTO 18
554 5
555 RCL 05
556 RCL 25
557 -
558 STO 15
559 ABS
560 X>Y?
561 RTN
562 GTO J
563♦LBL 18
564 RCL 05
565 STO 25
566 RCL 45
567 /
568 HMS
569 RCL 22
570 HMS+
571 STO 21
572 GTO J
573♦LBL I
574 FIX 4
575 RCL 15
576 RCL 45
577 /
578 HMS
579 X<0?
580 GTO 26
581 "LATE "
582 ARCL X
583 PROMPT
584♦LBL 26
585 CHS
586 "HOLD "
587 ARCL X
588 PROMPT
589♦LBL J
590 RCL 27
591 RCL 06
592 +
593 FIX 1
594 "IDL DME "
595 ARCL X
596 PROMPT
597♦LBL J
598 RCL 66
599 RCL 45
600 /
601 HMS
602 RCL 22
603 HMS+
604 FIX 4
605 "IDL TM "
606 ARCL X
607 PROMPT
608♦LBL 27
609 RCL 01
610 XEQ 13
611 STO 01
612 RCL 02
613 XEQ 13
614 STO 02
615 STO 03
616 ST- 01
617 RCL 01
618 2
619 /
620 ST+ 02
621 RCL 01
622 RCL 38
623 /
624 X<0?
625 CHS
626 STO 01
627 RCL 00
628 XEQ 05
629 STO 04
630 RCL 02
631 +
632 *
633 RCL 45
634 /
635 STO 02
636 RTN
```

```
637♦LBL 05
638 STO 04
639 RCL 52
640 *
641 RCL 53
642 +
643 RCL 04
644 RCL 50
645 *
646 RCL 51
647 +
648 RCL 29
649 -
650 RCL 24
651 +
652 COS
653 *
654 CHS
655 RCL 04
656 RCL 54
657 *
658 RCL 18
659 /
660 -
661 RTN
662♦LBL 29
663 RCL 00
664♦LBL 03
665 -12 E-06
666 *
667 1
668 +
669 /
670 RTN
671♦LBL 13
672 1
673 X<>Y
674 X>Y?
675 GTO 29
676 RCL 00
677♦LBL 06
678 36152
679 -
680 RCL 46
681 *
682 RCL 20
683 +
684 RCL 20
685 X<=Y?
686 X<>Y
687 SQRT
688 RCL Z
689 *
690 38.96
691 *
692 RTN
693♦LBL 02
694 CHS
695 FC? 00
696 RTN
697 FIX 1
698 RCL 28
699 +
700 STO 00
701 RCL 05
702 RCL 45
703 /
704 HMS
705 RCL 22
706 HMS+
707 STO 21
708 RCL 00
709 "EF < "
710 ARCL X
711 PROMPT
712♦LBL 39
713 PROMPT
714♦LBL H
715 STO 00
716 RCL 27
717 X<>Y
718 X<Y?
719 GTO 46
720 RCL 27
721 STO 02
722 55
723 STO 03
724 1
725 STO 04
726♦LBL 30
727 RCL IND 03
728 ST+ 02
729 RCL 02
730 RCL 00
731 X<=Y?
732 GTO 32
733 1
734 ST+ 04
735 5
736 RCL 04
737 X>Y?
738 GTO 31
739 1
740 ST+ 03
741 GTO 30
742♦LBL 46
743 RCL 07
744 RCL 09
745 *
746 STO 03
747 RCL 26
748 X<>Y
749 XEQ 03
750 RCL 03
751 XEQ 05
752 +
753 RCL 27
754 RCL 00
755 -
756 /
757 1/X
758 RCL 45
759 *
760 RCL 37
761 *
762 RCL 13
763 *
764 E↑X
765 STO 01
766 RCL 26
767 RCL 36
768 *
769 E↑X
770 RCL 35
771 *
772 STO Y
773 RCL 37
774 RCL 03
775 *
776 +
777 RCL 01
778 *
779 -
780 RCL 37
781 /
782 RCL 09
783 /
784 CHS
785 GTO 14
786♦LBL 31
787 RCL 18
788 GTO 14
789♦LBL 32
790 RCL 00
791 RCL 02
792 -
793 RCL IND 03
794 +
795 STO 01
```

```
796 32
797 ST+ 04
798 GTO IND 04
799♦LBL 33
800 RCL 07
801 GTO 14
802♦LBL 34
803 RCL 43
804 RCL 07
805 -
806 RCL 01
807 *
808 RCL IND 03
809 /
810 RCL 07
811 +
812 GTO 14
813♦LBL 35
814 RCL 12
815 GTO 14
816♦LBL 36
817 RCL 11
818 RCL 12
819 -
820 RCL 01
821 *
822 RCL IND 03
823 /
824 RCL 12
825 +
826 GTO 14
827♦LBL 37
828 RCL 62
829 RCL 13
830 *
831 RCL 09
832 /
833 RCL 60
834 *
835 RCL 11
836 +
837 RCL 18
838 -
839 RCL 60
840 X↑2
841 /
842 CHS
843 STO 00
844 RCL 45
845 RCL 01
846 *
847 RCL 61
848 /
849 STO 01
850 X↑2
851 RCL 00
852 *
853 RCL 62
854 RCL 13
855 *
856 RCL 09
857 /
858 RCL 01
859 *
860 +
861 RCL 11
862 +
863♦LBL 14
864 FIX 0
865 "H = "
866 ARCL X
867 GTO 39
868♦LBL a
869 ΣREG 01
870 CLΣ
871 ΣREG 11
872 CLΣ
873 CF 07
874 CF 06
875♦LBL 40
876 "H=? FT"
877 PROMPT
878 X<0?
879 GTO 41
880 STO 00
881 "DIR . SPD ?"
882 PROMPT
883 STO 50
884 FRC
885 1000
886 *
887 RCL 00
888 X<>Y
889 Σ+
890 RCL 11
891 STO 01
892 RCL 12
893 STO 02
894 RCL 15
895 STO 03
896 RCL 00
897 LASTX
898 Σ-
899 RCL 04
900 STO 11
901 RCL 05
902 STO 12
903 RCL 06
904 STO 15
905 RCL 50
906 INT
907 XEQ 42
908 RCL 00
909 X<>Y
910 Σ+
911 RCL 11
912 STO 04
913 RCL 12
914 STO 05
915 RCL 15
916 STO 06
917 RCL 01
918 STO 11
919 RCL 02
920 STO 12
921 RCL 03
922 STO 15
923 GTO 40
924♦LBL 41
925 RCL 13
926 RCL 01
927 *
928 RCL 16
929 X=0?
930 XEQ a
931 /
932 RCL 03
933 -
934 RCL 13
935 X↑2
936 RCL 16
937 /
938 RCL 14
939 -
940 STO 11
941 /
942 STO 52
943 RCL 13
944 RCL 16
945 /
946 STO 12
947 *
948 CHS
949 RCL 01
950 RCL 16
951 /
952 +
953 STO 53
954 RCL 13
```

```
955 RCL 04
956 *
957 RCL 16
958 /
959 RCL 06
960 -
961 RCL 11
962 /
963 STO 50
964 RCL 12
965 *
966 CHS
967 RCL 04
968 RCL 16
969 /
970 +
971 STO 51
972 0
973 STO 54
974 "WIND IN"
975 PROMPT
976♦LBL 42
977 300
978 X<>Y
979 X>Y?
980 GTO 43
981 60
982 X<>Y
983 X>Y?
984 RTN
985 FS? 06
986 RTN
987 FS? 07
988 GTO 44
989 SF 06
990 RTN
991♦LBL 43
992 FS? 07
993 RTN
994 FS? 06
995 GTO 45
996 SF 07
997 RTN
998♦LBL 44
999 360
1000 +
1001 RTN
1002♦LBL 45
1003 360
1004 -
1005 RTN
1006 .END.
```

References

1. Stein, Kenneth J.: New Procedures Key to Fuel Savings. *Aviat. Week & Space Technol.*, vol. 111, no. 9, Aug. 27, 1979, pp. 105–111.
2. Stein, Kenneth J.: Advanced Systems Aid Profile Descents. *Aviat. Week & Space Technol.*, vol. 111, no. 8, Aug. 20, 1979, pp. 57–62.
3. Heimbold, R. L.; Lee, H. P.; and Leffler, M. F.: *Development of Advanced Avionics Systems Applicable to Terminal-Configured Vehicles.* NASA CR-3280, 1980.
4. Knox, Charles E.; and Cannon, Dennis G.: *Development and Flight Test Results of a Flight Management Algorithm for Fuel-Conservative Descents in a Time-Based Metered Traffic Environment.* NASA TP-1717, 1980.
5. Knox, Charles E.: *Planning Fuel-Conservative Descents With or Without Time Constraints Using a Small Programmable Calculator—Algorithm Development and Flight Test Results.* NASA TP-2085, 1983.
6. *Manual of Barometry (WBAN)*—Volume I, First ed. U.S. Govt. Printing Off., 1963.

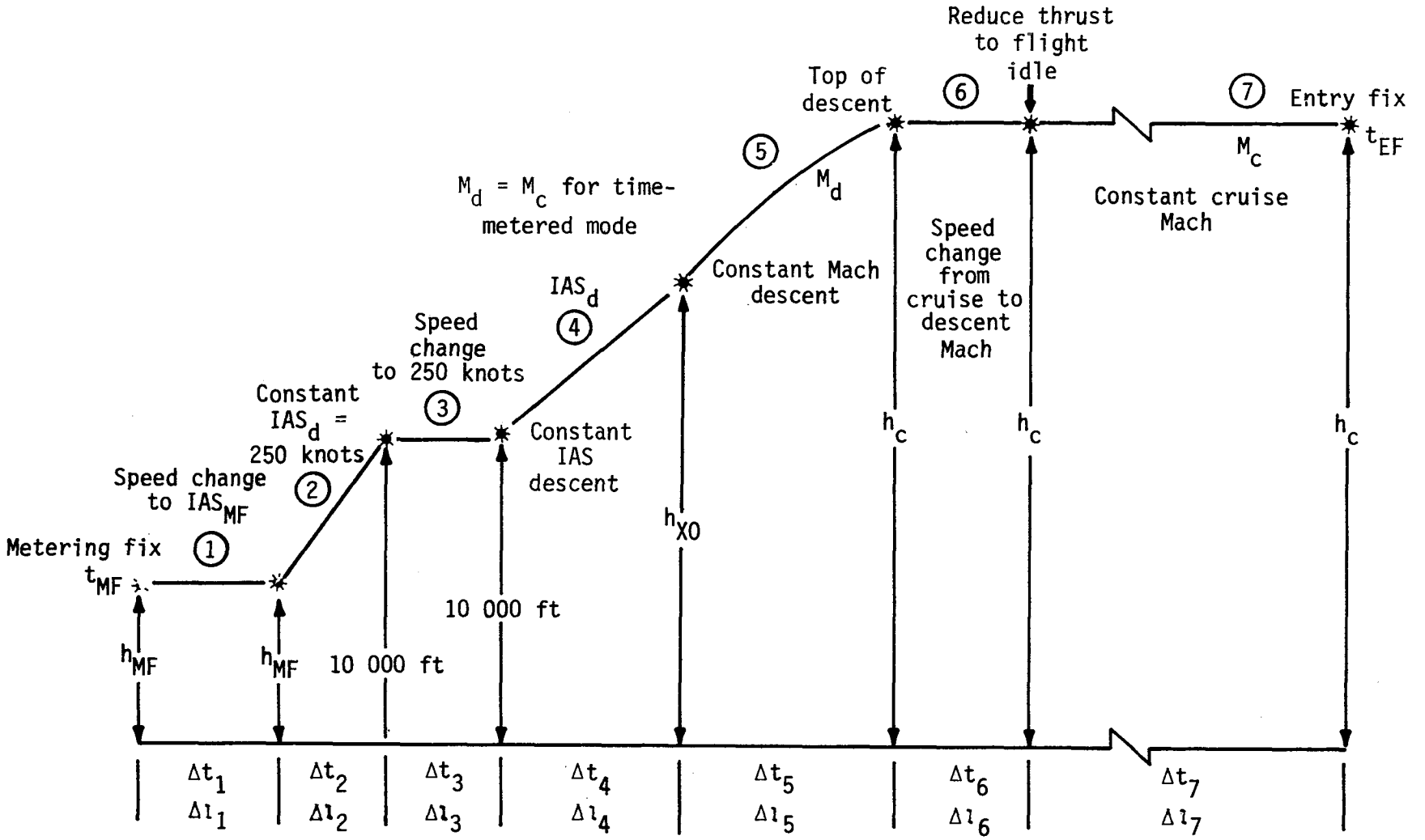

Figure 1. Vertical-plane geometry of computed descent path.

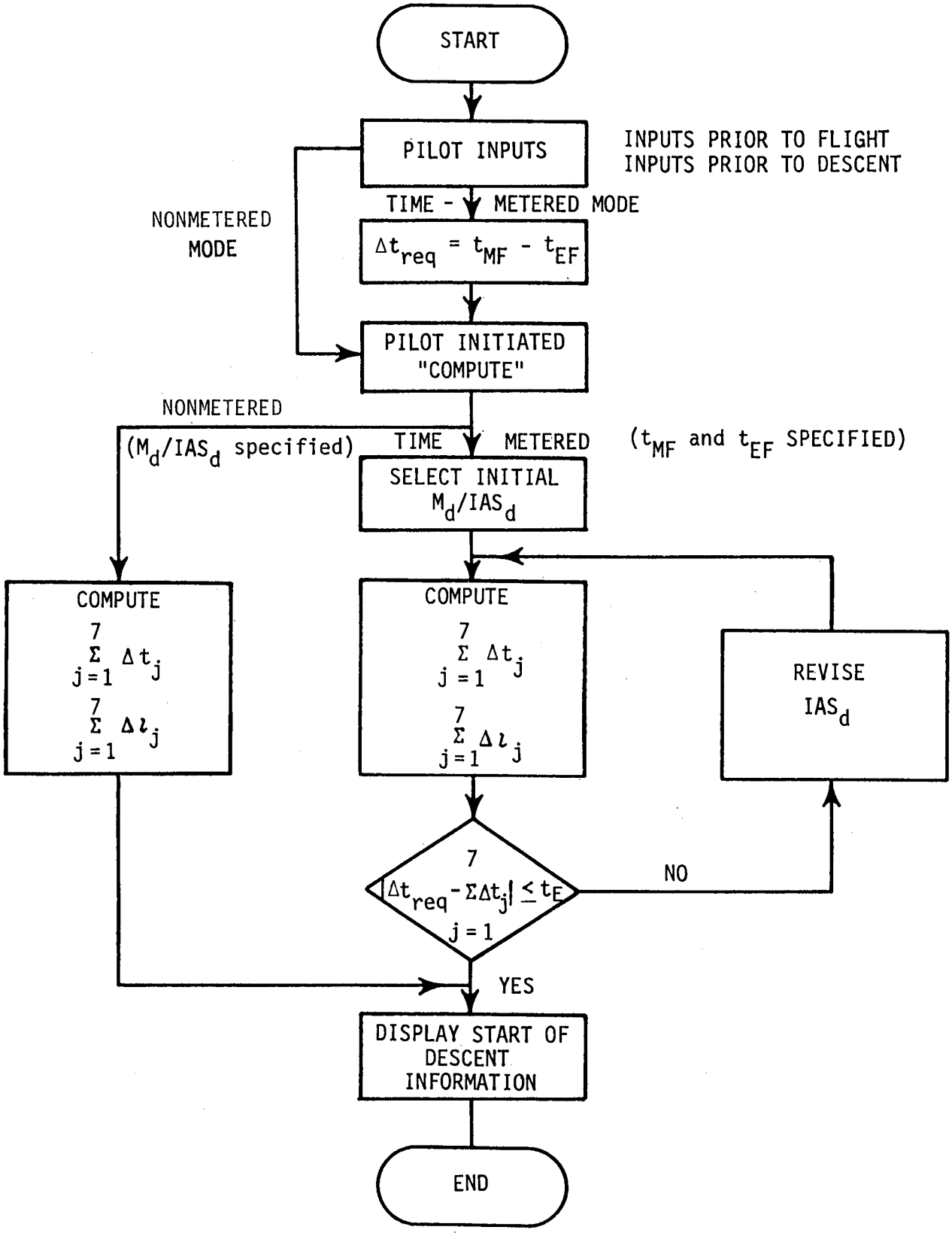

Figure 2. Logic flow of flight-management descent algorithm.

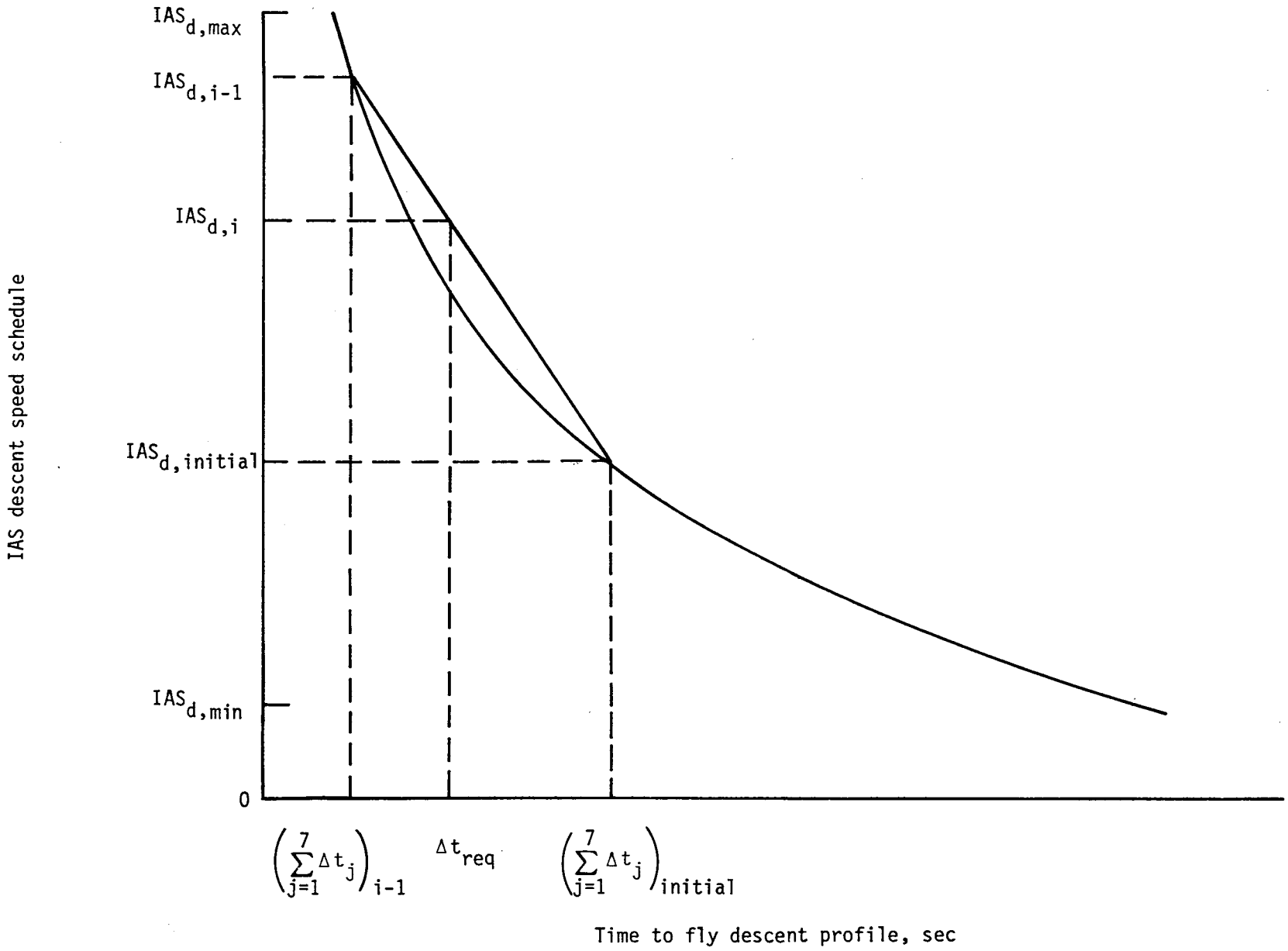

Figure 3. Schedule selection of indicated airspeed descent via interpolation.

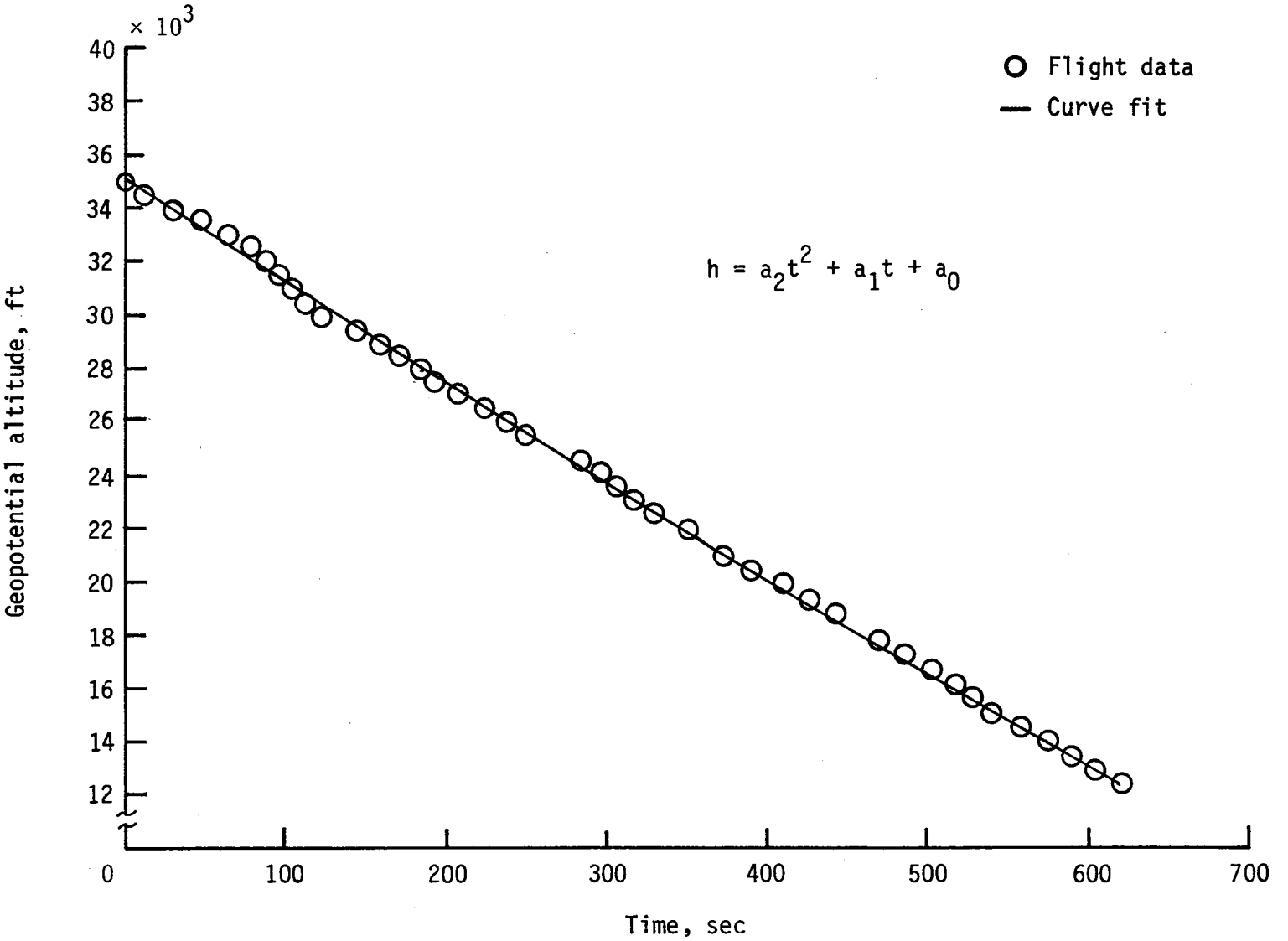

Figure 4. Quadratic curve fit of altitude plotted against time for DC-10 airplane executing a constant 280-knot indicated airspeed descent.

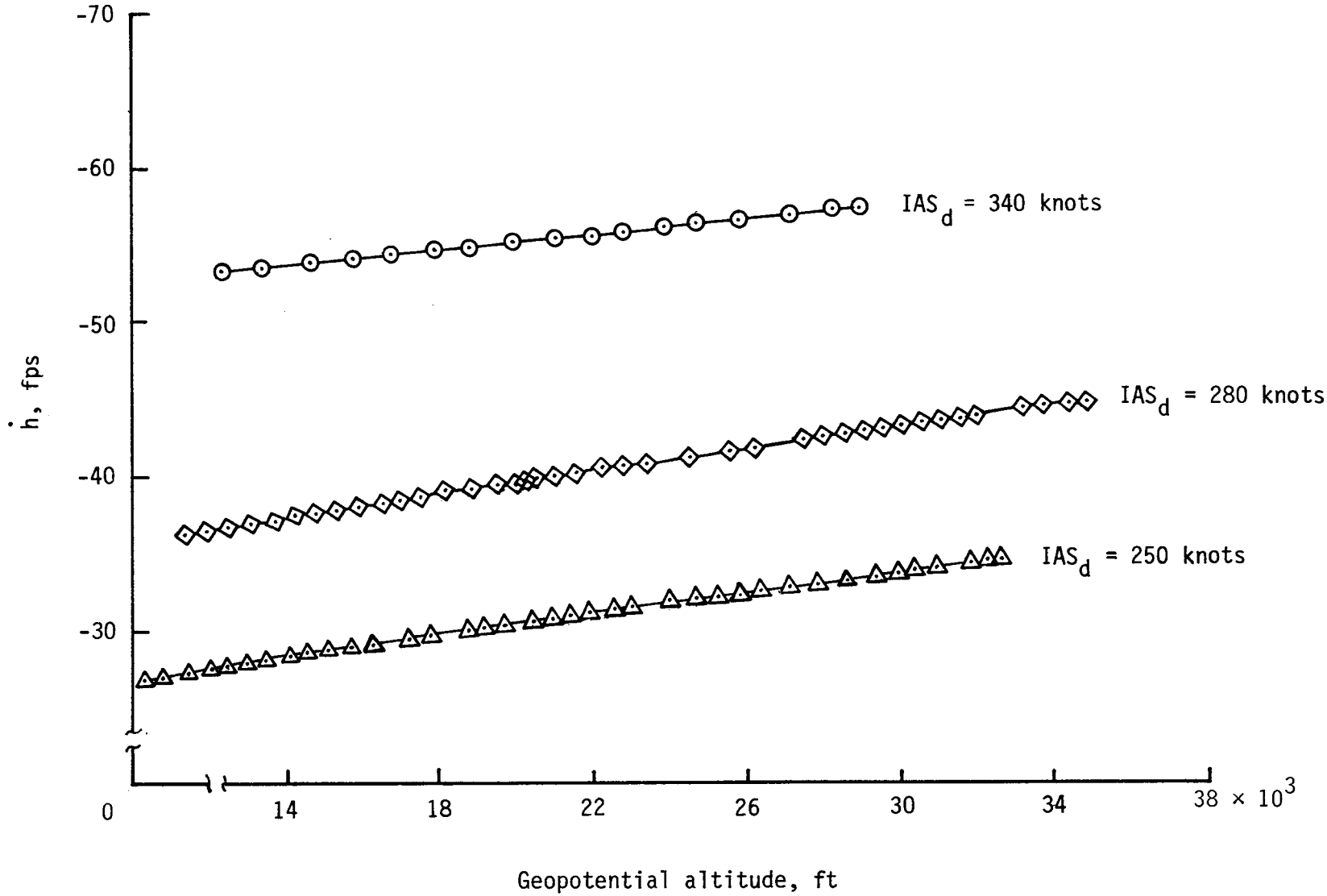

Figure 5. Vertical-speed model of DC-10 airplane for constant indicated airspeed descents (idle thrust).

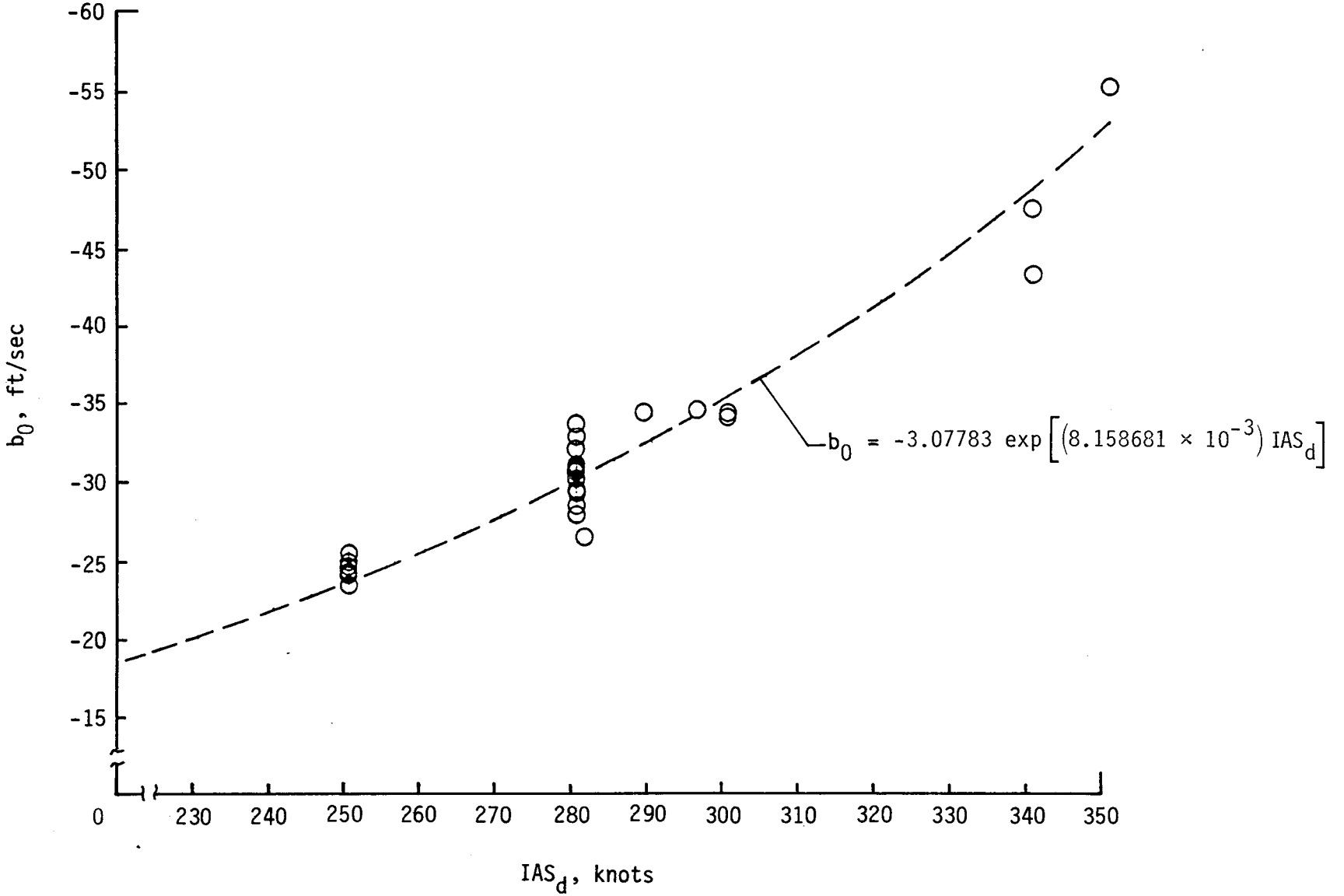

Figure 6. Modeled vertical speed at sea level (idle thrust) for DC-10 airplane.

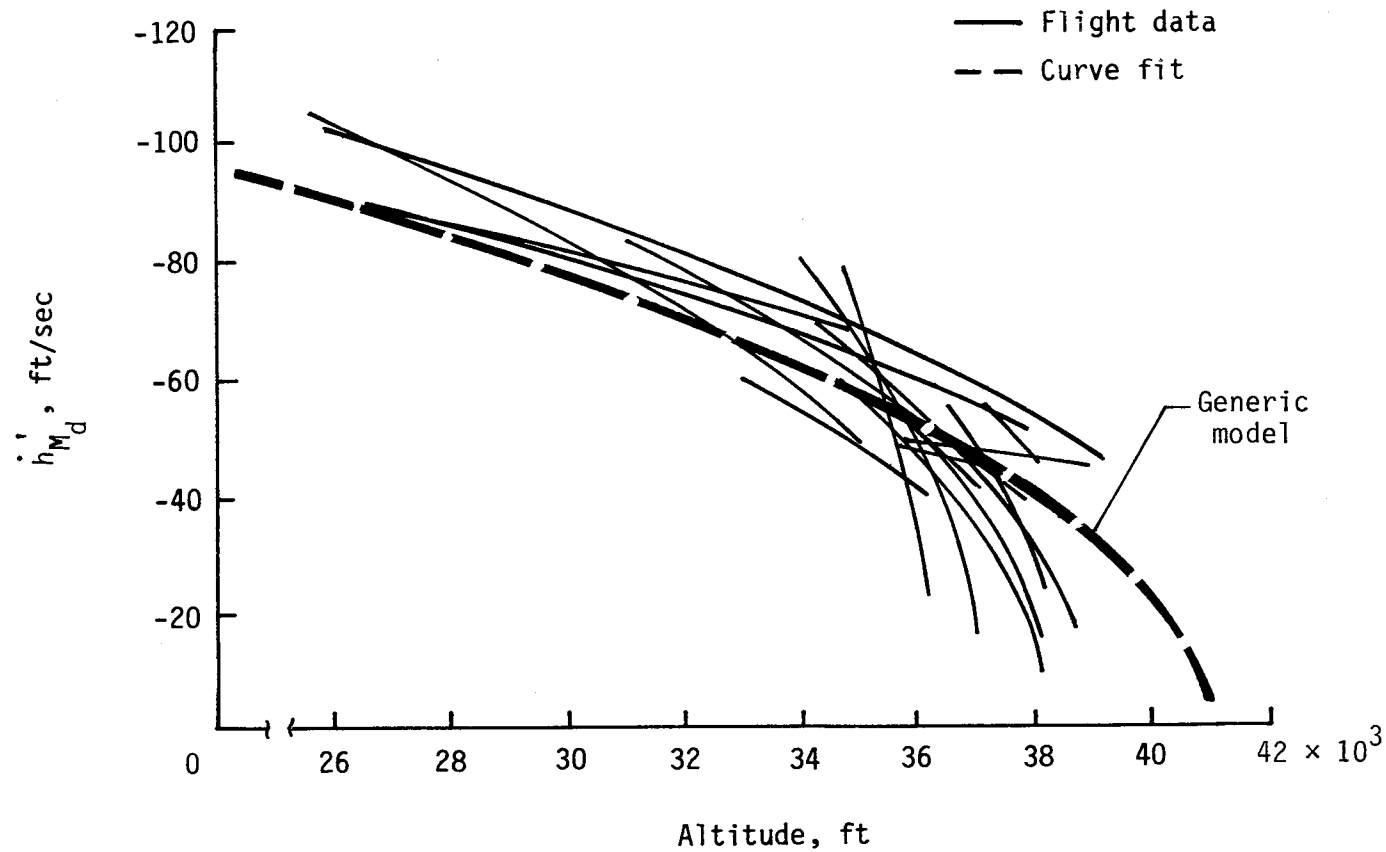

Figure 7. Flight data and generic parabolic model with $c_0 = -1.85$ sec^2/ft for constant Mach number descents (idle thrust) for DC-10 airplane.

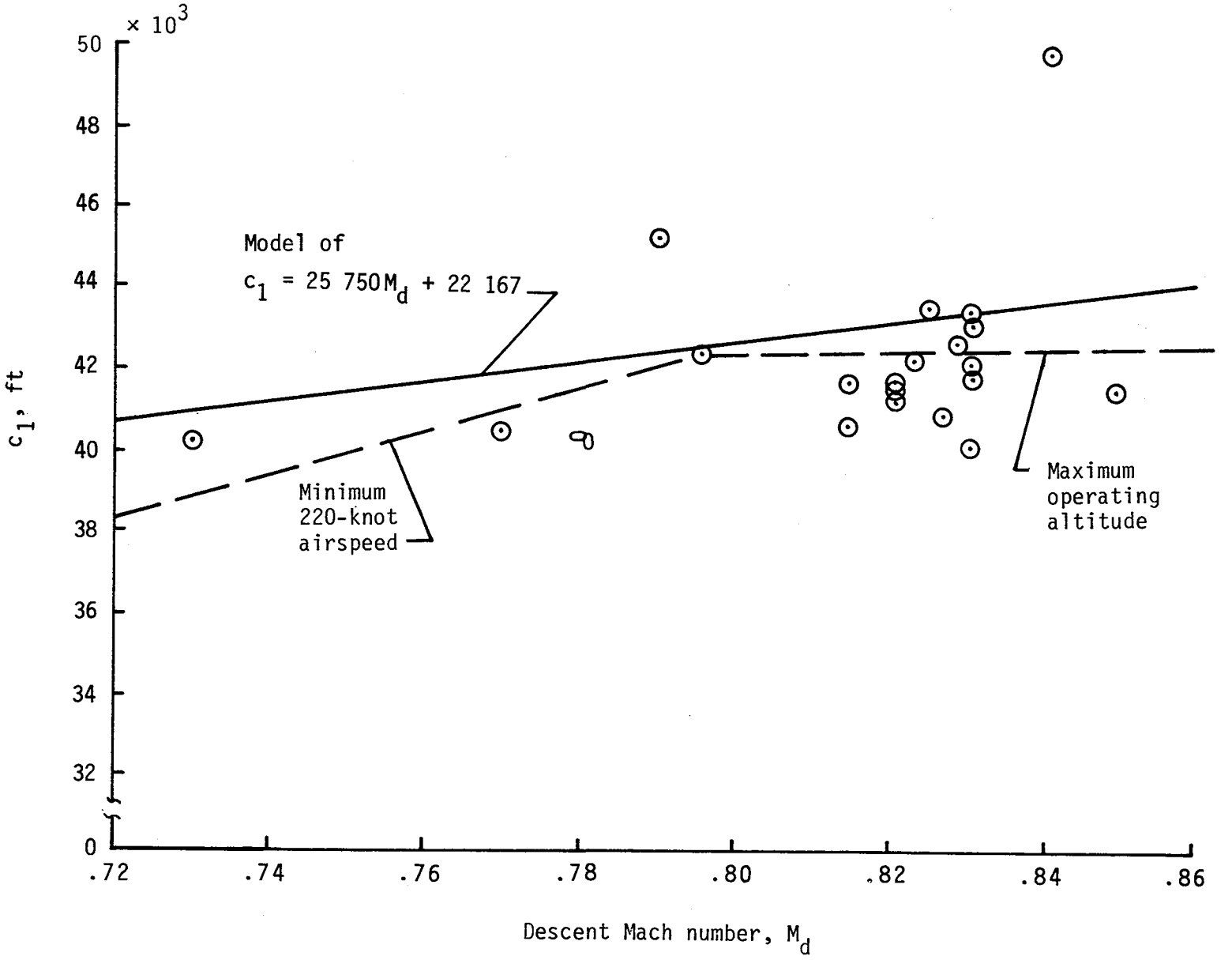

Figure 8. Model of c_1 for constant Mach number descents for DC-10 airplane.

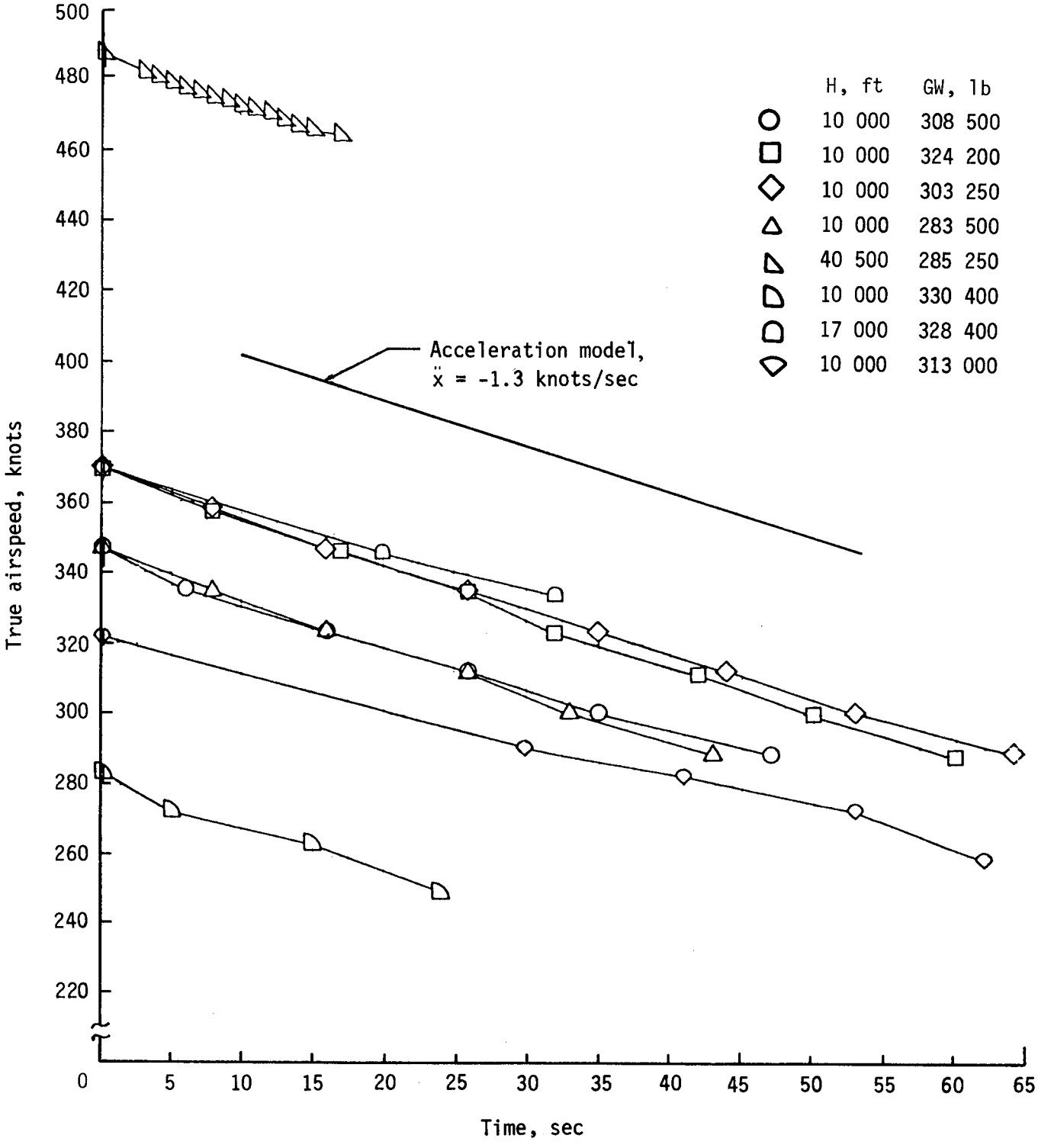

Figure 9. Modeled and actual true airspeed reduction in level flight (idle thrust) for DC-10 airplane.

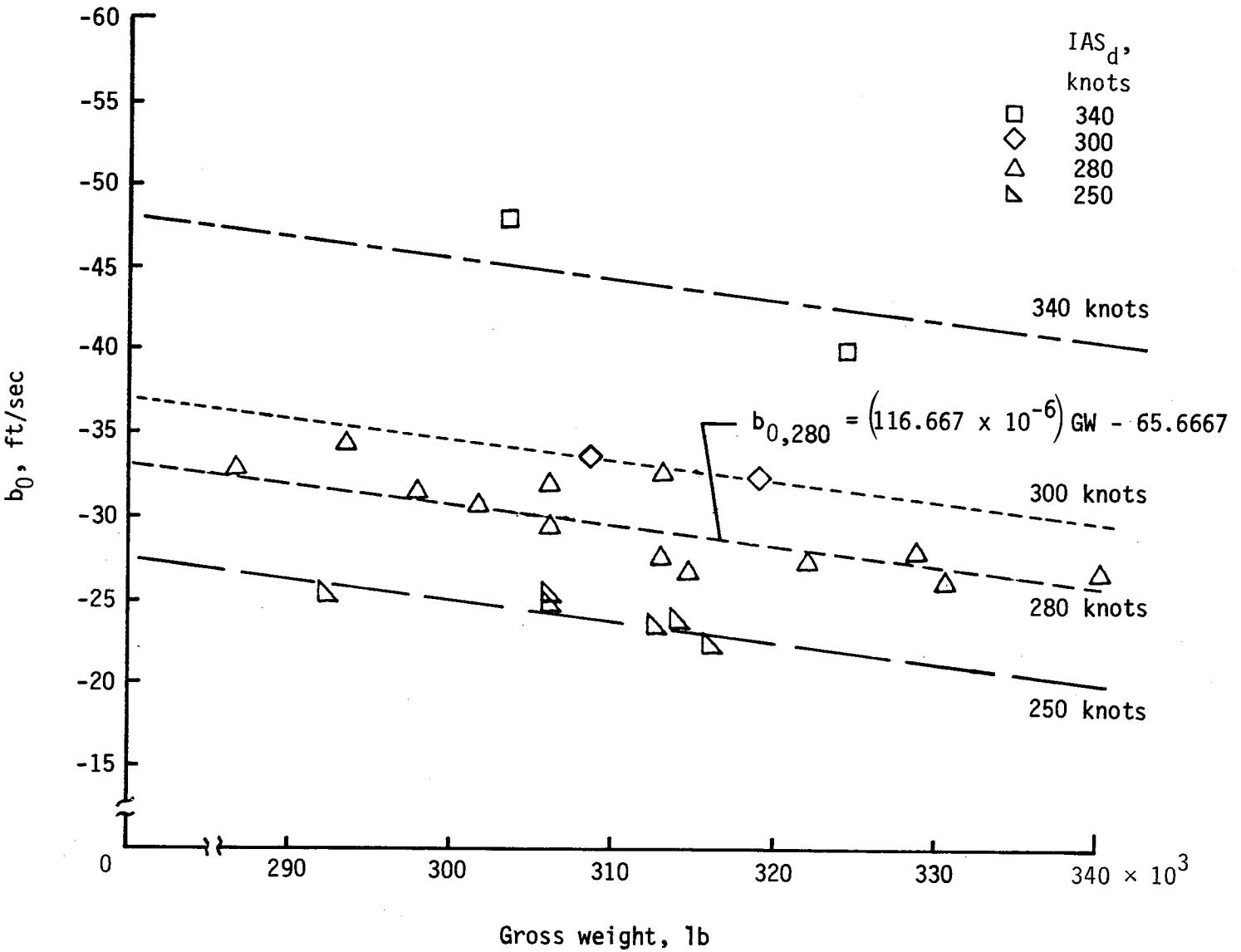

Figure 10. Vertical speed at sea level as a function of gross weight for DC-10 airplane.

L-84-12,910

Figure 11. Programmable descent calculator.

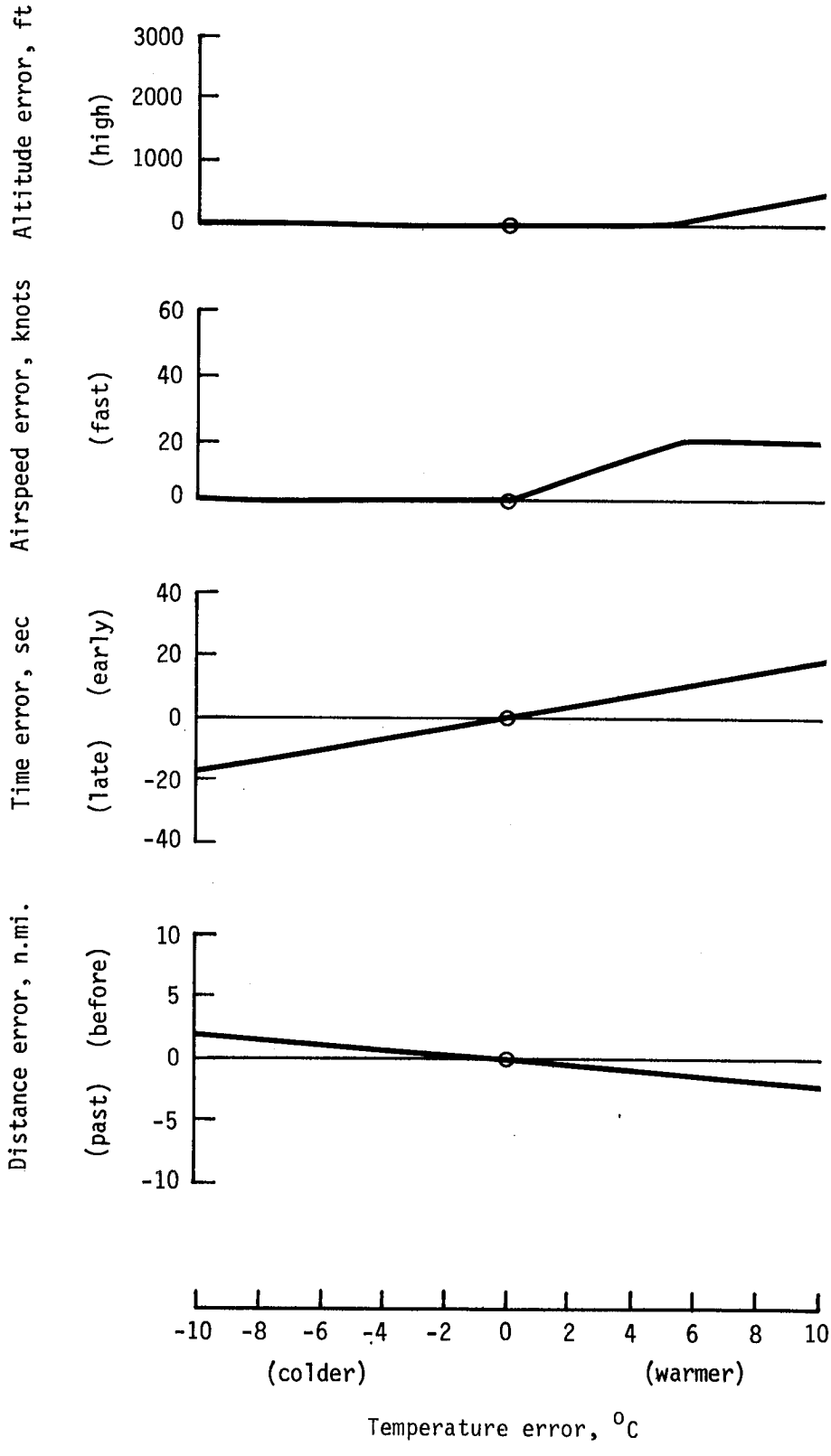

(a) Metering-fix crossing errors due to temperature error.

Figure 12. Metering-fix crossing errors.

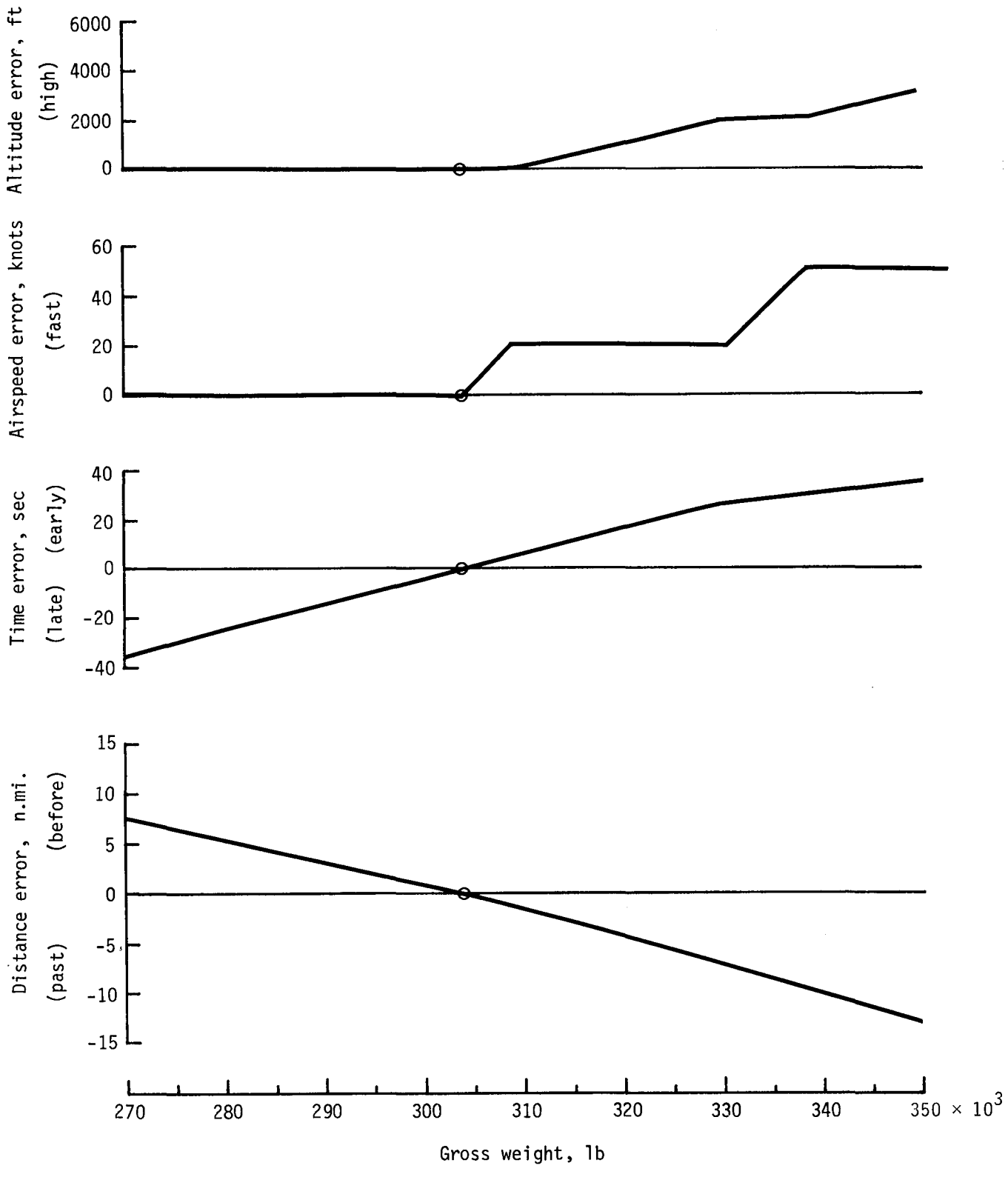

(b) Metering-fix crossing errors due to gross-weight variation.

Figure 12. Continued.

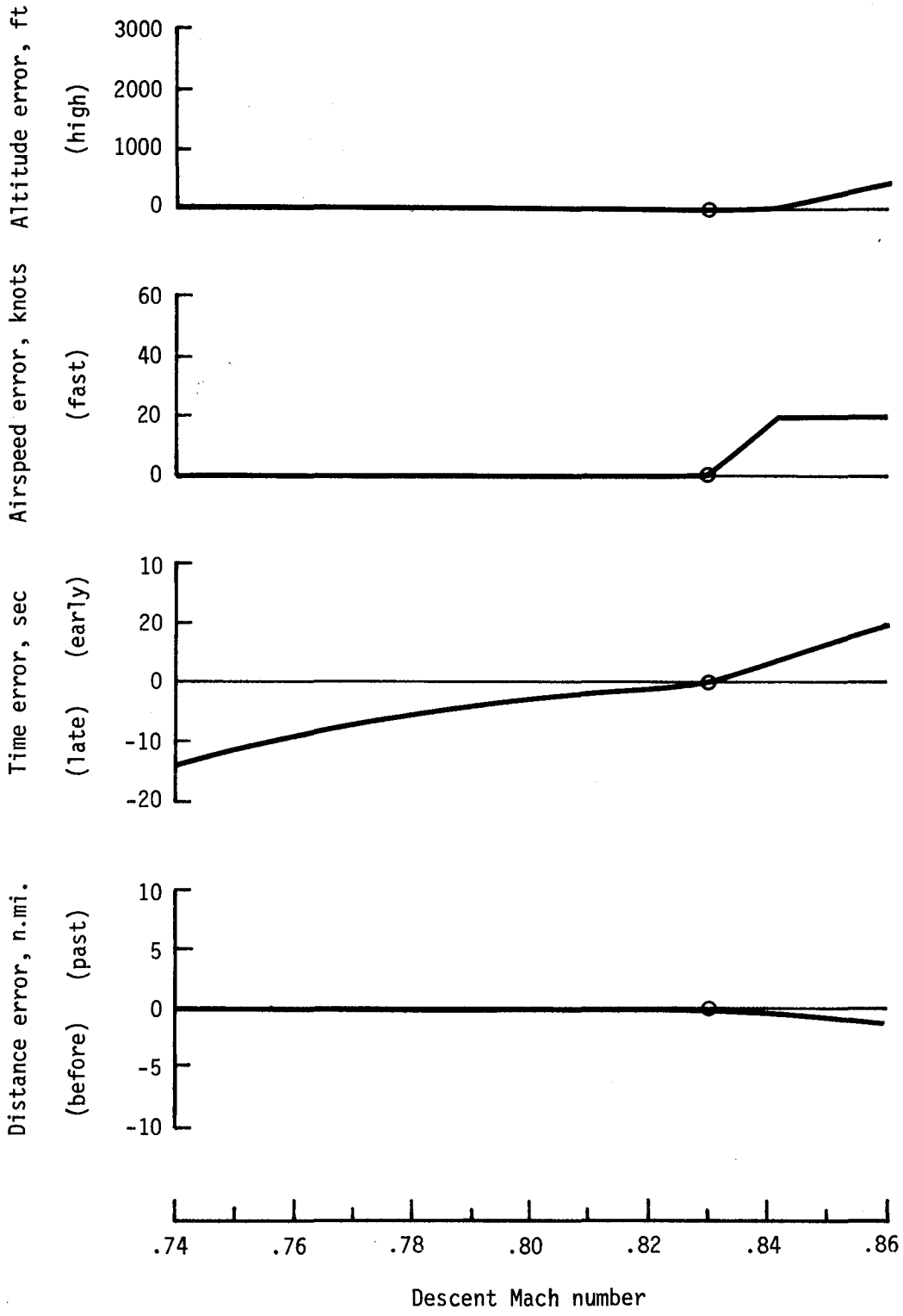

(c) Metering-fix crossing errors due to descent Mach number error.

Figure 12. Continued.

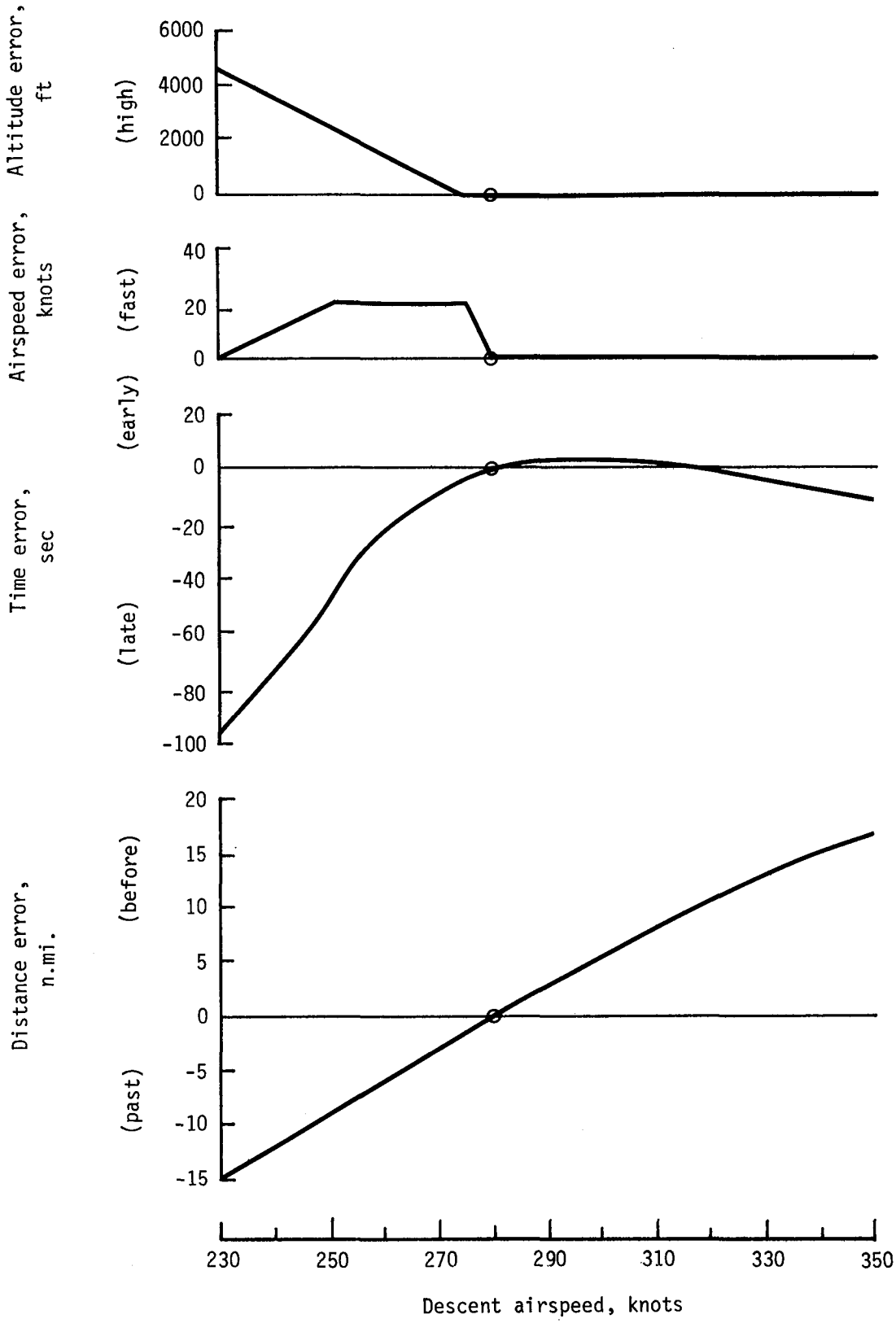

(d) Metering-fix crossing errors due to descent airspeed variation.

Figure 12. Continued.

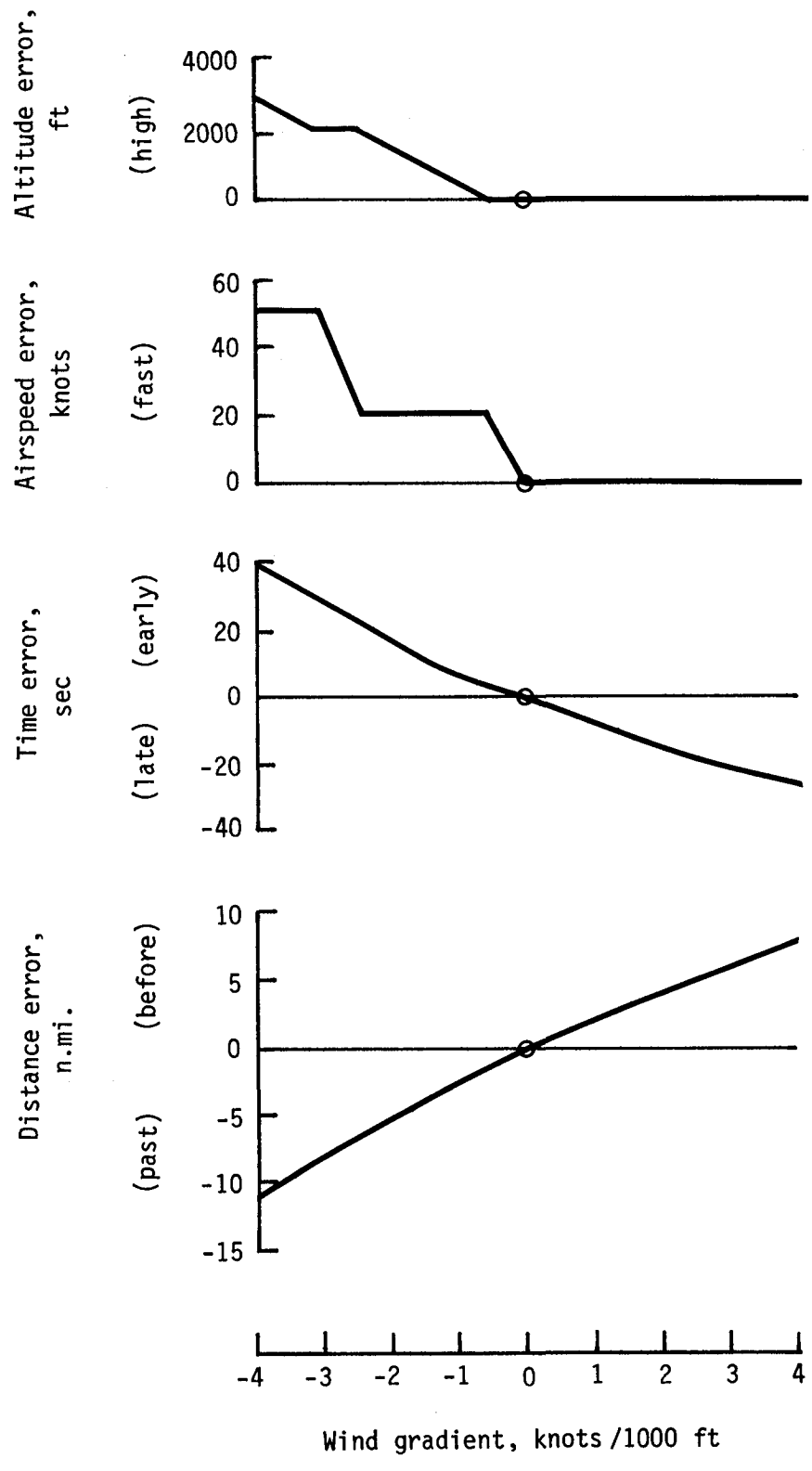

(e) Metering-fix crossing errors due to wind-gradient variation.

Figure 12. Concluded.

1. Report No.	2. Government Accession No.	3. Recipient's Catalog No.
NASA TP-2393		

4. Title and Subtitle	5. Report Date
Planning Fuel-Conservative Descents in an Airline Environment Using a Small Programmable Calculator—Algorithm Development and Flight Test Results	May 1985
	6. Performing Organization Code: 505-45-33-03
7. Author(s): Charles E. Knox, Dan D. Vicroy, and David A. Simmon	8. Performing Organization Report No.: L-15844
9. Performing Organization Name and Address: NASA Langley Research Center, Hampton, VA 23665	10. Work Unit No.
	11. Contract or Grant No.
12. Sponsoring Agency Name and Address: National Aeronautics and Space Administration, Washington, DC 20546	13. Type of Report and Period Covered: Technical Paper
	14. Sponsoring Agency Code

15. Supplementary Notes

Charles E. Knox and Dan D. Vicroy: Langley Research Center, Hampton, Virginia.
David A. Simmon: United Airlines, Inc., Chicago, Illinois.

16. Abstract

A simple, airborne, flight-management descent algorithm has been developed and programmed into a small programmable calculator. The algorithm may be operated in either a time mode or speed mode. The time mode was designed to aid the pilot in planning and executing a fuel-conservative descent to arrive at a metering fix at a time designated by the air traffic control system. The speed mode was designed for planning fuel-conservative descents when time is not a consideration. The descent path for both modes was calculated for a constant Mach/airspeed schedule from linear approximations of airplane performance with considerations given for the descent Mach/airspeed schedule, gross weight, wind, wind gradient, and nonstandard temperature effects. Flight tests, using the algorithm on the programmable calculator, have shown that the open-loop guidance could be useful to airline flight crews for planning and executing fuel-conservative descents.

17. Key Words (Suggested by Authors(s))	18. Distribution Statement
Fuel conservation Flight-management systems Airplanes Air traffic control Time-based metering	Unclassified—Unlimited Subject Category 06

19. Security Classif.(of this report)	20. Security Classif.(of this page)	21. No. of Pages	22. Price
Unclassified	Unclassified	75	A04

For sale by the National Technical Information Service, Springfield, Virginia 22161

NASA-Langley, 1985

National Aeronautics and Space Administration

Washington, D.C.
20546

Official Business
Penalty for Private Use, $300

THIRD-CLASS BULK RATE

Postage and Fees Paid
National Aeronautics and
Space Administration
NASA-451

NASA

POSTMASTER: If Undeliverable (Section 158 Postal Manual) Do Not Return